Distribution Agreement

In presenting this thesis or dissertation as a partial fulfillment of the requirements for an advanced degree from Emory University, I hereby grant to Emory University and its agents the non-exclusive license to archive, make accessible, and display my thesis or dissertation in whole or in part in all forms of media, now or hereafter known, including display on the world wide web. I understand that I may select some access restrictions as part of the online submission of this thesis or dissertation. I retain all ownership rights to the copyright of the thesis or dissertation. I also retain the right to use in future works (such as articles or books) all or part of this thesis or dissertation.

Signature:

_____ _____

Emily C. Woods Date

Genetic mechanisms of the *Clostridium difficile* response to host-produced antimicrobial peptides

By

Emily C. Woods
Doctor of Philosophy

Graduate Division of Biological and Biomedical Science
Microbiology and Molecular Genetics

_____
Shonna M. McBride, Ph.D.
Advisor

_____
Charles P. Moran, Ph.D.
Committee Member

_____
Philip N. Rather, Ph.D.
Committee Member

_____
William M. Shafer, Ph.D.
Committee Member

_____
David S. Weiss, Ph.D.
Committee Member

Accepted:

_____
Lisa A. Tedesco, Ph.D.
Dean of the James T. Laney School of Graduate Studies

_____
Date

Genetic mechanisms of the *Clostridium difficile* response to host-produced antimicrobial peptides

By

Emily C. Woods
B.S., Rhodes College, 2012

Advisor: Shonna M. McBride, Ph.D.

An abstract of
A dissertation submitted to the Faculty of the
James T. Laney School of Graduate Studies of Emory University
in partial fulfillment of the requirements for the degree of
Doctor of Philosophy

Graduate Division of Biological and Biomedical Science
Microbiology and Molecular Genetics

2017

Abstract

Genetic mechanisms of the *Clostridium difficile* response to host-produced antimicrobial peptides

By Emily C. Woods

As a leading cause of nosocomial infections, *Clostridium difficile* (also known as *Clostridiodes difficile*) is a major public health threat. *C. difficile* infections typically arise after administration of antibiotics, and account for about 20% of all antibiotic-associated diarrhea. Antibiotics alter the normal intestinal microbiota, making the host more susceptible to *C. difficile* infection. In addition to the commensal flora, the host's immune response is critical for warding off infection. The production of cationic antimicrobial peptides (CAMPs), such as LL-37 and lysozyme, in the intestines provides a defense against many intestinal pathogens. Despite the presence of these antimicrobials, *C. difficile* is able to survive in the colon and cause disease. *C. difficile* is able to survive because it is resistant to these CAMPs; however, the mechanisms by which *C. difficile* resists and responds to these CAMPs is unknown. We therefore investigated genetic mechanisms by which *C. difficile* responds to the CAMPs lysozyme and LL-37. Building upon previous work that had shown that lysozyme induces expression of the extracytoplasmic sigma factor, σ^V, we showed that σ^V regulates expression of the Dlt pathway. This pathway adds D-alanine to teichoic acids in the cell wall, thereby increasing *C. difficile* resistance to lysozyme. Both a *sigV* and a *dltD* mutant are more virulent in a hamster model of infection, underscoring the importance of this regulatory pathway to the course of infection *in vivo*. Additionally, we investigated how *C. difficile* responds to LL-37 by performing RNA-seq to determine which genes are induced in LL-37. We discovered an operon, *clnRAB*, which is specifically induced in response to LL-37. This operon encodes a GntR-family transcriptional regulator, ClnR, which acts as a global regulator, controlling expression of many genes involved in metabolism, transport, and transcriptional regulation. Our data indicate that this regulator responds to LL-37 as a signal that the bacterium is in the host environment and enables adaptation to this environment. Overall this work has furthered our understanding of how *C. difficile* interacts with the host innate immune system.

Genetic mechanisms of the *Clostridium difficile* response to host-produced antimicrobial peptides

By

Emily C. Woods
B.S., Rhodes College, 2012

Advisor: Shonna M. McBride, Ph.D.

A dissertation submitted to the Faculty of the
James T. Laney School of Graduate Studies of Emory University
in partial fulfillment of the requirements for the degree of
Doctor of Philosophy

Graduate Division of Biological and Biomedical Science
Microbiology and Molecular Genetics

2017

Acknowledgements

First, I would like to thank my advisor, Shonna. She has been incredibly patient with me throughout the blunders that come with being a student in training. I am immensely grateful that she devoted so much effort and energy to me over these past several years.

I also would never have survived this process without the support of the other McBride lab members, both past and present. Not only did they help to make the lab a place I enjoyed being, but also the scientific and life advice that they have given me along the way has proved invaluable.

The unwavering support and encouragement of my parents has been indispensible. Even when I doubted myself, they remained certain that I could persist. Their support has been a huge blessing.

Samarth has been a steady source of joy in my life. He remained a calming presence in the midst of all the drama that comes with graduate school. I cannot imagine making it through the last year and a half of my graduate school experience without him.

Unfortunately I do not have the space to thank other individuals by name; however, I realize that completion of a doctoral degree is never a solo achievement, and I am immensely grateful for the many other individuals and communities who have supported me on this journey.

Table of Contents

List of Tables and Figures

Chapter 2

Chapter 3

Chapter 1: Introduction

I: *Clostridium difficile*

a. *Clostridium difficile* poses a significant burden on the healthcare system

Clostridium (Clostridiodes) difficile is one of the leading nosocomial infections in the United States and represents the most common cause of nosocomial diarrhea worldwide (1, 2). In 2011, the Centers for Disease Control and Prevention (CDC) estimates that 453,000 cases of *C. difficile* infection (CDI) occurred in the United States, resulting in approximately 29,000 deaths (3). CDI recurs in close to 20% of patients and often necessitates expensive treatment and lengthy hospital stays; CDI therefore results in significant healthcare costs (1, 3-5). In 2008, it was estimated that CDI was responsible for $4.8 billion in excess healthcare spending (4).

Since the early 2000s, a new strain of *C. difficile*, known as the 027 ribotype (also referred to as NAP1 or BPI in other classification systems), has become epidemic (6-8). These strains are associated with increased severity and mortality, higher toxin production, and higher rates of recurrence and treatment failure (8-12). The rise of these strains has therefore exacerbated the burden of CDI on the healthcare system.

b. Risks for infection

A variety of factors have been associated with an increased risk for contracting CDI. These include older age, use of acid-suppressing drugs, immunosuppression (especially chemotherapy), and the presence of additional chronic diseases (13, 14). The two most important risk factors, however, are exposure to antibiotics and exposure to healthcare settings (14, 15). Given the importance of these risk factors, they will each be discussed in greater depth.

Exposure to antibiotics is the primary risk factor for developing CDI. CDI accounts for about 20% of all antibiotic associated diarrhea (AAD), although it likely accounts for a higher percentage of AAD in the hospital setting (16, 17). Out of all patients receiving antibiotics in a hospital setting, about 15% will develop CDI (18). All antibiotics except tetracyclines have been associated with subsequent CDI, however clindamycin and third-generation cephalosporins have the strongest association with CDI (13, 19, 20). The epidemic 027 strains are strongly associated with fluoroquinolone exposure because they are often resistant to this class of antibiotics (21, 22). Those who receive antibiotics have a heightened susceptibility to CDI for up to 3 months (23).

The primary mechanism by which antibiotic exposure leads to increased susceptibility to CDI is the dysbiosis of the gut microbiota (24). A healthy individual is colonized by a diverse compilation of bacteria in the gut that provide colonization resistance against *C. difficile*. Antibiotic treatment induces a number of changes that make it easier for *C. difficile* to colonize the colon and cause disease. First, antibiotic treatment disrupts the composition of the gut microbiota (25, 26). Because some intestinal bacterial species can directly inhibit *C. difficile* growth, the loss of these species enables *C. difficile* colonization (27, 28). The decreased diversity of bacteria, particularly of the butyrogenic Firmicutes family, means *C. difficile* has less competition for resources and space in the colon (29-31). Moreover, when particular types of bacteria are lost from the microbiota, the metabolic activities of these bacteria are also lost. These changes in the available nutrients and metabolic by-products can drastically change the environment in the colon (32-34). For example, with the loss of bacteria that metabolize complex carbohydrates, there is decreased production of short-chain fatty acids (SCFA),

which regulates immune function in the gut (34, 35). Antibiotic treatment can lead to increased availability of amino acids, which are a preferred nutrition source for *C. difficile* (34). *C. difficile* is also able to metabolize many of the sugar alcohols, such as mannitol and sorbitol, which are increased in the intestines after antibiotic treatment (26, 36). Antibiotics are also associated with a decrease in bacteria that hydrolyze primary bile acids into secondary bile acids (37, 38). Secondary bile acids inhibit *C. difficile* growth, whereas primary bile acids stimulate germination of *C. difficile* spores (39-41). A decrease in secondary bile acids and increase in primary bile acids therefore creates a favorable environment for *C. difficile* outgrowth and colonization (37, 38).

Exposure to healthcare settings is the other main risk factor for CDI, because healthcare settings can easily become contaminated with *C. difficile* spores from infected patients. As a strict anaerobe, *C. difficile* is dependent on the hardy spore form to transmit between hosts (42). Spores are resistant to alcohol-based hand sanitizers and most standard environmental cleaning products (43-45). In addition, spores can survive on surfaces for several months (46). It is therefore not surprising that 21% of hospitalized patients are colonized with *C. difficile* (although it is important to note than only about a third of these colonized patients present with symptoms of disease) (47). Efforts by hospitals to use appropriate sporicidal cleaning products to disinfect surfaces, to quickly diagnose and isolate infected patients, to enforce proper hand-washing by healthcare professionals, and to reduce unnecessary antibiotic use can decrease the incidence of CDI (46, 48-50). Nevertheless, close to 70% of CDI cases are healthcare associated, so healthcare settings remain a significant risk factor for development of CDI (51).

c. Pathogenesis

C. difficile can cause a broad spectrum of disease severity, which ranges from asymptomatic carriage to death (24, 47). In between those extremes, afflicted individuals can experience mild or severe diarrhea, pseudomembranous colitis, and/or toxic megacolon (52). The severity of symptoms depends on a combination of host and bacterial strain characteristics, but ultimately all of the disease symptoms are attributable to the *C. difficile* toxins (24).

The primary *C. difficile* toxins, TcdA and TcdB, are encoded on the pathogenicity locus (PaLoc), which includes *tcdR, tcdA, tcdB, tcdC* and *tcdE* (53). TcdR is a sigma factor that regulates expression of the PaLoc (54). TcdC is an anti-sigma factor for TcdR (55). TcdE encodes a holin that is predicted to be important for release of toxins from the cell (56). TcdA (Toxin A, enterotoxin) and TcdB (Toxin B, cytotoxin) are toxic to colonocytes due to their glucosyltransferase activity (57). Upon entering colonocytes via receptor-mediated endocytosis, these toxins transfer glucosyl moieties onto the host GTPase, Rho, thereby inactivating this critical host protein (57-59). Inactivation of Rho leads to disaggregation of actin, increased intracellular calcium concentrations, increased membrane permeability, and ultimately cell death through either necrosis or apoptosis (57). Epithelial cell death releases factors that stimulate inflammation, and the neutrophils and other immune effectors recruited to the area can cause additional tissue damage (57, 60, 61).

In addition to toxins A and B, some strains, including the epidemic 027 strains, also produce a binary toxin (62, 63). Binary toxin ADP-ribosylates actin, resulting in microfilament protrusions on epithelial cells, which can aid colonization of *C. difficile* on the surface of these cells (64).

II. Innate immunity in CDI

a. Immune responses in the intestines

The intestinal tract has evolved a complex, multi-tiered system to provide immune protection from the large volume of foreign material that enters the gut (65, 66). The first line of protection is the physical barrier of a thick mucus layer (67). A second general protection against pathogens is provided by antimicrobial peptides (AMPs) (68, 69). Commensal bacteria provide additional protection through colonization competition, secretion of antimicrobials, and immune modulation (28, 70). More specialized responses are provided by the epithelial cells which line the lumen of the intestines and by the gut-associated lymphoid tissue (GALT) (71). The contribution of each of these aspects of protection in the gut will be explored in more detail.

Mucus is a coating of the intestinal epithelia that creates a physical barrier between the gut lumen and the epithelial layer (72). Mucus is secreted by mucin-secreting cells, and is composed of many varieties of mucin, a heavily glycosylated protein (72). Although some bacteria are able to adhere to and/or metabolize mucins, the thick nature of the mucus layer is largely impermeable to bacteria (73, 74). Mucus therefore effectively prevents most intestinal bacteria from directly contacting host surfaces (72).

AMPs are a class of molecules produced by the innate immune system, and a wide variety of AMPs can be found in the intestines (68, 69, 75). In most cases, AMPs are cationic (CAMPs). The surface of bacterial cells is typically highly negatively charged, so the CAMPs are electrostatically attracted to the surface of bacteria and can form pores in bacterial membranes (71, 76). In addition to their direct antimicrobial

effects, many AMPs also have chemotactic or immunomodulatory effects (65, 76). A number of AMPs are produced and released constitutively by Paneth cells in the small intestines and/or by the epithelial cells of the intestines (65, 69, 71). Many AMPs are also released by neutrophils when these immune cells are activated at the site of an infection (68, 71). A few of the key AMPs found in the intestines include the α- and ß-defensins, LL-37 (cathelicidin), BP1, lysozyme, CCL20, and PLA2 (65, 66). Lysozyme and LL-37 will be discussed in more detail in subsequent sections.

As mentioned previously, the commensal gut microbiota provide an additional deterent to pathogens, a term called colonization resistance (77). Colonization resistance occurs through a variety of mechanisms. First of all, the commensal microbiota can deplete the available metabolites, making it difficult for newcomers to obtain adequate nutrition (78). By Freter's nutrient-niche hypothesis, a bacteria can only colonize the intestines if it is able to metabolize a growth-limiting nutrient better than its competitors (78). This hypothesis has been supported by evidence that particular *E. coli* strains are unable to colonize the gut only when strains with similar nutrient requirements are present (79). The commensal bacteria also block potential mucin binding sites (78). In addition to these passive mechanisms of exclusion, the commensal microbiota can actively hinder pathogens via the production of their own AMPs, known as bacteriocins (28, 78). Some commensal bacteria also play a role in bile acid metabolism (80). Because some forms of bile acids have antimicrobial effects, the metabolism of the bile acids by bacteria can help maintain an environment unfavorable to colonization by pathogens (80). Moreover, commensal bacteria help to stimulate a baseline level of activity from the host immune system (70, 81-83). For example, many commensal bacteria secrete molecules

such as short-chain fatty acids and butyrate that can stimulate host production of AMPs (70). Additionally, commensal bacteria have been shown to induce mucin production, secretory IgA production, and promote differentiation of Th17 cells (pro-inflammatory helper T cells) (70, 83). This combination of mechanisms enables the commensal bacteria to create a formidable colonization barrier to *C. difficile*.

Although many of these defense mechanisms act constitutively, there are also aspects of the intestinal defense that are only activated when pathogens are detected. For example, epithelial cells can trigger an immune reaction in response to pathogens (84). Located below the mucus layer, the epithelial cells of the intestines can detect when aberrant bacteria have breached the mucus barrier (70, 85). Epithelial cells express a number of toll-like receptors (TLRs), which sense a variety of bacteria-specific molecules, such as lipopolysaccharide (LPS), peptidoglycan (PG), lipoteichoic acid (LTA), and flagellin (83). Similarly, invasive bacteria can activate cytosolic NOD-like receptors (NLRs). Binding of a bacterial molecule to a TLR or NLR triggers a signaling cascade that results in the release of pro-inflammatory cytokines, such as the interleukins IL-1 and IL-8 (83, 84). These cytokines then serve to recruit and activate other components of the immune system at the site of the sensed pathogen (83).

Beyond these initial innate immune responses, an adaptive immune response to specific pathogens can develop. In the intestines, the adaptive immune response is primarily mediated through the gut-associated lymphoid tissues (GALT) (86). A key component of the GALT is M cells, which extend into the lumen of the gut to sample any antigens that are present there (86). The M cells then present these antigens to dendritic cells in the sub-epithelium (86). Also located in the sub-epithelium are T cells and IgA-

producing B cells (87). Antigens are ultimately presented to B cells in follicles within the Peyer's patches of the GALT, thereby stimulating an antibody response (87).

b. Immune responses to CDI

Evidence from animal models of CDI indicates that the innate immune response is critical to eliminating the infection. Resolution of disease in the mouse model of infection typically occurs at the time before the adaptive immune response has had the chance to fully activate and before the composition of the commensal microflora has returned to normal, implying that an early response from the innate immune system is responsible for the clearance of infection (88). Moreover, mice lacking components of the innate immune system, such as MyD88, TLR4, TLR5, innate lymphoid cells, and Nod1, experience greater mortality when challenged with *C. difficile* (89-93). In addition, *Rag1*$^{-/-}$ mice, which lack an adaptive immune response, recover from the acute phase of CDI similar to wild-type mice, indicating that the innate response is more critical for initial resolution of symptoms than the adaptive response (93).

Although the surface layer protein (SLP) and flagellin of *C. difficile* have been demonstrated to trigger the immune response (94, 95), the primary route of activation of the innate immune response appears to be through the effects of toxins A and B on epithelial cells (88, 96). These toxins, especially toxin B, stimulate the NF-kB pathway, which leads to the production of pro-inflammatory cytokines (97, 98). Particularly notable is the release of IL-8 and CXCL8 (98, 99). IL-8 and CXCL8 act as chemoattractants for neutrophils (99). A massive influx of neutrophils into the mucosa of the colon, resulting in pseudomembranous colitis, is pathognomonic for CDI (90, 100).

A second wave of inflammation can also occur once the epithelial layer is destroyed and the underlying mucosal cells begin responding to the effects of the toxins (88, 101).

After this initial innate immune response, an adaptive immune response is initiated, resulting in the production of antibodies (101). About 60% of healthy adults in the U.S. have detectable anti-*C. difficile* antibodies (102, 103). At the time of colonization, individuals with higher anti-toxin A IgG levels are less likely to develop symptoms than individuals with lower anti-toxin A IgG levels, suggesting the importance of these antibodies in preventing the development of disease (104). Similarly, higher levels of anti-*C. difficile* IgM and IgG levels during disease correlate with a decreased likelihood of recurrence, indicating that these antibodies are important for final eradication of the pathogen (105, 106). Attempts to create a vaccine that can stimulate production of these protective antibodies is currently an area of active research in the field (107-109).

III. Lysozyme

a. Source and mechanism of action

Lysozyme is a CAMP produced by a variety of cell types in the human body and in other animals (110). In macrophages and neutrophils, lysozyme is stored in granules until released (71, 111). Lysozyme represents 2.5% of the total protein produced by macrophages (112). Within the upper gastrointestinal tract, it is produced and released constitutively by cells in the stomach and Paneth cells in the small intestine (71, 110). Lysozyme can typically be found at concentrations of about 4 mg/L in the feces of

healthy individuals (113). Mucosal secretions may contain lysozyme concentrations of up to 5 mg/ml, and this level can fluctuate based on inflammatory conditions (114, 115).

Lysozyme acts as an antimicrobial primarily by cleaving the peptidoglycan that composes bacterial cell walls. Lysozyme specifically cleaves between the *N*-acetylmuramic acid (MurNAC) and *N*-acetylglucosamine (GlcNAc) components of peptidoglycan (116, 117). Cleavage of the peptidoglycan layer subsequently results in death of bacterial cells due to osmotic stress (65). Some evidence suggests that lysozyme may also have antimicrobial effects in addition to its catalytic cleavage of peptidoglycan. Lysozyme with mutations in its active site retains the ability to disrupt bacterial membranes, suggesting that the cationic charge associated with lysozyme may also contribute to its antimicrobial effects (118).

b. Bacterial resistance mechanisms to lysozyme

Given the long co-evolution of bacteria with lysozyme, bacteria have evolved a variety of mechanisms to resist the effects of lysozyme (119). In general, Gram-negative bacteria are much less susceptible to lysozyme than Gram-positive bacteria, because the Gram-negative peptidoglycan is thinner and is protected by an outer membrane (65). In contrast, Gram-positive bacteria have evolved a number of specific resistance mechanisms, which can be grouped into two main types: modifications of peptidoglycan and other surface modifications (119).

A variety of modifications to peptidoglycan can confer lysozyme resistance. Several species including *Staphylococcus aureus, Enterococcus faecalis,* and *Bacillus subtilis* add an acetyl group to MurNAc using the O-acetyltransferase, OatA (120-122). In both *B. subtilis* and *E. faecalis*, *oatA* expression is regulated by the extracytoplasmic

function sigma factor, σ^V, which is induced in lysozyme (121, 122). Similarly, *Lactobacillus plantarum* can acetylate GlcNAc (123). Conversely, deacetylating either MurNAc (as in *B. subtilis*) or GlcNAc (as in *Bacillus cereus, Bacillus anthracis,* or several streptococci) can also provide resistance (124-126). All of these modifications are thought to confer resistance by altering binding for the active site of lysozyme (119).

Bacteria may also alter other surface components to prevent the action of lysozyme. For example, in *B. subtilis* the *dlt* operon D-alanylates teichoic acids, which adds a positive charge to teichoic acids, thereby helping to repulse cationic lysozyme (122, 127). Like *oatA*, the *dlt* operon is regulated by σ^V in response to lysozyme (122). In other species, such as *S. aureus*, the presence of wall teichoic acids is important for lysozyme resistance, regardless of D-alanylation (128). In the case of *S. aureus*, teichoic acids appear to act as a physical barrier to prevent access of lysozyme to its target in peptidoglycan (128).

c. Role in CDI

Because lysozyme is produced in the gastrointestinal tract and by neutrophils, *C. difficile* is exposed to lysozyme during the natural course of infection (110). Nevertheless, only a few lysozyme resistance mechanisms have been characterized in *C. difficle* to date. It has been shown that σ^V is necessary for lysozyme resistance in *C. difficile* (129). Moreover, lysozyme binds directly to RsiV, the anti-sigma factor that controls σ^V activity (130). One gene in the *sigV* regulon, *pdaV*, deacetylates GlcNAc and confers resistance to lysozyme (129). However the contribution of *pdaV* to lysozyme resistance does not account for the full level of lysozyme resistance in a *sigV* mutant (129). Based on these observations, additional resistance mechanisms under the

regulation of σ^V must exist. We therefore sought additional σ^V-regulated lysozyme resistance mechanisms. Because σ^V regulates the *dlt* operon in *B. subtilis*, we hypothesized that the *dlt* operon in *C. difficile* is regulated by σ^V (131). The results of our experiments addressing this hypothesis are described in Chapter 2.

IV. LL-37

a. Structure, source, and mechanism of action

LL-37 is also known as human cathelicidin, as it is the only CAMP of the cathelicidin class produced in humans (132, 133). Cathelicidins are a family of CAMPs that are well-conserved throughout mammals and which share a number of characteristics (134, 135). The N-terminal portion of these proteins contains the cathelin domain and is evolutionarily the most well-conserved portion of these molecules (135). In contrast, the C-terminal portion of the protein diverges greatly between different organisms (135). The C-terminal portion must be proteolytically cleaved from the cathelin domain before it becomes antimicrobially active (136).

LL-37 begins as an 18 kDa precursor protein (hCAP18), but is ultimately cleaved by extracellular proteases to a 37 amino acid peptide (132, 136). The name LL-37 refers to the length of the peptide and the fact that the N-terminus begins with two consecutive leucines (136). LL-37 contains 11 positively charged amino acids and 5 negatively charged amino acids, for a net charge of +6 at physiological pH. Due to these charges, the linear α-helix of LL-37 is amphipathic with a hydrophobic region surrounded by cationic regions (137). The cationic charge is thought to account for the antimicrobial effects of

this CAMP, because the cationic charge influences binding to LPS, pore formation, and membrane leakage (138, 139).

Distinct from its role as an antimicrobial, LL-37 has a number of immunomodulatory effects. For example, LL-37 is chemotaxic for monocytes, neutrophils, and T-cells and can stimulate the release of several pro-inflammatory cytokines, including IL-1ß and IL-8 (140, 141). LL-37 can also prolong the acute immune response by preventing neutrophil and epithelial cell apoptosis (142, 143). On the other hand, LL-37 can modulate the immune response by binding and neutralizing immune-stimulatory lipopolysaccharide (LPS) from Gram-negative bacteria (144). Additionally, it limits the amount of TNF-α released by LPS-induced macrophages (145). Moreover, LL-37 promotes wound healing by stimulating angiogenesis and migration of keratinocytes (146, 147).

Given its broad role in the immune response, it is not surprising that cathelicidin is produced by a wide range of immune cell types. It is produced by neutrophils, natural killer cells, macrophages, and mast cells (148-150). In each of these cell types, it is stored in granules prior to release upon stimulation (151). In addition, cathelicidin is produced by epithelial cells, including colonic epithelial cells and the mucosa (152). Epithelial expression of catehlicidin is typically constitutive, but can be induced to higher levels by butyrate, vitamin D_3, and several cytokines (151, 153, 154). Expression levels typically decrease with age (155).

b. Bacterial resistance mechanisms

Bacteria have evolved a variety of resistance mechanisms to evade killing by LL-37. Several species, including *Streptococcus pneumoniae* and *Neisseria gonnorhoeae*,

extrude LL-37 via RND efflux pumps (156, 157). Bacteria in the respiratory tract can increase resistance to LL-37 by increasing the amount of phosphorylcholine in LPS (158). Similarly, phosphoethanolamine modifications to Lipid A of LPS confer LL-37 resistance in *Acinetobacter baumanii* and *N. gonorhoeae* (159-161). *Salmonella enterica, Pseudomonas aeruginosa, S. pyogenes,* and *Escherichia coli* secrete proteases that specifically degrade LL-37 (162, 163). Lastly, several bacteria, including *Vibrio cholerae, Shigella,* and *E. coli*, are able to decrease intestinal production of LL-37 during infection (164, 165).

c. Role of LL-37 in CDI

The production of LL-37 by the colonic epithelium and by immune cells makes this CAMP important at the site of CDI (151). In a mouse model of CDI, CRAMP (the mouse homolog of LL-37) expression was found to increase about two-fold during infection (166). Addition of exogenous LL-37 to mice decreases tissue damage and inflammation caused by toxin A (166). Nevertheless, CRAMP deficient mice have a similar level of intestinal inflammation when exposed to toxin A as wild-type mice, suggesting that endogenous levels of CRAMP expression may not be sufficient to limit the damage inflicted by *C. difficile* (166). These findings indicate that LL-37 likely plays a role in CDI.

Given that LL-37 is produced at the site of infection and appears to play a role in CDI, it would be expected that *C. difficile* has evolved mechanisms to withstand the antibacterial effects of LL-37. McQuade et al. investigated LL-37 resistance in a number of *C. difficile* isolates and found that resistance varies across strains, with MICs ranging from 8-48 μg/ml (167). These MIC values are similar to other Gram-positive enteric

pathogens such as *Enterococcus faecalis* (30 μg/ml) (132). The level of LL-37 resistance in *C. difficile* increases after exposure to sub-MIC levels of LL-37 (167). This finding implies that *C. difficile* has inducible mechanisms of resistance to LL-37. But, *C. difficile* resistance mechanisms for LL-37 have not yet been identified.

V. Specific Aims

Because the processes of colonization and resistance of innate host immune factors are early steps in the course of infection, a better understanding of these processes in *C. difficile* could enable the development of preventative and/or early-acting therapeutics. Yet much remains unknown about these processes. In particular, the role of host-produced CAMPs in CDI is a largely unexplored topic. In order to colonize the colon and cause disease, *C. difficile* must resist killing by these molecules. Although deacetylation of peptidoglycan has been shown to confer lysozyme resistance in *C. difficile*, it does not account for the full level of resistance seen in this organism (129). No additional mechanisms of resistance to lysozyme and no mechanisms of resistance to LL-37 have been identified in *C. difficile*. The goal of my dissertation was to identify and characterize specific mechanisms of lysozyme and LL-37 resistance in *C. difficile*. Herein, I investigated *C. difficile* CAMP resistance through the following specific aims:

1. Characterize the role of the Dlt pathway in lysozyme resistance in *C. difficile*.
2. Identify and characterize LL-37 resistance mechanisms in *C. difficile*.

References

1. **Bouza E.** 2012. Consequences of *Clostridium difficile* infection: understanding the healthcare burden. Clin Microbiol Infect **18 Suppl 6:**5-12.
2. **McGlone SM, Bailey RR, Zimmer SM, Popovich MJ, Tian Y, Ufberg P, Muder RR, Lee BY.** 2012. The economic burden of *Clostridium difficile*. Clin Microbiol Infect **18:**282-289.
3. **Lessa FC, Mu Y, Bamberg WM, Beldavs ZG, Dumyati GK, Dunn JR, Farley MM, Holzbauer SM, Meek JI, Phipps EC, Wilson LE, Winston LG, Cohen JA, Limbago BM, Fridkin SK, Gerding DN, McDonald LC.** 2015. Burden of *Clostridium difficile* infection in the United States. N Engl J Med **372:**825-834.
4. **Dubberke ER, Olsen MA.** 2012. Burden of *Clostridium difficile* on the healthcare system. Clin Infect Dis **55 Suppl 2:**S88-92.
5. **Magee G, Strauss ME, Thomas SM, Brown H, Baumer D, Broderick KC.** 2015. Impact of *Clostridium difficile*-associated diarrhea on acute care length of stay, hospital costs, and readmission: a multicenter retrospective study of inpatients, 2009-2011. Am J Infect Control **43:**1148-1153.
6. **Loo VG, Poirier L, Miller MA, Oughton M, Libman MD, Michaud S, Bourgault AM, Nguyen T, Frenette C, Kelly M, Vibien A, Brassard P, Fenn S, Dewar K, Hudson TJ, Horn R, Rene P, Monczak Y, Dascal A.** 2005. A predominantly clonal multi-institutional outbreak of *Clostridium difficile*-associated diarrhea with high morbidity and mortality. N Engl J Med **353:**2442-2449.

7. **McDonald LC, Killgore GE, Thompson A, Owens RC, Jr., Kazakova SV, Sambol SP, Johnson S, Gerding DN.** 2005. An epidemic, toxin gene-variant strain of *Clostridium difficile*. N Engl J Med **353:**2433-2441.

8. **Warny M, Pepin J, Fang A, Killgore G, Thompson A, Brazier J, Frost E, McDonald LC.** 2005. Toxin production by an emerging strain of *Clostridium difficile* associated with outbreaks of severe disease in North America and Europe. Lancet **366:**1079-1084.

9. **Marsh JW, Arora R, Schlackman JL, Shutt KA, Curry SR, Harrison LH.** 2012. Association of relapse of *Clostridium difficile* disease with BI/NAP1/027. J Clin Microbiol **50:**4078-4082.

10. **Pepin J, Valiquette L, Cossette B.** 2005. Mortality attributable to nosocomial *Clostridium difficil*e-associated disease during an epidemic caused by a hypervirulent strain in Quebec. Can Med Assoc J **173:**1037-1042.

11. **Rao K, Micic D, Natarajan M, Winters S, Kiel MJ, Walk ST, Santhosh K, Mogle JA, Galecki AT, LeBar W, Higgins PD, Young VB, Aronoff DM.** 2015. *Clostridium difficile* ribotype 027: relationship to age, detectability of toxins A or B in stool with rapid testing, severe infection, and mortality. Clin Infect Dis **61:**233-241.

12. **Cloud J, Kelly CP.** 2007. Update on *Clostridium difficile* associated disease. Curr Opin Gastroenterol **23:**4-9.

13. **Bignardi GE.** 1998. Risk factors for *Clostridium difficile* infection. J Hosp Infect **40:**1-15.

14. **Tariq R, Khanna S.** 2017. *Clostridium difficile* infection: updates in management. Indian J Gastroenterol **36:**3-10.

15. **Khanafer N, Vanhems P, Barbut F, Luxemburger C, group CDIS.** 2017. Factors associated with *Clostridium difficile* infection: a nested case-control study in a three year prospective cohort. Anaerobe **44:**117-123.

16. **Varughese CA, Vakil NH, Phillips KM.** 2013. Antibiotic-associated diarrhea: a refresher on causes and possible prevention with probiotics--continuing education article. J Pharm Pract **26:**476-482.

17. **Hogenauer C, Hammer HF, Krejs GJ, Reisinger EC.** 1998. Mechanisms and management of antibiotic-associated diarrhea. Clin Infect Dis **27:**702-710.

18. **McFarland LV.** 1998. Epidemiology, risk factors and treatments for antibiotic-associated diarrhea. Dig Dis **16:**292-307.

19. **Slimings C, Riley TV.** 2014. Antibiotics and hospital-acquired *Clostridium difficile* infection: update of systematic review and meta-analysis. J Antimicrob Chemother **69:**881-891.

20. **Baines SD, Saxton K, Freeman J, Wilcox MH.** 2006. Tigecycline does not induce proliferation or cytotoxin production by epidemic *Clostridium difficile* strains in a human gut model. J Antimicrob Chemother **58:**1062-1065.

21. **Vardakas KZ, Konstantelias AA, Loizidis G, Rafailidis PI, Falagas ME.** 2012. Risk factors for development of *Clostridium difficile* infection due to BI/NAP1/027 strain: a meta-analysis. Int J Infect Dis **16:**e768-773.

22. **O'Connor JR, Johnson S, Gerding DN.** 2009. *Clostridium difficile* infection caused by the epidemic BI/NAP1/027 strain. Gastroenterology **136:**1913-1924.

23. **Hensgens MP, Goorhuis A, Dekkers OM, Kuijper EJ.** 2012. Time interval of increased risk for *Clostridium difficile* infection after exposure to antibiotics. J Antimicrob Chemother **67:**742-748.

24. **Pothoulakis C.** 1996. Pathogenesis of *Clostridium difficile*-associated diarrhoea. Eur J Gastroenterol Hepatol **8:**1041-1047.

25. **Keeney KM, Yurist-Doutsch S, Arrieta MC, Finlay BB.** 2014. Effects of antibiotics on human microbiota and subsequent disease. Annu Rev Microbiol **68:**217-235.

26. **Theriot CM, Koenigsknecht MJ, Carlson PE, Jr., Hatton GE, Nelson AM, Li B, Huffnagle GB, J ZL, Young VB.** 2014. Antibiotic-induced shifts in the mouse gut microbiome and metabolome increase susceptibility to *Clostridium difficile* infection. Nat Commun **5:**3114.

27. **Rolfe RD, Helebian S, Finegold SM.** 1981. Bacterial interference between *Clostridium difficile* and normal fecal flora. J Infect Dis **143:**470-475.

28. **Drissi F, Buffet S, Raoult D, Merhej V.** 2015. Common occurrence of antibacterial agents in human intestinal microbiota. Front Microbiol **6:**441.

29. **Borriello SP.** 1990. The influence of the normal flora on *Clostridium difficile* colonisation of the gut. Ann Med **22:**61-67.

30. **Wilson KH, Perini F.** 1988. Role of competition for nutrients in suppression of *Clostridium difficile* by the colonic microflora. Infect Immun **56:**2610-2614.

31. **Antharam VC, Li EC, Ishmael A, Sharma A, Mai V, Rand KH, Wang GP.** 2013. Intestinal dysbiosis and depletion of butyrogenic bacteria in *Clostridium difficile* infection and nosocomial diarrhea. J Clin Microbiol **51:**2884-2892.

32. **Ferreyra JA, Wu KJ, Hryckowian AJ, Bouley DM, Weimer BC, Sonnenburg JL.** 2014. Gut microbiota-produced succinate promotes *C. difficile* infection after antibiotic treatment or motility disturbance. Cell host & microbe **16:**770-777.

33. **Britton RA, Young VB.** 2012. Interaction between the intestinal microbiota and host in *Clostridium difficile* colonization resistance. Trends Microbiol **20:**313-319.

34. **Theriot CM, Young VB.** 2015. Interactions between the gastrointestinal microbiome and *Clostridium difficile*. Annu Rev Microbiol **69:**445-461.

35. **Pham TA, Lawley TD.** 2014. Emerging insights on intestinal dysbiosis during bacterial infections. Curr Opin Microbiol **17:**67-74.

36. **Ng KM, Ferreyra JA, Higginbottom SK, Lynch JB, Kashyap PC, Gopinath S, Naidu N, Choudhury B, Weimer BC, Monack DM, Sonnenburg JL.** 2013. Microbiota-liberated host sugars facilitate post-antibiotic expansion of enteric pathogens. Nature **502:**96-99.

37. **Buffie CG, Bucci V, Stein RR, McKenney PT, Ling L, Gobourne A, No D, Liu H, Kinnebrew M, Viale A, Littmann E, van den Brink MR, Jenq RR, Taur Y, Sander C, Cross JR, Toussaint NC, Xavier JB, Pamer EG.** 2015. Precision microbiome reconstitution restores bile acid mediated resistance to *Clostridium difficile*. Nature **517:**205-208.

38. **Sistrunk JR, Nickerson KP, Chanin RB, Rasko DA, Faherty CS.** 2016. Survival of the fittest: how bacterial pathogens utilize bile to enhance infection. Clin Microbiol Rev **29:**819-836.

39. **Sorg JA, Sonenshein AL.** 2010. Inhibiting the initiation of *Clostridium difficile* spore germination using analogs of chenodeoxycholic acid, a bile acid. J Bacteriol **192:**4983-4990.

40. **Giel JL, Sorg JA, Sonenshein AL, Zhu J.** 2010. Metabolism of bile salts in mice influences spore germination in *Clostridium difficile*. PLoS One **5:**e8740.

41. **Wilson KH.** 1983. Efficiency of various bile salt preparations for stimulation of *Clostridium difficile* spore germination. J Clin Microbiol **18:**1017-1019.

42. **Paredes-Sabja D, Shen A, Sorg JA.** 2014. *Clostridium difficile* spore biology: sporulation, germination, and spore structural proteins. Trends Microbiol **22:**406-416.

43. **Fawley WN, Underwood S, Freeman J, Baines SD, Saxton K, Stephenson K, Owens RC, Jr., Wilcox MH.** 2007. Efficacy of hospital cleaning agents and germicides against epidemic *Clostridium difficile* strains. Infect Control Hosp Epidemiol **28:**920-925.

44. **Edwards AN, Karim ST, Pascual RA, Jowhar LM, Anderson SE, McBride SM.** 2016. Chemical and stress resistances of *Clostridium difficile* spores and vegetative cells. Front Microbiol **7:**1698.

45. **Ali S, Moore G, Wilson AP.** 2011. Spread and persistence of *Clostridium difficile* spores during and after cleaning with sporicidal disinfectants. J Hosp Infect **79:**97-98.

46. **Vrtis MC.** 2008. *Clostridium difficile*: preventing epidemic outbreaks in home health. Home Healthc Nurse **26:**563-571.

47. **McFarland LV, Mulligan ME, Kwok RY, Stamm WE.** 1989. Nosocomial acquisition of *Clostridium difficile* infection. N Engl J Med **320:**204-210.

48. **Valiquette L, Cossette B, Garant MP, Diab H, Pepin J.** 2007. Impact of a reduction in the use of high-risk antibiotics on the course of an epidemic of *Clostridium difficile*-associated disease caused by the hypervirulent NAP1/027 strain. Clin Infect Dis **45 Suppl 2:**S112-121.

49. **Louh IK, Greendyke WG, Hermann EA, Davidson KW, Falzon L, Vawdrey DK, Shaffer JA, Calfee DP, Furuya EY, Ting HH.** 2017. *Clostridium difficile* infection in acute care hospitals: systematic review and best practices for prevention. Infect Control Hosp Epidemiol **38:**476-482.

50. **Fisher A, Dembry LM.** 2017. Norovirus and *Clostridium difficile* outbreaks: squelching the wildfire. Curr Opin Infect Dis **30:**440-447.

51. **Lessa FC.** 2013. Community-associated *Clostridium difficile* infection: how real is it? Anaerobe **24:**121-123.

52. **Borriello SP.** 1998. Pathogenesis of *Clostridium difficile* infection. J Antimicrob Chemother **41 Suppl C:**13-19.

53. **Kuehne SA, Cartman ST, Heap JT, Kelly ML, Cockayne A, Minton NP.** 2010. The role of toxin A and toxin B in *Clostridium difficile* infection. Nature **467:**711-713.

54. **Mani N, Dupuy B.** 2001. Regulation of toxin synthesis in *Clostridium difficile* by an alternative RNA polymerase sigma factor. Proc Natl Acad Sci U S A **98:**5844-5849.

55. **Dupuy B, Govind R, Antunes A, Matamouros S.** 2008. *Clostridium difficile* toxin synthesis is negatively regulated by TcdC. J Med Microbiol **57:**685-689.

56. **Govind R, Fitzwater L, Nichols R.** 2015. Observations on the role of TcdE isoforms in *Clostridium difficile* toxin secretion. J Bacteriol doi:10.1128/JB.00224-15.

57. **Di Bella S, Ascenzi P, Siarakas S, Petrosillo N, di Masi A.** 2016. *Clostridium difficile* toxins A and B: insights into pathogenic properties and extraintestinal effects. Toxins (Basel) **8:**E134.

58. **Just I, Fritz G, Aktories K, Giry M, Popoff MR, Boquet P, Hegenbarth S, von Eichel-Streiber C.** 1994. *Clostridium difficile* toxin B acts on the GTP-binding protein Rho. J Biol Chem **269:**10706-10712.

59. **von Eichel-Streiber C, Boquet P, Sauerborn M, Thelestam M.** 1996. Large clostridial cytotoxins--a family of glycosyltransferases modifying small GTP-binding proteins. Trends Microbiol **4:**375-382.

60. **Savidge TC, Pan WH, Newman P, O'Brien M, Anton PM, Pothoulakis C.** 2003. *Clostridium difficile* toxin B is an inflammatory enterotoxin in human intestine. Gastroenterology **125:**413-420.

61. **Jafari NV, Kuehne SA, Bryant CE, Elawad M, Wren BW, Minton NP, Allan E, Bajaj-Elliott M.** 2013. *Clostridium difficile* modulates host innate immunity via toxin-independent and dependent mechanism(s). PLoS One **8:**e69846.

62. **Kuehne SA, Collery MM, Kelly ML, Cartman ST, Cockayne A, Minton NP.** 2014. Importance of toxin A, toxin B, and CDT in virulence of an epidemic *Clostridium difficile* strain. J Infect Dis **209:**83-86.

63. **Perelle S, Gibert M, Bourlioux P, Corthier G, Popoff MR.** 1997. Production of a complete binary toxin (actin-specific ADP-ribosyltransferase) by *Clostridium difficile* CD196. Infect Immun **65:**1402-1407.

64. **Schwan C, Stecher B, Tzivelekidis T, van Ham M, Rohde M, Hardt WD, Wehland J, Aktories K.** 2009. *Clostridium difficile* toxin CDT induces formation of microtubule-based protrusions and increases adherence of bacteria. PLoS Pathog **5:**e1000626.

65. **Muller CA, Autenrieth IB, Peschel A.** 2005. Innate defenses of the intestinal epithelial barrier. Cell Mol Life Sci **62:**1297-1307.

66. **Tollin M, Bergman P, Svenberg T, Jornvall H, Gudmundsson GH, Agerberth B.** 2003. Antimicrobial peptides in the first line defence of human colon mucosa. Peptides **24:**523-530.

67. **Dupont A, Heinbockel L, Brandenburg K, Hornef MW.** 2014. Antimicrobial peptides and the enteric mucus layer act in concert to protect the intestinal mucosa. Gut Microbes **5:**761-765.

68. **Eckmann L.** 2005. Defence molecules in intestinal innate immunity against bacterial infections. Curr Opin Gastroen **21:**147-151.

69. **Wah J, Wellek A, Frankenberger M, Unterberger P, Welsch U, Bals R.** 2006. Antimicrobial peptides are present in immune and host defense cells of the human respiratory and gastrointestinal tracts. Cell Tissue Res **324:**449-456.

70. **Caballero S, Pamer EG.** 2015. Microbiota-mediated inflammation and antimicrobial defense in the intestine. Annu Rev Immunol **33:**227-256.

71. **Dommett R, Zilbauer M, George JT, Bajaj-Elliott M.** 2005. Innate immune defence in the human gastrointestinal tract. Mol Immunol **42:**903-912.

72. **Lievin-Le Moal V, Servin AL.** 2006. The front line of enteric host defense against unwelcome intrusion of harmful microorganisms: mucins, antimicrobial peptides, and microbiota. Clin Microbiol Rev **19:**315-337.

73. **Van Klinken BJ, Dekker J, Buller HA, Einerhand AW.** 1995. Mucin gene structure and expression: protection vs. adhesion. Am J Physiol **269:**G613-627.

74. **Berg RD.** 1996. The indigenous gastrointestinal microflora. Trends Microbiol **4:**430-435.

75. **Cunliffe RN, Mahida YR.** 2004. Expression and regulation of antimicrobial peptides in the gastrointestinal tract. J Leukoc Biol **75:**49-58.

76. **Hancock RE, Diamond G.** 2000. The role of cationic antimicrobial peptides in innate host defences. Trends Microbiol **8:**402-410.

77. **Hand TW.** 2016. The role of the microbiota in shaping infectious immunity. Trends Immunol **37:**647-658.

78. **Stecher B, Hardt WD.** 2011. Mechanisms controlling pathogen colonization of the gut. Curr Opin Microbiol **14:**82-91.

79. **Leatham MP, Banerjee S, Autieri SM, Mercado-Lubo R, Conway T, Cohen PS.** 2009. Precolonized human commensal *Escherichia coli* strains serve as a barrier to *E. coli* O157:H7 growth in the streptomycin-treated mouse intestine. Infect Immun **77:**2876-2886.

80. **Nie YF, Hu J, Yan XH.** 2015. Cross-talk between bile acids and intestinal microbiota in host metabolism and health. J Zhejiang Univ Sci B **16:**436-446.

81. **Mahida YR.** 2004. Microbial-gut interactions in health and disease: epithelial cell responses. Best Pract Res Clin Gastroenterol **18:**241-253.

82. **Sartor RB.** 2001. Induction of mucosal immune responses by bacteria and bacterial components. Curr Opin Gastroenterol **17:**555-561.

83. **Perez-Lopez A, Behnsen J, Nuccio SP, Raffatellu M.** 2016. Mucosal immunity to pathogenic intestinal bacteria. Nat Rev Immunol **16:**135-148.

84. **Maaser C, Kagnoff MF.** 2002. Role of the intestinal epithelium in orchestrating innate and adaptive mucosal immunity. Z Gastroenterol **40:**525-529.

85. **Maynard CL, Elson CO, Hatton RD, Weaver CT.** 2012. Reciprocal interactions of the intestinal microbiota and immune system. Nature **489:**231-241.

86. **Ohno H.** 2016. Intestinal M cells. J Biochem **159:**151-160.

87. **Mason KL, Huffnagle GB, Noverr MC, Kao JY.** 2008. Overview of gut immunology. Adv Exp Med Biol **635:**1-14.

88. **Sun X, Hirota SA.** 2015. The roles of host and pathogen factors and the innate immune response in the pathogenesis of *Clostridium difficile* infection. Mol Immunol **63:**193-202.

89. **Jarchum I, Liu M, Lipuma L, Pamer EG.** 2011. Toll-like receptor 5 stimulation protects mice from acute *Clostridium difficile* colitis. Infect Immun **79:**1498-1503.

90. **Jarchum I, Liu M, Shi C, Equinda M, Pamer EG.** 2012. Critical role for MyD88-mediated neutrophil recruitment during Clostridium difficile colitis. Infect Immun **80:**2989-2996.

91. **Hasegawa M, Yamazaki T, Kamada N, Tawaratsumida K, Kim Y-G, Núñez G, Inohara N.** 2011. Nucleotide-binding oligomerization domain 1 mediates recognition of *Clostridium difficile* and induces neutrophil recruitment and protection against the pathogen. The Journal of Immunology **186:**4872-4880.

92. **Ryan A, Lynch M, Smith SM, Amu S, Nel HJ, McCoy CE, Dowling JK, Draper E, O'Reilly V, McCarthy C, O'Brien J, Ni Eidhin D, O'Connell MJ, Keogh B, Morton CO, Rogers TR, Fallon PG, O'Neill LA, Kelleher D, Loscher CE.** 2011. A role for TLR4 in *Clostridium difficile* infection and the recognition of surface layer proteins. PLoS Pathog **7:**e1002076.

93. **Abt MC, Lewis BB, Caballero S, Xiong H, Carter RA, Susac B, Ling L, Leiner I, Pamer EG.** 2015. Innate immune defenses mediated by two ILC subsets are critical for protection against acute *Clostridium difficile* infection. Cell Host Microbe **18:**27-37.

94. **Ausiello CM, Cerquetti M, Fedele G, Spensieri F, Palazzo R, Nasso M, Frezza S, Mastrantonio P.** 2006. Surface layer proteins from *Clostridium difficile* induce inflammatory and regulatory cytokines in human monocytes and dendritic cells. Microbes and Infection **8:**2640-2646.

95. **Yoshino Y, Kitazawa T, Ikeda M, Tatsuno K, Yanagimoto S, Okugawa S, Yotsuyanagi H, Ota Y.** 2013. *Clostridium difficile* flagellin stimulates toll-like receptor 5, and toxin B promotes flagellin-induced chemokine production via TLR5. Life Sci **92:**211-217.

96. **Mahida YR, Makh S, Hyde S, Gray T, Borriello SP.** 1996. Effect of *Clostridium difficil*e toxin A on human intestinal epithelial cells: induction of interleukin 8 production and apoptosis after cell detachment. Gut **38:**337-347.

97. **He D, Sougioultzis S, Hagen S, Liu J, Keates S, Keates AC, Pothoulakis C, LaMont JT.** 2002. *Clostridium difficile* toxin A triggers human colonocyte IL-8 release via mitochondrial oxygen radical generation. Gastroenterology **122:**1048-1057.

98. **Abt MC, McKenney PT, Pamer EG.** 2016. *Clostridium difficile* colitis: pathogenesis and host defence. Nat Rev Microbiol **14:**609-620.

99. **Jefferson KK, Smith MF, Bobak DA.** 1999. Roles of intracellular calcium and NF- κ B in the *Clostridium difficile* toxin A-induced up-regulation and secretion of IL-8 from human monocytes. The Journal of Immunology **163:**5183.

100. **Kelly CP, Becker S, Linevsky JK, Joshi MA, O'Keane JC, Dickey BF, LaMont JT, Pothoulakis C.** 1994. Neutrophil recruitment in *Clostridium difficile* toxin A enteritis in the rabbit. J Clin Invest **93:**1257-1265.

101. **Solomon K.** 2013. The host immune response to *Clostridium difficile* infection. Ther Adv Infect Dis **1:**19-35.

102. **Kelly CP, Pothoulakis C, Orellana J, LaMont JT.** 1992. Human colonic aspirates containing immunoglobulin A antibody to *Clostridium difficile* toxin A inhibit toxin A-receptor binding. Gastroenterology **102:**35-40.

103. **Sanchez-Hurtado K, Corretge M, Mutlu E, McIlhagger R, Starr JM, Poxton IR.** 2008. Systemic antibody response to *Clostridium difficile* in colonized

patients with and without symptoms and matched controls. J Med Microbiol **57:**717-724.

104. **Kyne L, Warny M, Qamar A, Kelly CP.** 2000. Asymptomatic carriage of *Clostridium difficile* and serum levels of IgG antibody against toxin A. N Engl J Med **342:**390-397.

105. **Kyne L, Warny M, Qamar A, Kelly CP.** 2001. Association between antibody response to toxin A and protection against recurrent *Clostridium difficile* diarrhoea. Lancet **357:**189-193.

106. **Katchar K, Taylor CP, Tummala S, Chen X, Sheikh J, Kelly CP.** 2007. Association between IgG2 and IgG3 subclass responses to toxin A and recurrent *Clostridium difficile*-associated disease. Clin Gastroenterol Hepatol **5:**707-713.

107. **Kelly CP, Kyne L.** 2011. The host immune response to *Clostridium difficile*. J Med Microbiol **60:**1070-1079.

108. **Cox AD, St Michael F, Aubry A, Cairns CM, Strong PC, Hayes AC, Logan SM.** 2013. Investigating the candidacy of a lipoteichoic acid-based glycoconjugate as a vaccine to combat *Clostridium difficile* infection. Glycoconj J **30:**843-855.

109. **Ghose C, Eugenis I, Edwards AN, Sun X, McBride SM, Ho DD.** 2015. Immunogenicity and protective efficacy of *Clostridium difficile* spore proteins. Anaerobe **37:**85-95.

110. **Mason DY, Taylor CR.** 1975. The distribution of muramidase (lysozyme) in human tissues. J Clin Pathol **28:**124-132.

111. **West BC, Rosenthal AS, Gelb NA, Kimball HR.** 1974. Separation and characterization of human neutrophil granules. Am J Pathol **77:**41-66.

112. **Gordon S, Todd J, Cohn ZA.** 1974. In vitro synthesis and secretion of lysozyme by mononuclear phagocytes. J Exp Med **139:**1228-1248.

113. **Costongs GM, Hemrika MH, Engels LG, Bos LP, Bas BM, Flendrig JA, Janson PC.** 1987. Faecal lysozyme: determination, reference intervals and some data in gastro-intestinal disease. Clin Chim Acta **167:**125-134.

114. **Klass HJ, Neale G.** 1978. Serum and faecal lysozyme in inflammatory bowel disease. Gut **19:**233-239.

115. **Laaberki MH, Pfeffer J, Clarke AJ, Dworkin J.** 2011. O-Acetylation of peptidoglycan is required for proper cell separation and S-layer anchoring in *Bacillus anthracis*. J Biol Chem **286:**5278-5288.

116. **Berger LR, Weiser RS.** 1957. The beta-glucosaminidase activity of egg-white lysozyme. Biochim Biophys Acta **26:**517-521.

117. **Ganz T.** 2004. Antimicrobial polypeptides. J Leukoc Biol **75:**34-38.

118. **Ibrahim HR, Matsuzaki T, Aoki T.** 2001. Genetic evidence that antibacterial activity of lysozyme is independent of its catalytic function. FEBS Lett **506:**27-32.

119. **Nawrocki KL, Crispell EK, McBride SM.** 2014. Antimicrobial peptide resistance mechanisms of Gram-positive bacteria. Antibiotics **3:**461-492.

120. **Herbert S, Bera A, Nerz C, Kraus D, Peschel A, Goerke C, Meehl M, Cheung A, Gotz F.** 2007. Molecular basis of resistance to muramidase and cationic antimicrobial peptide activity of lysozyme in staphylococci. PLoS Pathog **3:**e102.

121. **Le Jeune A, Torelli R, Sanguinetti M, Giard J-C, Hartke A, Auffray Y, Benachour A.** 2010. The extracytoplasmic function sigma factor SigV plays a key role in the original model of lysozyme resistance and virulence of *Enterococcus faecalis*. PLoS One **5:**e9658.

122. **Guariglia-Oropeza V, Helmann JD.** 2011. *Bacillus subtilis* Sigma(V) confers lysozyme resistance by activation of two cell wall modification pathways, peptidoglycan O-acetylation and D-alanylation of teichoic acids. J Bacteriol **193:**6223-6232.

123. **Bernard E, Rolain T, Courtin P, Guillot A, Langella P, Hols P, Chapot-Chartier M-P.** 2011. Characterization of O-acetylation of N-acetylglucosamine: a novel structural variation of bacterial peptidoglycan. . J Biol Chem **286:**23950-23958.

124. **Vollmer W, Tomasz A.** 2000. The *pgdA* gene encodes for a peptidoglycan N-acetylglucosamine deacetylase in *Streptococcus pneumoniae*. J Biol Chem **275:**20496-20501.

125. **Psylinakis E, Boneca IG, Mavromatis K, Deli A, Hayhurst E, Foster SJ, Varum KM, Bouriotis V.** 2005. Peptidoglycan N-acetylglucosamine deacetylases from *Bacillus cereus*, highly conserved proteins in *Bacillus anthracis*. J Biol Chem **280:**30856-30863.

126. **Kobayashi K, Sudiarta IP, Kodama T, Fukushima T, Ara K, Ozaki K, Sekiguchi J.** 2012. Identification and characterization of a novel polysaccharide deacetylase C (PdaC) from *Bacillus subtilis*. J Biol Chem **287:**9765-9776.

127. **Perego M, Glaser P, Minutello A, Strauch MA, Leopold K, Fischer W.** 1995. Incorporation of D-alanine into lipoteichoic acid and wall teichoic acid in *Bacillus subtilis*: identification of genes and regulation. J Biol Chem **270:**15598-15606.

128. **Bera A, Biswas R, Herbert S, Kulauzovic E, Weidenmaier C, Peschel A, Götz F.** 2007. Influence of wall teichoic acid on lysozyme resistance in *Staphylococcus aureus*. J Bacteriol **189:**280-283.

129. **Ho TD, Williams KB, Chen Y, Helm RF, Popham DL, Ellermeier CD.** 2014. *Clostridium difficile* extracytoplasmic function σ factor σ V regulates lysozyme resistance and is necessary for pathogenesis in the hamster model of infection. Infect Immun **82:**2345-2355.

130. **Hastie JL, Williams KB, Bohr LL, Houtman JC, Gakhar L, Ellermeier CD.** 2016. The Anti-sigma Factor RsiV Is a bacterial receptor for lysozyme: co-crystal structure determination and demonstration that binding of lysozyme to RsiV is required for σ V activation. PLoS Genet **12:**e1006287.

131. **Ho TD, Hastie JL, Intile PJ, Ellermeier CD.** 2011. The *Bacillus subtilis* extracytoplasmic function σ factor σ (V) is induced by lysozyme and provides resistance to lysozyme. J Bacteriol **193:**6215-6222.

132. **Dürr UHN, Sudheendra US, Ramamoorthy A.** 2006. LL-37, the only human member of the cathelicidin family of antimicrobial peptides. BBA - Biomembranes **1758:**1408-1425.

133. **Cowland JB, Johnsen AH, Borregaard N.** 1995. hCAP-18, a cathelin/pro-bactenecin-like protein of human neutrophil specific granules. FEBS Lett **368:**173-176.

134. **Scocchi M, Wang S, Zanetti M.** 1997. Structural organization of the bovine cathelicidin gene family and identification of a novel member. FEBS Lett **417:**311-315.

135. **Gennaro R, Zanetti M.** 2000. Structural features and biological activities of the cathelicidin-derived antimicrobial peptides. Peptide Science **55:**31-49.

136. **Gudmundsson GH, Agerberth B, Odeberg J, Bergman T, Olsson B, Salcedo R.** 1996. The human gene *FALL39* and processing of the cathelin precursor to the antibacterial peptide LL-37 in granulocytes. Eur J Biochem **238:**325-332.

137. **Johansson J, Gudmundsson GH, Rottenberg ME, Berndt KD, Agerberth B.** 1998. Conformation-dependent antibacterial activity of the naturally occurring human peptide LL-37. J Biol Chem **273:**3718-3724.

138. **Nagaoka I, Hirota S, Niyonsaba F, Hirata M, Adachi Y, Tamura H, Tanaka S, Heumann D.** 2002. Augmentation of the lipopolysaccharide-neutralizing activities of human cathelicidin CAP18/LL-37-derived antimicrobial peptides by replacement with hydrophobic and cationic amino acid residues. Clin Diagn Lab Immunol **9:**972-982.

139. **Wang G, Epand RF, Mishra B, Lushnikova T, Thomas VC, Bayles KW, Epand RM.** 2012. Decoding the functional roles of cationic side chains of the major antimicrobial region of human cathelicidin LL-37. Antimicrob Agents Chemother **56:**845-856.

140. **Chertov O, Michiel DF, Xu L, Wang JM, Tani K, Murphy WJ, Longo DL, Taub DD, Oppenheim JJ.** 1996. Identification of defensin-1, defensin-2, and

CAP37/azurocidin as T-cell chemoattractant proteins released from interleukin-8-stimulated neutrophils. J Biol Chem **271:**2935-2940.

141. **Chertov O, Ueda H, Xu LL, Tani K, Murphy WJ, Wang JM, Howard OM, Sayers TJ, Oppenheim JJ.** 1997. Identification of human neutrophil-derived cathepsin G and azurocidin/CAP37 as chemoattractants for mononuclear cells and neutrophils. J Exp Med **186:**739-747.

142. **Otte JM, Zdebik AE, Brand S, Chromik AM, Strauss S, Schmitz F, Steinstraesser L, Schmidt WE.** 2009. Effects of the cathelicidin LL-37 on intestinal epithelial barrier integrity. Regul Pept **156:**104-117.

143. **Nagaoka I, Tamura H, Hirata M.** 2006. An antimicrobial cathelicidin peptide, human CAP18/LL-37, suppresses neutrophil apoptosis via the activation of formyl-peptide receptor-like 1 and P2X7. J Immunol **176:**3044-3052.

144. **Larrick JW, Hirata M, Balint RF, Lee J, Zhong J, Wright SC.** 1995. Human CAP18: a novel antimicrobial lipopolysaccharide-binding protein. Infect Immun **63:**1291-1297.

145. **Zughaier SM, Shafer WM, Stephens DS.** 2005. Antimicrobial peptides and endotoxin inhibit cytokine and nitric oxide release but amplify respiratory burst response in human and murine macrophages. Cell Microbiol **7:**1251-1262.

146. **Koczulla R, von Degenfeld G, Kupatt C, Krotz F, Zahler S, Gloe T, Issbrucker K, Unterberger P, Zaiou M, Lebherz C, Karl A, Raake P, Pfosser A, Boekstegers P, Welsch U, Hiemstra PS, Vogelmeier C, Gallo RL, Clauss M, Bals R.** 2003. An angiogenic role for the human peptide antibiotic LL-37/hCAP-18. J Clin Invest **111:**1665-1672.

147. **Tokumaru S, Sayama K, Shirakata Y, Komatsuzawa H, Ouhara K, Hanakawa Y, Yahata Y, Dai X, Tohyama M, Nagai H, Yang L, Higashiyama S, Yoshimura A, Sugai M, Hashimoto K.** 2005. Induction of keratinocyte migration via transactivation of the epidermal growth factor receptor by the antimicrobial peptide LL-37. J Immunol **175:**4662-4668.

148. **Di Nardo A, Vitiello A, Gallo RL.** 2003. Cutting edge: mast cell antimicrobial activity is mediated by expression of cathelicidin antimicrobial peptide. J Immunol **170:**2274-2278.

149. **Sorensen O, Arnljots K, Cowland JB, Bainton DF, Borregaard N.** 1997. The human antibacterial cathelicidin, hCAP-18, is synthesized in myelocytes and metamyelocytes and localized to specific granules in neutrophils. Blood **90:**2796-2803.

150. **Buchau AS, Morizane S, Trowbridge J, Schauber J, Kotol P, Bui JD, Gallo RL.** 2010. The host defense peptide cathelicidin is required for NK cell-mediated suppression of tumor growth. J Immunol **184:**369-378.

151. **Vandamme D, Landuyt B, Luyten W, Schoofs L.** 2012. A comprehensive summary of LL-37, the factotum human cathelicidin peptide. Cell Immunol **280:**22-35.

152. **Hase K, Eckmann L, Leopard JD, Varki N, Kagnoff MF.** 2002. Cell differentiation is a key determinant of cathelicidin LL-37/human cationic antimicrobial protein 18 expression by human colon epithelium. Infect Immun **70:**953-963.

153. **Kida Y, Shimizu T, Kuwano K.** 2006. Sodium butyrate up-regulates cathelicidin gene expression via activator protein-1 and histone acetylation at the promoter region in a human lung epithelial cell line, EBC-1. Mol Immunol **43:**1972-1981.

154. **Gombart AF.** 2009. The vitamin D-antimicrobial peptide pathway and its role in protection against infection. Future Microbiol **4:**1151-1165.

155. **Alvarez-Rodriguez L, Lopez-Hoyos M, Garcia-Unzueta M, Amado JA, Cacho PM, Martinez-Taboada VM.** 2012. Age and low levels of circulating vitamin D are associated with impaired innate immune function. J Leukoc Biol **91:**829-838.

156. **Shafer WM, Qu X, Waring AJ, Lehrer RI.** 1998. Modulation of *Neisseria gonorrhoeae* susceptibility to vertebrate antibacterial peptides due to a member of the resistance/nodulation/division efflux pump family. Proc Natl Acad Sci USA **95:**1829-1833.

157. **Zahner D, Zhou X, Chancey ST, Pohl J, Shafer WM, Stephens DS.** 2010. Human antimicrobial peptide LL-37 induces MefE/Mel-mediated macrolide resistance in *Streptococcus pneumoniae*. Antimicrob Agents Chemother **54:**3516-3519.

158. **Lysenko ES, Gould J, Bals R, Wilson JM, Weiser JN.** 2000. Bacterial phosphorylcholine decreases susceptibility to the antimicrobial peptide LL-37/hCAP18 expressed in the upper respiratory tract. Infect Immun **68:**1664-1671.

159. **Napier BA, Burd EM, Satola SW, Cagle SM, Ray SM, McGann P, Pohl J, Lesho EP, Weiss DS.** 2013. Clinical use of colistin induces cross-resistance to host antimicrobials in *Acinetobacter baumannii*. MBio **4:**e00021-00013.

160. **Hobbs MM, Anderson JE, Balthazar JT, Kandler JL, Carlson RW, Ganguly J, Begum AA, Duncan JA, Lin JT, Sparling PF, Jerse AE, Shafer WM.** 2013. Lipid A's Structure Mediates Neisseria gonorrhoeae Fitness during Experimental Infection of Mice and Men. mBio **4:**e00892-00813.

161. **Kandler JL, Joseph SJ, Balthazar JT, Dhulipala V, Read TD, Jerse AE, Shafer WM.** 2014. Phase-Variable Expression of lptA Modulates the Resistance of Neisseria gonorrhoeae to Cationic Antimicrobial Peptides. Antimicrob Agents Chemother **58:**4230-4233.

162. **Schmidtchen A, Frick IM, Andersson E, Tapper H, Bjorck L.** 2002. Proteinases of common pathogenic bacteria degrade and inactivate the antibacterial peptide LL-37. Mol Microbiol **46:**157-168.

163. **Guina T, Yi EC, Wang H, Hackett M, Miller SI.** 2000. A PhoP-regulated outer membrane protease of *Salmonella enterica* serovar Typhimurium promotes resistance to alpha-helical antimicrobial peptides. J Bacteriol **182:**4077-4086.

164. **Islam D, Bandholtz L, Nilsson J, Wigzell H, Christensson B, Agerberth B, Gudmundsson G.** 2001. Downregulation of bactericidal peptides in enteric infections: a novel immune escape mechanism with bacterial DNA as a potential regulator. Nat Med **7:**180-185.

165. **Chakraborty K, Ghosh S, Koley H, Mukhopadhyay AK, Ramamurthy T, Saha DR, Mukhopadhyay D, Roychowdhury S, Hamabata T, Takeda Y, Das S.** 2008. Bacterial exotoxins downregulate cathelicidin (hCAP-18/LL-37) and human beta-defensin 1 (HBD-1) expression in the intestinal epithelial cells. Cell Microbiol **10:**2520-2537.

166. **Hing TC, Ho S, Shih DQ, Ichikawa R, Cheng M, Chen J, Chen X, Law I, Najarian R, Kelly CP, Gallo RL, Targan SR, Pothoulakis C, Koon HW.** 2013. The antimicrobial peptide cathelicidin modulates *Clostridium difficile*-associated colitis and toxin A-mediated enteritis in mice. Gut **62:**1295-1305.

167. **McQuade R, Roxas B, Viswanathan VK, Vedantam G.** 2012. *Clostridium difficile* clinical isolates exhibit variable susceptibility and proteome alterations upon exposure to mammalian cationic antimicrobial peptides. Anaerobe **18:**614-620.

Chapter 2: The *Clostridium difficile* Dlt Pathway Is Controlled by the Extracytoplasmic Function Sigma Factor σ^V in Response to Lysozyme

Emily C. Woods[1], Kathryn L. Nawrocki[1], Jose M. Suárez[1], Shonna M. McBride[1]

[1]Department of Microbiology and Immunology, Emory Antibiotic Resistance Center, Emory University School of Medicine, Atlanta, Georgia, USA

Published in

Infection and Immunity

June 2016 Volume 84 Issue 6

E.C.W. performed experiments and contributed to the writing and editing of the manuscript.

K.L.N. assisted with the animal experiments.

J.M.S. generated the *dlt* mutant.

S.M.M. performed experiments and contributed to the writing and editing of the manuscript.

ABSTRACT

Clostridium difficile (also known as *Peptoclostridium difficile*) is a major nosocomial pathogen and a leading cause of antibiotic-associated diarrhea throughout the world. Colonization of the intestinal tract is necessary for *C. difficile* to cause disease. Host-produced antimicrobial proteins (AMPs), such as lysozyme, are present in the intestinal tract and can deter colonization by many bacterial pathogens, yet *C. difficile* is able to survive in the colon in the presence of these AMPs. Our prior studies established that the Dlt pathway, which increases the surface charge of the bacterium by addition of D-alanine to teichoic acids, is important for *C. difficile* resistance to a variety of AMPs. We sought to determine what genetic mechanisms regulate expression of the Dlt pathway. In this study, we show that a *dlt* null mutant is severely attenuated for growth in lysozyme and that expression of the *dltDABC* operon is induced in response to lysozyme. Moreover, we found that a mutant lacking the extracytoplasmic function (ECF) sigma factor, σ^V, does not induce *dlt* expression in response to lysozyme, indicating that σ^V is required for regulation of lysozyme-dependent D-alanylation of the cell wall. Using reporter gene fusions and 5' RACE analysis, we identified promoter elements necessary for lysozyme-dependent and lysozyme-independent *dlt* expression. In addition, we observed that both a *sigV* mutant and a *dlt* mutant are more virulent in a hamster model of infection. These findings demonstrate that cell wall D-alanylation in *C. difficile* is induced by lysozyme in a σ^V-dependent manner and that this pathway impacts virulence *in vivo*.

INTRODUCTION

Clostridium difficile (*Peptoclostridium difficile*) causes nearly half a million infections in the United States each year, representing a significant public health threat (1). In order to cause infection, *C. difficile* must colonize the colon. As an important interface between the host and microbiota, the colon is an environment rich in host innate immune molecules and bacterial-derived antimicrobials made by the indigenous microbiota (2-6). These innate immune molecules and bacterially produced antimicrobials include a variety of cationic antimicrobial peptides (CAMPs), such as lysozyme, LL-37, defensins, and bacteriocins (2, 4, 7-9). Understanding how *C. difficile* is able to resist killing in this antimicrobial-laden environment could better our understanding of the factors that contribute to the progression of *C. difficile* infections.

A common resistance mechanism to CAMPs in many bacteria is the alteration of the cell surface charge (10-12). One mechanism for increasing the surface charge is through the addition of D-alanine (D-ala) to teichoic acids in the cell wall (10, 12, 13). The addition of D-ala is mediated by four proteins, DltA, DltB, DltC, and DltD, encoded by the *dlt* operon (13). The Dlt pathway confers lysozyme resistance to *Bacillus subtilis* and *Enterococcus faecalis* (14, 15). Previously, we demonstrated that the D-alanylation of the cell wall via the Dlt pathway is important for resistance of *C. difficile* to several CAMPs and other antimicrobials, including nisin, gallidermin, polymyxin B, and vancomycin (12).

How the Dlt pathway is regulated in *C. difficile* is unknown. Expression of *dlt* increases in *C. difficile* in the presence of CAMPs (12), but the mechanisms that control this expression remain unidentified. Although a putative DeoR-family regulator (CD2850) is co-transcribed as part of the *C. difficile dlt* operon, it does not appear to be necessary for *dlt* expression *in vitro* (12). The availability of sugars may play a role in regulating *dlt*

expression in *C. difficile*, as evidenced by a CcpA binding site located within *dltD* and differential expression of the operon in the presence of glucose (16). In *B. subtilis,* the *dlt* operon is regulated by the alternative sigma factor, σ^D, the sporulation regulatory protein, Spo0A, and the extracytoplasmic function (ECF) sigma factors, σ^X and σ^V (15, 17-19). ECF sigma factors are a class of alternative sigma factors broadly involved in functions at the cell surface (20). ECF sigma factors are typically regulated by anti-sigma factors that are located in the cell membrane, which makes ECF sigma factors uniquely suited to regulate genes, such as *dlt*, that are needed to respond to changes in the cell surface (20). *C. difficile* encodes orthologs of Spo0A, σ^V (also known as *csfV* or *sigV*) and σ^D. Moreover, σ^V is necessary for lysozyme resistance in *C. difficile* (21). In fact, the *C. difficile* σ^V anti-sigma factor, RsiV, binds lysozyme and may serve as a direct lysozyme receptor, as it does in *B. subtilis* (22). An ortholog of σ^X has not been identified in any sequenced *C. difficile* isolate, but *C. difficile* strains encode an additional ECF sigma factor, σ^T *(csfT* or *sigT)*. Based on the presence of alternative sigma factors in *C. difficile* that are comparable to those that regulate *dlt* in *B. subtilis*, we hypothesized that σ^V, σ^T, or σ^D may regulate the *dlt* operon of *C. difficile* in response to CAMPs.

To test this hypothesis, we characterized growth, D-alanylation of the cell wall and gene expression profiles of *dlt*, *sigV*, *sigT* and *sigD* null mutants in the presence of the antimicrobials, lysozyme and polymyxin B. In addition, we characterized expression from the *dlt* promoter to determine regions that are responsible for antimicrobial-dependent expression. Our results demonstrate that σ^V is an important regulator of *dlt* expression and that σ^V is necessary for controlling D-alanylation of the *C. difficile* cell wall in response to lysozyme.

MATERIALS AND METHODS

Bacterial strains and growth conditions

The bacterial strains and plasmids used in this study are listed in **Table 1**. *Escherichia coli* strains were grown aerobically in Luria broth (Teknova) at 37˚C (23). Cultures were supplemented with 20 μg chloramphenicol ml^{-1} (Sigma-Aldrich) or 100 μg ampicillin ml^{-1} (Cayman Chemical Company) as needed. *C. difficile* strains were grown in brain heart infusion medium supplemented with 2% yeast extract (BHIS; Becton, Dickinson, and Company) or on BHIS agar plates (24) at 37˚C in an anaerobic chamber (Coy Laboratory Products) as previously described (25-27). BHIS medium was supplemented with 0.6–1.0 mg lysozyme ml^{-1} (Fisher Scientific), 150–200 μg polymyxin B ml^{-1} (Sigma-Aldrich), 2 μg thiamphenicol ml^{-1} (Sigma-Aldrich), 0.5 μg kanamycin ml^{-1} or 0.5 μg nisin ml^{-1} (MP Biomedicals) as needed.

Strain and plasmid construction

The oligonucleotides used in this study are listed in **Table 2**. Primers were designed based on *C. difficile* strain 630 (GenBank accession NC_009089.1), unless otherwise specified. Genomic DNA from strain 630Δ*erm* served as template for PCR amplifications, except where the use of strain R20291 (GenBank accession NC_013316.1) is noted. PCR, cloning, and plasmid DNA isolation were performed according to standard protocols (25). To create null mutations in *C. difficile* strain 630Δ*erm*, the group II intron from pCE240 was re-targeted using the primers listed in **Table 2**, as previously described (28-30). To select for TargeTron insertional disruptions, transconjugants were exposed to 5 μg erythromycin ml^{-1} (Sigma-Aldrich) and 50 μg kanamycin ml^{-1} (Sigma-Aldrich) to select against *E. coli*.

To generate alkaline phosphatase reporter gene promoter fusions, regions of various lengths upstream of *dltD* were PCR-amplified from either *C. difficile* strain 630Δ*erm* or R20291 genomic DNA, as noted for the primers listed in **Table 2**. For site-directed mutagenesis of the promoter region, mutations were generated via Splicing by Overlap Extension (SOEing) PCR using the primers listed in **Table 2**. These products were independently ligated into the *Eco*RI/*Bam*HI sites of pMC358 (31) to generate the plasmids listed in **Table 2**. Plasmids were confirmed by sequencing (Eurofins MWG Operon) and introduced into *E. coli* strain MC101 by transformation. The resulting *E. coli* strains were then conjugated to *C. difficile* strain 630Δ*erm* or MC361, selecting for thiamphenicol resistance, as previously described (12, 32).

To complement the *sigV* mutant, the *sigV* coding sequence was cloned into pMC211 to place expression of *sigV* under the control of the nisin-inducible *cpr* promoter, as previously described (33, 34). The resulting plasmid (pMC360) was conjugated with MC361 as described above. Strains 630Δ*erm* and MC361 containing the empty pMC211 vector served as controls.

Phase contrast microscopy

C. difficile strains were grown in BHIS alone or supplemented with 1 mg lysozyme ml^{-1} as described above. 1 ml of actively growing culture was removed from the anaerobic chamber, centrifuged at full speed for 1 min, and resuspended in 5 μl supernatant. 2 μl of resuspended pellet was placed on top of a thin layer of 0.7% agarose on a microscope slide. For comparison of the 630Δ*erm* and JIR8094 strains, 250 μl of actively growing *C. difficile* cultures in BHIS at an OD_{600} of 0.50 was plated on 70:30 agar (35). After 24 hours, growth was scrapped from these plates, resuspended in BHIS, and 2 μl was placed on top of a thin

layer of 0.7% agarose on a microscope slide. Phase contrast microscopy was performed using an X100 Ph3 oil-immersion objective on a Nikon Eclipse Ci-L microscope.

Quantitative Reverse Transcription PCR analysis (qRT-PCR)

Actively growing *C. difficile* cultures were diluted to an OD_{600} of approximately 0.05 in BHIS alone or with 1.0 mg lysozyme ml^{-1} or 200 μg polymyxin B ml^{-1}. Cultures were grown to an OD_{600} of 0.5, harvested into cold 1:1 ethanol:acetone, and stored at -80˚C. Alternatively, for *in vitro* toxin expression experiments, 250 μl of actively growing *C. difficile* cultures in BHIS at an OD_{600} of 0.50 was plated on 70:30 agar. After 12 hours, growth from these plates was scraped into cold 1.5:1.5:3 ethanol:acetone:water, and stored at -80˚C. In addition, cecal contents from animals infected with *C. difficile* were collected post-mortem into cold 1:1 ethanol:acetone and stored at -80˚C. RNA was purified and treated with DNaseI before cDNA synthesis as previously described (36-38). 50 μg of RNA was used as template for cDNA generation from *in vitro* samples, and 200 μg of RNA was used as template for cDNA generation from cecal samples. The IDT PrimerQuest tool was used to design qRT-PCR primers (http://www.idtdna.com/Scitools/Applications/Primerquest). Each qRT-PCR reaction was performed in technical triplicate for at least three biological replicates. *rpoC* served as an internal control transcript to normalize expression for relative quantification. The means and standard error of the means for the transcriptional ratios of variable and control sets are presented and compared using either a one- or two-way analysis of variance with Dunnett's or Sidak's multiple comparisons tests, as indicated.

Alkaline phosphatase activity assay

C. difficile strains containing the promoter-reporter gene fusions listed in **Table 1** were grown to mid-logarthmic phase (OD_{600} ~0.5), 1 ml samples were harvested in duplicate,

and pelleted cells were stored at -20˚C. The samples were analyzed for alkaline phosphatase (AP) activity as previously described (31). Briefly, samples were washed in 0.5 ml wash buffer (10 mM Tris-HCl, pH 8.0, 10 mM $MgSO_4$) and resuspended in 800 μl of assay buffer (1 M Tris-HCl, pH 8.0, 0.1 M $ZnCl_2$). 50 μl 0.1% SDS and 50 μl chloroform were added to the samples, which were then vortexed for 15 sec. Samples were incubated for 5 min at 37˚C then for 5 min on ice. After rewarming to room temperature, 100 μl of 0.4% pNP (p-nitrophenyl phosphate in 1 M Tris-HCl, pH 8.0) was added to samples in 10 sec intervals. Samples were mixed by inversion and incubated at 37˚C until the development of yellow color. To stop the reaction, 100 μl of 1 M KH_2PO_4 was added in 10 sec intervals and the samples were placed on ice. Developed samples were then centrifuged at 4˚C for 5 minutes and the supernatant OD_{550} and OD_{420} values recorded. AP activity was calculated as follows: $((OD_{420} - (1.75*OD_{550}))*1000)/(OD_{600}*Vol*time)$. OD_{600} refers to the absorbance of the culture at 600 nm at the time of sample collection. Vol is the volume of sample analyzed (1 ml). Time is the total reaction time from addition of pNP to the addition of stop buffer. Results are represented as the means of calculated AP activity and standard errors of the means from at least three biological replicates, each performed as technical duplicates. Data were excluded from analysis if technical duplicates varied from each other by greater than 25%. Data were analyzed with a two-way analysis of variance with Dunnett's multiple comparisons tests. Data from site-directed mutagenesis constructs were analyzed using the two-tailed Student's *t* test with correction for multiple comparisons by the Holm-Sidak method.

Quantification of D-alanine ester content in teichoic acids

The amount of D-alanine esters incorporated into teichoic acids of cell walls was quantified as previously described, with minor modifications (12, 39, 40). Cultures were grown anaerobically at 37˚C in BHIS or in BHIS supplemented with 0.6 mg lysozyme ml^{-1} or 150 μg polymyxin B ml^{-1}. 50 ml was harvested by centrifugation at an OD_{600} of 0.5, and cell pellets were stored at -20˚C. Cell pellets were washed three times with 1 ml 0.1 M MES (Sigma Aldrich), pH 6.0 before boiling for 15 min in 0.5 ml 0.2% SDS, 0.1 M MES, pH 6.0 to partially purify cell walls. Pelleted cell walls were then washed four times with 1 ml 0.1 M MES, pH 6.0. The washed and pelleted cell walls were dried on a tabletop vacuum centrifuge heated to 55˚C. Total cell wall contents were determined by weighing the dried pellets. To release D-alanine residues, the pellets were resuspended in 0.5 ml 0.1 M sodium pyrophosphate (Sigma Aldrich), pH 8.3 and incubated at 60˚C for 3 h. The samples were then centrifuged and the supernatant was transferred to a fresh tube for use in the quantification assay, as described previously (12). Results are the means and standard errors of the means from at least three biological replicates, each performed as technical duplicates. Data were analyzed using a two-way analysis of variance with Dunnett's multiple comparisons tests.

5' Rapid Amplification of cDNA Ends (5' RACE)

RNA was purified from cells collected as described above for qRT-PCR. After DNase I treatment, the RNA was used as a template to generate cDNA using the Roche 5'/3' RACE 2nd generation kit, according to the manufacturer's protocol. Primer oMC1023 was used for first-strand synthesis, and oMC1024 and the Roche oligo-T primer were used for the subsequent PCR amplification step. The resulting cDNA products were purified and either

sequenced directly (Eurofins MWG Operon) or cloned into pCR2.1 (Invitrogen TOPO TA cloning kit) before sequencing.

Animal studies

All animal studies were approved in advance by the Emory University Institutional Animal Care and Use Committee (IUCAC). Female Syrian golden hamsters (*Mesocricetus auratus;* Charles River Laboratories) were housed individually in sterile cages in an animal biosafety level 2 facility within the Emory University Division of Animal Resources. Hamsters were provided sterile water and rodent feed pellets *ad libitum*. To induce susceptibility to infection with *C. difficile*, hamsters were orally gavaged once with clindamycin (30 mg/kg body weight) 7 days prior to inoculation with *C. difficile* (41, 42). Hamsters were inoculated by oral gavage with approximately 5000 *C. difficile* spores, which were prepared as described previously (33). After preparation, spores were diluted in PBS with 1% bovine serum albumin to prevent clumping of spores and stored at room temperature in glass vials to prevent adhesion to plastic. Prior to plating, aliquots of spores were heated for 20 minutes at 55˚C. Spores were enumerated by plating these heated aliquots on BHIS + 0.1% taurocholate to induce germination. Spore preparations were heated for 20 minutes at 55˚C prior to inoculating animals. Multiple cohorts of hamsters were tested for each strain of *C. difficile* (630Δ*erm*, MC319, MC361, JIR8094, TCD20, or a one-to-one mixture of 630Δ*erm* and MC319) for a total of at least 12 hamsters per strain. A hamster treated with clindamycin, but not inoculated with *C. difficile*, served as a negative control for each cohort. After inoculation, hamsters were weighed at least once per day and fecal samples were collected daily. Hamsters were monitored for disease symptoms and considered moribund if they either lost ≥ 15% of their highest body weight or developed symptoms of diarrhea,

lethargy, and wet tail. To prevent unnecessary suffering, hamsters meeting either of these criteria were euthanized. Cecal contents were collected at the time of morbidity (post-mortem). Colony forming units (CFU) were enumerated from daily fecal samples and from cecal samples by resuspension in 1x PBS, serial dilution, and plating onto TCCFA agar (43, 44). CFU were enumerated after 48 h incubation on TCCFA. For samples from animals co-infected with 630Δ*erm* and MC319, samples were plated on both TCCFA and TCCFA with 2 μg/ml erythromycin to distinguish between the strains. These CFU counts were then used to calculate the competitive index (CI) for MC319, using the formula CI = number of MC319 CFU/ml over number of 630Δ*erm* CFU/ml (in cecal contents) divided by number of MC319 spores/ml over number of 630Δ*erm* spores/ml (in original inoculum). Differences in CFU counts were analyzed using a one-way analysis of variance with Dunnett's multiple comparisons tests, and differences in survival were analyzed using log-rank regression.

Accession numbers. *C. difficile* strain 630 (GenBank accession NC_009089.1); *C. difficile* strain R20291 (NC_013316.1). The locus tags for individual genes mentioned in the text are listed in **Table 2**.

Statistical analysis. All statistical analysis was performed using GraphPad Prism version 6.00 for Mac OS X, GraphPad Software (La Jolla, CA, USA).

RESULTS

Impact of *sigD, sigT* and *sigV* disruption on CAMP resistance

In order to test our hypothesis that Dlt-mediated CAMP resistance is regulated by alternative sigma factors in *C. difficile*, insertion mutants were generated in *sigV*, *sigD* and *sigT* in strain 630Δ*erm* using group II intron targeting (28, 45). In previous work, we

generated a *C. difficile* mutant with a non-functional *dltDABC* operon (12), but this mutant was derived from the parent strain JIR8094, which is non-motile and has a virulence defect (46). Unlike JIR8094, 630Δ*erm* retains the virulence profile of the clinical parent strain, 630, and is therefore a more clinically relevant strain (47-49) The *dlt* mutation was regenerated in the strain 630Δ*erm* background for these studies. The growth phenotype of these mutants was then assessed in the presence of the antimicrobials, lysozyme and polymyxin B (**Fig. 1**). The strain R20291, a clinical isolate of the epidemic 027 ribotype, was also included in order to assess the antimicrobial sensitivities of this clinically relevant strain. All of the mutants had growth comparable to the parent strain in BHIS; however, the *dlt* and *sigV* mutants both had attenuated growth in BHIS supplemented with 1 mg/ml lysozyme (**Fig. 1A**). The lysozyme-deficient growth phenotype was more pronounced in the *dlt* mutant than in the *sigV* mutant. The R20291 strain, had a slight growth defect in lysozyme when compared to the 630Δ*erm* strain. Growth of the *dlt* mutant was also attenuated in BHIS supplemented with 200 μg/ml polymyxin B (**Fig. 1B**). These findings validate earlier studies that D-alanylation by the Dlt pathway is important for CAMP resistance (12) and suggest that σ^V is a candidate regulator of *dlt* in lysozyme. The attenuated growth of the *sigV* mutant in lysozyme was complemented by expression of *sigV* from a plasmid, similar to previous studies (**Fig. S1**, (21)). The *sigV* mutant did not, however, have a growth defect in polymyxin B (**Fig. 1B**), demonstrating that σ^V is not necessary for *dlt* regulation in polymyxin B. In contrast to the phenotype observed for *sigV*, neither a *sigT* nor a *sigD* mutant were attenuated for growth in lysozyme (**Fig. 1A**). The *sigT* and *sigD* mutants were slightly attenuated for growth in polymyxin B during log phase, but ultimately achieved the same cell density as the parent strain (**Fig. 1B**). These

results indicate that σ^T and σ^D are not critical for regulation of the *dlt* operon in *C. difficile* in response to polymyxin B or lysozyme.

***dlt* and *sigV* expression are induced by CAMPs**

Based on the similar phenotypes of the *dlt* and *sigV* mutants when grown in CAMPs, we further explored σ^V as a potential regulator of the Dlt pathway in response to antimicrobials. We hypothesized that if σ^V regulates *dlt* expression in response to CAMPs, then expression of *sigV* and the *dlt* operon would be simultaneously induced upon exposure to these compounds. Using qRT-PCR, we detected significantly higher *dltD* expression in 630Δ*erm* and R20291 cells grown in 1.0 mg lysozyme ml^{-1} or 200 μg polymyxin B ml^{-1}, compared to cells grown in BHIS alone. (**Fig. 2A**). The increase in *dltD* expression during growth in lysozyme or polymyxin B was more pronounced in the R20291 strain (~15-fold) than in 630Δ*erm* (~8-fold). The expression of *dltD* was greater during growth in lysozyme than in polymyxin B for both R20291 and 630Δ*erm*. But, there was no significant change in *dltD* expression for the *sigV* mutant during growth in lysozyme. This result strongly suggests that σ^V is necessary for increased *dlt* expression in response to lysozyme. Similar to *dltD* regulation, we found that *sigV* expression increases in both R20291 and 630Δ*erm* in response to lysozyme (**Fig. 2A**), with a larger fold-change in R20291 (~80-fold vs. 40-fold, respectively).

In contrast, the *sigV* mutant had a similar change in *dltD* expression during growth in polymyxin B as the parent strain, indicating that a mechanism(s) other than σ^V can regulate *dlt* in response to polymyxin B (**Fig. 2B**). In polymyxin B, *sigV* expression was only marginally higher in the 630Δ*erm* background compared to untreated 630Δ*erm*, suggesting that the adaptive response to polymyxin B is not σ^V-dependent in this strain (**Fig. 2B**). In

contrast, R20291 induced *sigV* and *dlt* transcript more than strain 630Δ*erm* in polymyxin B. These data suggest that R20291 and 630Δ*erm* may have different mechanisms for regulating *dlt* gene expression during growth in polymyxin B, and that σ^V is not a significant regulator of the adaptive response to polymyxin B in the 630Δ*erm* strain. As expected, *sigV* was not expressed in the *sigV* mutant under any condition tested (**Fig. 2**).

***dlt* and *sigV* mutants have altered morphology in lysozyme**

Because *dltD* and *sigV* expression was increased in lysozyme, and growth of these mutants was also affected by lysozyme, we hypothesized that lysozyme has a greater impact on the cell wall of these mutants than on the parent strain. To test this, we used phase contrast microscopy to assess the cellular morphology of the *dlt* and *sigV* mutants during growth in lysozyme (**Fig. 3**). Although the *sigV* and *dlt* mutants have normal morphology in BHIS medium (**Fig. 3A-C**), both mutants displayed altered phenotypes in lysozyme compared to the parent strain, 630Δ*erm*. In both mutant strains, some of the bacteria took on a curved morphology (**Fig 3F and G**). In addition, many of the *dlt* and *sigV* mutant cells lysed during growth in lysozyme, and some of the *dlt* mutant cells appeared elongated. Although more lytic cells were observed in the *sigV* mutant than the *dlt* mutant, the *dlt* mutant grew much more slowly in lysozyme than the *sigV* strain (**Fig. 1A**), suggesting that the *dlt* cells were dying more rapidly. Hence, lysozyme is more effective against *C. difficile* that lack σ^V or cannot incorporate D-alanine into the cell wall.

Similar to the *sigV* and *dlt* mutants, R20291 adopted altered morphologies and phenotypes in lysozyme, including curved cell shapes, elongated cells, and apparent cell lysis (**Fig. 3H**). The more dramatic effect of lysozyme on cell morphology in R20291 compared to

630Δ*erm* parallels the slight growth defect that we observed in R20291 in lysozyme (**Fig. 1A**). These findings indicate that strain R20291 is more affected by lysozyme than 630Δ*erm*.

D-alanylation of the cell wall increases upon exposure to CAMPs

The Dlt pathway is responsible for catalyzing the addition of D-alanine (D-ala) to teichoic acids in the cell wall of *C. difficile* (12, 13). To determine if the observed increases in *dlt* expression affect D-alanylation of the cell wall, we examined the D-ala content of R20291, 630Δ*erm*, and the *sigV* and *dlt* mutants, grown with and without polymyxin B or lysozyme. We calculated the amount of D-ala esters present in purified cell walls of 630Δ*erm*, R20291, the *sigV* mutant, and the *dlt* mutant grown in BHIS alone or in BHIS supplemented with 0.6 mg lysozyme ml^{-1} or 150 μg polymyxin B ml^{-1} as described in Materials and Methods (**Fig. 4**). As previously observed, the *dlt* mutant had undetectable D-ala content in the cell wall (12). As expected from *dlt* expression analyses, the relative D-ala content in 630Δ*erm* and R20291 was higher in cells exposed to lysozyme or polymyxin B than for cells grown in BHIS alone. D-ala content was higher in 630Δ*erm* than in R20291 in BHIS and with added lysozyme, suggesting that these strains inherently differ in their ability to D-alanylate teichoic acids. The D-ala content of the *sigV* mutant in BHIS alone was similar to that of 630Δ*erm*. The *sigV* mutant did not have a significantly altered amount of D-ala when exposed to lysozyme or polymyxin B. These data demonstrate that σ^V is not necessary for basal-level D-alanylation of the cell wall that occurs in the absence of CAMPs, but σ^V is required for increased D-alanylation in the presence of lysozyme.

Identification of *dlt* promoter elements

To evaluate the potential promoter elements necessary for σ^V-dependent and independent transcription of the *dlt* operon, we created a series of transcriptional fusions of

the predicted *dltD* promoter to a *phoZ* (alkaline phosphatase) reporter (31). Segments upstream of the *dltD* translational start site (TSS) were amplified and ligated to the *phoZ* reporter gene within a plasmid vector (**Fig. 5A**). The resultant plasmids were conjugated independently into 630Δ*erm* and the *sigV* mutant. To assess potential promoter functions of this region, the resultant strains were grown with or without lysozyme and assayed for alkaline phosphatase (AP) activity (**Table 3**).

Initially, reporter fusions containing the 600 bp region upstream of the *dltD* start codon from strains 630Δ*erm* or R20291 were assessed for activity in both the 630Δ*erm* and *sigV* mutant strains (Pdlt_{600}*::phoZ* and Pdlt_{600}*::phoZ* (R20291); **Table 3**). As predicted, this region contains the necessary promoter elements to support transcription, as evidenced by AP activity. Despite multiple nucleotide differences between the P*dlt* sequences of the R20291 and 630Δ*erm* strains (**Fig. 5B**), the AP activity generated from the respective promoter fusions (expressed in the 630Δ*erm* background) were comparable, indicating that these sequence changes do not affect promoter activity. Importantly, these fusions demonstrated lysozyme-dependent induction of activity in 630Δ*erm*, but only lower, constitutive-level activity was observed in the *sigV* mutant. These results demonstrate that σ^V is required for lysozyme-dependent expression from the *dlt* promoter.

To determine the minimal sequence required for transcription, we examined activity from increasingly larger portions of sequence, beginning at 25 nt upstream of the *dltD* TSS. Segments from 25-75 nt upstream of the *dltD* TSS (Pdlt_{25}*::phoZ*, Pdlt_{50}*::phoZ,* and Pdlt_{75}*::phoZ* fusions) did not generate significant AP activity in the 630Δ*erm* or *sigV* backgrounds, indicating that the 75 bp upstream region is not sufficient for transcription. The Pdlt_{100}*::phoZ* fusion had modest AP activity, demonstrating that the 100 bp region upstream

of the *dltD* TSS is sufficient for transcription. The AP activity of the Pdlt_{100}::*phoZ* fusion was not inducible in lysozyme, which suggests that this region does not contain sequence elements necessary for lysozyme-dependent induction of transcription. Additionally, there were no differences between AP activity of Pdlt_{100}::*phoZ* in the parent strain or *sigV* mutant. Thus, the sequence between 75-100 bp upstream of the *dltD* start codon contains the minimal promoter elements for constitutive, low-level transcription of the operon, but is not sufficient for σ^V-dependent transcription.

Sequence analyses of the region revealed two direct repeat sequences spanning from nt -73 to -85 and nt -116 to -128, suggesting that these areas could be involved in regulation. We created constructs using additional nucleotides (Pdlt_{112}::*phoZ*, Pdlt_{119}::*phoZ* and Pdlt_{130}::*phoZ*) to investigate the function of this region. Lysozyme-inducible AP activity was observed with all three constructs in the parent strain, with the highest constitutive and lysozyme-induced activity found for the Pdlt_{130}*::phoZ* fusion (**Table 3**). Lower promoter activity was observed with the Pdlt_{112}::*phoZ* and Pdlt_{119}::*phoZ* in the parent and *sigV* strains, suggesting the direct repeat region may be involved in lysozyme-independent (constitutive) expression of *dlt*. AP activity from Pdlt_{112}::*phoZ* and Pdlt_{119}::*phoZ* in the *sigV* mutant was not inducible in lysozyme. Therefore, the segment 112 bp upstream of the *dltD* TSS contains a sequence necessary for lysozyme-dependent and σ^V-dependent induction of transcription (**Fig. 5B**)

In addition to the direct repeat sequences mentioned above, two segments of complementary sequence were identified at nt -131 to -139 and nt -157 to -165. Additional reporter fusion constructs were generated to examine these larger segments of the P*dlt* upstream region for differences in regulation (Pdlt_{140}::*phoZ*, Pdlt_{150}::*phoZ*, Pdlt_{160}::*phoZ* and

P*dlt*$_{170}$::*phoZ*). The constructs containing promoter segments from -130 to -150 nt upstream of the *dltD* TSS in the 630Δ*erm* strain demonstrated similar levels of AP activity to each other. The *sigV* mutant had lower AP activity with all of these constructs when grown in BHIS, than in medium containing lysozyme. Higher AP activity was observed for 630Δ*erm* strains expressing the P*dlt*$_{160}$::*phoZ* or P*dlt*$_{170}$::*phoZ* fusions, than with the shorter promoter segments. In fact, the P*dlt*$_{170}$::*phoZ* reporter fusion had higher AP activity with or without lysozyme than fusions containing more upstream sequence (P*dlt*$_{200}$::*phoZ,* P*dlt*$_{300}$::*phoZ*, or P*dlt*$_{600}$::*phoZ*). These data suggest that the region 170-200 nt upstream of the *dltD* TSS may contain elements that negatively affect σ^V-independent promoter activity; however, the factors that contribute to this regulation are not known.

To further characterize the *dlt* operon promoter elements and identify potential sites of RNA polymerase binding, we performed 5' RACE analysis on mRNA extracted from 630Δ*erm* grown in the presence of 1 mg/ml lysozyme. This analysis revealed transcriptional start sites at 30 bp and 35 bp upstream of the predicted *dltD* translational start (**Fig. 5B**). The location of transcriptional start sites 5 nt apart suggests that two unique, but perhaps overlapping, promoters are involved in *dlt* transcription. However, these transcriptional start sites and the anticipated -10 and -35 sites (**Fig. 5B**) are positioned in a segment that was insufficient for reporter expression (P*dlt*$_{75}$*::phoZ*, **Table 3**). Together, these results suggest that RNA polymerase initiates transcription from promoters within the 75 nt upstream of the *dltD* start codon, but additional upstream sequence is needed to facilitate transcription.

Based on the 5' RACE results, we predicted that σ^A and/or σ^V -10 promoter elements may be located either 49-42 bp or 51-45 bp upstream of the *dltD* TSS (**Fig. 5B**). We therefore performed site-directed mutagenesis on the nucleotides at positions -43, -51, -92, -

93, and -95 bp upstream of the *dltD* TSS. The AP activity from Pdlt_{300}G-95A::*phoZ,* Pdlt_{300}C-93A::*phoZ,* Pdlt_{300}G-92A::*phoZ,* Pdlt_{300}T-51C::*phoZ* were all comparable to the activity observed from the native-sequence Pdlt_{300}::*phoZ* construct in both the parent strain and *sigV* mutant carrying these constructs during growth in BHIS and lysozyme (**Table 4**). Therefore, we conclude that T-51, G-92, C-93, and G-95 are not essential for constitutive or lysozyme-dependent expression of *dlt*. However, the Pdlt_{300}T-43C::*phoZ* fusion had negligible AP activity in the parent strain in either BHIS or lysozyme. Further, the *sigV* mutant containing the Pdlt_{300}T-43C::*phoZ* construct also lacked expression in BHIS and lysozyme. Hence, nucleotide T-43 is critical for both constitutive and σ^V-dependent, lysozyme-induced transcription of *dlt*. These results strongly suggest that σ^A and σ^V-dependent promoters overlap at T-43. Alternatively, it is possible that σ^V-dependent expression in lysozyme is indirect. In that case, overlapping σ^A-dependent promoters would be used for both constitutive and lysozyme-induced expression with lysozyme-induction mediated by a regulatory factor controlled by σ^V.

In order to test whether separate σ^A- and σ^V-dependent promoters overlap at T-43, we performed site-directed mutagenesis at the nucleotides -48 and -38 bp upstream of the *dlt* TSS (**Figure 5B**). If distinct -10 promoter elements overlap at T-43, the -48 and -38 nucleotides would be the initial and final nucleotides of these elements, respectively. The Pdlt_{300}T-48C::*phoZ* fusion had negligible AP activity in both the parent strain and the *sigV* mutant in BHIS or in lysozyme, suggesting that the T-48 is a necessary for both constitutive and lysozyme-dependent transcription (**Table 4**). Compared to the native-sequence Pdlt_{300}::*phoZ* construct, AP activity from Pdlt_{300}A-38C::*phoZ* was lower in the parent strain and the *sigV* mutant in both BHIS and lysozyme. However, the mutation at A-38 did not abolish

the induction of activity in lysozyme in the parent strain, indicating that σ^V-dependent transcription was retained. Therefore, A-38 may be important for basal *dlt* transcription, as well as σ^V-dependent transcription in lysozyme.

σ^V and the Dlt pathway impact *C. difficile* virulence *in vivo*

Because the *sigV* and *dlt* mutants are more sensitive to lysozyme (**Fig. 1A**), we hypothesized that these mutants would be less fit *in vivo*. In a previous study, Ho et al. demonstrated that a *sigV* mutant is significantly attenuated in a hamster model of infection (21). However, that study was performed in the JIR8094 strain, which is attenuated for virulence *in vivo* (46, 50). To determine the relative impacts of the *dlt* and *sigV* mutations on virulence, hamster infections were performed using the *dlt* and *sigV* isogenic mutants derived from the 630Δ*erm* strain.

Seven days after a single dose of clindamycin, hamsters were gavaged with approximately 5000 spores of 630Δ*erm*, *dltD* or *sigV*, as described in the Materials and Methods. Fecal samples were collected daily and cecal samples were collected at the point of morbidity (post-mortem) to enumerate CFU. Hamsters infected with the *sigV* mutant reached morbidity significantly faster than those infected with 630Δ*erm* (46.2 h ± 17.9 h 630Δ*erm* v. 33.2 h ± 6.3 h *sigV*), demonstrating that σ^V affects virulence *in vivo* (**Fig. 6A**). At the point of morbidity, the ceca of hamsters infected with the *sigV* mutant contained significantly more CFU than those infected with 630Δ*erm*, indicating that this mutant has a growth advantage in the host (**Fig. 6B**). Hamsters infected with the *dlt* mutant also reached morbidity significantly earlier than those infected with 630Δ*erm* (46.2 h ± 17.9 h 630Δ*erm* v. 35.8 h ± 5.0 h *dlt*), but hamsters infected with the *dlt* mutant strain had similar CFU counts in cecal samples compared to the parent strain. These data suggest that the lack of D-ala in the cell wall

contributes to increased virulence *in vivo*, but does not provide a growth advantage to the bacterium.

To determine if the increased virulence observed with *dlt* mutant infections could be due to an altered ability of the host to recognize the bacterium (*i.e.*, immune system response to the lipoteichoic acid antigen), we performed competitive infections with 1:1 mixtures of 630Δ*erm* and *dlt* mutant spores. Hamsters co-infected with the mixture of 630Δ*erm* and *dlt* mutant spores reached morbidity earlier than those infected with the 630Δ*erm* alone and at a rate comparable to those infected with the *dlt* mutant alone (35.4 h ± 5.1 h for co-infection v. 46.2 h ± 17.9 h for 630Δ*erm* and 35.8 h ± 5.0 h for *dlt*). The *dlt* mutant therefore remains more virulent than 630Δ*erm*, even when 630Δ*erm* is present. The total number of CFU recovered from the ceca of co-infected hamsters was comparable to the number of CFU recovered from the ceca of hamsters infected with either 630Δ*erm* or the *dlt* mutant alone. Similar numbers of 630Δ*erm* and *dlt* CFU were recovered from the ceca of co-infected hamsters (**Fig. 6B**), and the mean competitive index for the *dlt* mutant was 1.2 (**Fig. 6C**), suggesting that neither strain had a significant competitive advantage *in vivo*.

Because our results for *sigV* mutant infections differed from results previously obtained in the JIR8094 background (21), we performed an additional experiment using JIR8094 and TCD20 strains (kindly provided by C. Ellermeier), to determine the basis for this variability (**Fig. S6**). In our hands, animals infected with JIR8094 strain succumbed to infection 3.7 days later on average than the 630Δ*erm* infected animals, similar to results obtained by other investigators (47, 51). The animals infected with strain TCD20 (JIR8094 *csfV*/*sigV* mutant) presented with symptoms of CDI and became moribund faster than those infected with the JIR8094 parent strain (133.2 ± 75.2 h v. 76.9 ± 12.9 h for TCD20). This is

in contrast to the findings of Ho et al., which observed a much longer time to morbidity with the JIR8094 strain and low morbidity with the JIR8094 *sigV* mutant (TCD20). Thus, both *sigV* mutant strains caused animals to become moribund more quickly than the parental strain-infected animals.

DISCUSSION

Resistance to CAMPs can enable the survival of bacterial pathogens within the host (52, 53). As an intestinal pathogen, *C. difficile* encounters many CAMPs in the gut, including those produced by the host and indigenous microbiota (2, 4, 7-9, 54, 55). One mechanism that enables *C. difficile* to resist killing by CAMPs is the altering of cell surface charge via the Dlt pathway, which adds D-alanines to cell wall teichoic acids (12, 13). In this paper, we demonstrate that expression of the Dlt pathway is regulated by the extracytoplasmic function sigma factor, σ^V. Moreover, we show that regulation of *dlt* by σ^V occurs in response to the host-produced CAMP, lysozyme, and that the incorporation of D-alanine into the cell wall is critical for lysozyme resistance.

The other alternative sigma factors examined, σ^T and σ^D, did not significantly contribute to *dlt* expression under the conditions tested. Similar to previous findings, we observed that *sigT* expression increased about 2-fold in the presence of lysozyme (data not shown, (30)), implying that σ^T could contribute to lysozyme resistance through a mechanism other than Dlt. The *sigT* mutant also demonstrated a modest growth delay in polymyxin B (**Fig. 1**), but σ^T did not appear to influence *dlt* transcription in polymyxin B (**Fig. S3**), suggesting that σ^T contributes to polymyxin B resistance through an alternate mechanism. The *sigV* mutant did not demonstrate a growth defect in polymyxin B (**Fig. 1**) and the *sigV*

mutant induced *dlt* expression in polymyxin B similar to the parent strain (**Fig. 2B**). Thus, polymyxin B induces *dlt* expression through a σ^D-, σ^T- and σ^V-independent mechanism.

Because the ribotype 027 epidemic strains have proven very successful in colonizing and causing disease (56-58), we considered that these strains might have increased resistance to lysozyme. As evidenced by growth assays (**Fig. 1**), the R20291 strain (027 ribotype) was more sensitive to both lysozyme and polymyxin B than the 630Δ*erm* strain (012 ribotype). Examination of *dlt* expression in R20291 showed that this strain induced *dlt* transcription more robustly than 630Δ*erm* in polymyxin B and lysozyme (**Fig. 2**). But, analyses of D-alanine cell wall content revealed that R20291 incorporated less total D-alanine than 630Δ*erm* at baseline and in the tested CAMPs. Moreover, R20291 had greater morphological cell changes in lysozyme than strain 630Δ*erm* (**Fig. 3**). But, the R20291 strain had significantly more D-alanine incorporation when grown in polymyxin B than in BHIS alone, while no significant change in D-alanine content was observed for 630Δ*erm* in polymyxin B (**Fig. 4**). The difference in *dlt* transcription by these strains was not explained by the nucleotide changes in their *dlt* promoter sequences, as demonstrated with reporter fusions to the R20291 and 630Δ*erm* promoters (**Fig. S2**). Based on these results, it is likely that R20291 encodes a regulatory factor that influences *dlt* transcription in response to polymyxin B, which is not present in the 630Δ*erm* strain.

Our results identified the *dlt* operon as part of the σ^V regulon of *C. difficile*. In a previous study, Ho *et al*. identified σ^V as important for lysozyme resistance in *C. difficile* (21), and identified several σ^V-dependent transcripts including a peptidoglycan deacetylase, putative exported proteins, an ABC transporter system and many genes of unknown function, but *dlt* was not detected. σ^V and other ECF sigma factors have been shown to regulate *dlt*

expression in *Bacillus subtilis*. *C. difficile* strain 630 has three identified ECF sigma factors, σ^T, σ^V, and σ^W (30), but σ^W is encoded in only a few strains (59). The R20291 genome encodes multiple sigma factors and putative regulatory proteins that are not present in strain 630. It is possible that in R20291 these regulators, or σ^D, are involved in transcription of *dlt* in response to other CAMPs or host conditions.

Though likely, these results do not definitively prove that σ^V directly regulates *dlt* in response to lysozyme. 5' RACE identified multiple transcriptional start sites, which would be expected if σ^A and σ^V directly mediate RNA polymerase binding from distinct promoters. The transcriptional start sites that we identified are 5 bp apart, which is close enough that two distinct promoters would likely overlap at nt T-43 (**Fig. 5B**). Site-directed mutagenesis of nucleotides within the predicted -10 promoter elements revealed that a single nucleotide changes at -43 or -48 upstream of the *dlt* TSS was sufficient to abolish lysozyme-dependent and independent *dlt* expression (**Table 4**). In addition, mutagenesis of A-38 decreased both lysozyme-dependent and independent *dlt* expression, without abolishing induction of *dlt* expression in lysozyme. These findings imply that the promoter region required for σ^A and σ^V-dependent transcription of *dlt* overlap. Moreover, a reporter fusion containing the putative -10 and -35 elements (Pdlt_{75}*::phoZ*) was not sufficient for activity, and full σ^V-dependent transcription was achieved only when additional upstream sequence was included (Pdlt_{130}*::phoZ*). We hypothesize that the tandem repeats contained within this 130 bp region may be important for binding of additional σ^V-dependent regulatory factors. The region that is necessary for a σ^V-dependent lysozyme response (130-75 bp upstream of the *dltD* TSS) is farther upstream than the predicted locations of the promoters, based on the transcriptional start sites identified (**Fig. 5**). A construct containing only the 130-75 bp region had no AP

activity, with or without added lysozyme (**Table 4**). These results indicate that this region does not contain sufficient elements for transcription initiation. Moreover, AP activity peaked with the Pdlt_{170}*::phoZ* construct, which suggests that the regions of complementarity that we identified within this 170 bp region could be involved in secondary structures that impact transcription. Further studies are needed to identify additional factors that bind this region and influence *dlt* transcription.

Despite the increased sensitivity of the *sigV* and *dlt* mutants to lysozyme *in vitro* (**Fig. 1B**), both of these mutants demonstrated increased virulence *in vivo* (**Fig. 6A**). It is unlikely that this increased virulence is due to increased toxin production, because we observed similar levels of *tcdA* expression in both mutants *in vitro* (**Fig. S4A**). Levels of toxin expression in the cecal contents of infected hamsters at the time of morbidity were also similar between strains, although the cecal contents of hamsters infected with the *sigV* mutant trended towards higher toxin levels (**Fig. S4B**). Given the importance of σ^V and Dlt in lysozyme resistance *in vitro*, one might expect that the lack of cell wall modification in the *dlt* and *sigV* mutants would make the bacteria more susceptible to innate immune clearance. However, the presence of cell wall modifications, while protective against innate immune effectors, are also immunogenic and may increase the host response to the pathogen. Thus, it is possible that the increased virulence of the *dlt* mutant may be due to an altered host immune response to this mutant. D-alanylated lipoteichoic acid (LTA) is an epitope for the host receptor, toll-like receptor 2 (TLR2) (60, 61). In most pathogens investigated, the lack of a functional Dlt pathway results in decreased virulence (14, 62-64). But it is possible that D-alanylation of LTA may be a mechanism by which *C. difficile* can mask the immunogenic portions of LTA and evade an immune response. Such a mechanism would be similar to how

D-alanylation of LTA in *Staphylococcus aureus* masks antigenic portions of peptidoglycan resulting in decreased virulence because the immune system can better respond to antigens that are unmasked in the mutant (65). But in CDI, a more robust immune response leads to greater intestinal injury (55, 66, 67). Because the *dlt* mutant lacks D-alanylated LTA (**Fig. 4**), this mutant may elicit a stronger immune response, which causes more severe disease symptoms than the parent strain. In co-infection experiments, hamsters reached morbidity at a rate comparable to those infected with the *dlt* mutant alone (**Fig. 6A**), which would be expected if an enhanced immune response to the mutant leads to increased virulence. However, the parent strain did not have a colonization advantage during co-infection (**Fig. 6B** and **C**), as might be expected if the *dlt* mutant is more readily recognized by the immune system.

σ^V has been established as an important factor for colonization and virulence in *E. faecalis,* though in *E. faecalis* a *sigV* mutant is less virulent than the parent strain and σ^V does not control *dlt* expression (68). In *C. difficile*, the *sigV* mutant retains a baseline level of D-alanylated LTA (**Fig. 4**), but is unable to induce other σ^V-dependent modifications to the cell surface. The immunogenicity of σ^V-dependent surface modifications is unknown, but our results suggest that σ^V plays a role in host colonization and may affect recognition of the pathogen by the host. Moreover, the increased virulence that we observed for the *sigV* mutant contradicts an earlier finding of attenuated virulence for a *C. difficile sigV* mutant (21). This previous study was performed with a *sigV* mutant in the strain JIR8094 background. JIR8094 colonizes the intestine more slowly than 630Δ*erm,* has lower toxin A and B production (**Fig. S5A**), is non-motile, has lower expression of flagellar genes and is overall less virulent (46-48, 50, 69). The virulence defects of this strain explain the shorter average time to morbidity

with our parent strain compared to that of Ho, *et al*. Moreover, in our hands, this *sigV* mutant (TCD20) was more virulent than the parent strain (**Fig. S6**). Our results with JIR8094 are more similar to previously published experiments with this strain (47) than the results obtained by Ho, *et al*. Possible reasons for the discrepancies observed between our results and those of Ho, *et al*. may be due to differences in the spore preparation, timing of clindamycin administration, variations in hamster genetics or differences in the microbiome of the animals used in these studies.

A number of other questions remain to be answered about the regulation of *dlt* and the role of σ^V in *C. difficile*. Does σ^V directly regulate *dlt* expression? Are the tandem repeats upstream of *dlt* binding sites for a regulatory factor? What factors regulate *dlt* expression in response to other triggers, such as polymyxin B? Despite these remaining questions, our finding that σ^V regulates the Dlt pathway in *C. difficile* in response to lysozyme represents an important insight into the mechanisms that enable *C. difficile* colonization. These results underscore the complex relationship between mechanisms of antimicrobial resistance and the effects of these modifications on virulence. Mutants in more virulent isolates, such as R20291, may allow for further study of these mechanisms in the mouse model of CDI, which would enable more detailed investigation of the immune response to cell wall modifications. Surviving the innate immune response is a critical step in the process of disease progression, and therefore represents a key window of opportunity for therapeutic intervention and prevention of pathogenesis. Identifying ways to increase *C. difficile* susceptibility to innate immune responses may help extend the utility and efficacy of our current antibiotic therapies.

FUNDING INFORMATION

This research was supported by the U.S. National Institutes of Health through research grants DK087763, DK101870, AI109526 and AI116933 to S.M.M., T32 GM008169 to E.C.W., and T32 AI106699 to K.L.N. The content of this manuscript is solely the responsibility of the authors and does not necessarily reflect the official views of the National Institutes of Health.

ACKNOWLEDGEMENTS

We give special thanks thank Rita Tamayo for providing us with the *sigD* mutant (RT1075) and Craig Ellermeier for strains JIR8094 and TCD20. We also give thanks to Bill Shafer, Charles Moran, Joanna Goldberg and members of the McBride lab for helpful suggestions and discussions during the course of this work. We also thank Jeremy Boss for use of the Bio-Rad CFX96 real-time PCR detection system.

Table 1. Bacterial Strains and plasmids

Plasmid or Strain	Relevant genotype or features	Source, construction or reference
Strains		
E. coli		
HB101	F$^-$ *mcrB mrr hsdS20*(r_B^- m_B^-) *recA13 leuB6 ara-14 proA2 lacY1 galK2 xyl-5 mtl-1 rpsL20*	B. Dupuy
MC101	HB101 pRK24	B. Dupuy
MC277	HB101 pRK24 pMC211	(33)
MC314	HB101 pRK24 pMC235	This study
MC355	HB101 pRK24 pMC286	This study
MC373	HB101 pRK24 pMC316	This study
MC445	HB101 pRK24 pMC358	(31)
MC463	HB101 pRK24 pMC364	This study
MC464	HB101 pRK24 pMC362	This study
MC466	HB101 pRK24 pMC373	This study
MC468	HB101 pRK24 pMC375	(31)
MC469	HB101 pRK24 pMC376	This study
MC535	HB101 pRK24 pMC390	This study
MC580	HB101 pRK24 pMC455	This study
MC581	HB101 pRK24 pMC456	This study
MC616	HB101 pRK24 pMC467	This study
MC617	HB101 pRK24 pMC468	This study
MC628	HB101 pRK24 pMC470	This study
MC629	HB101 pRK24 pMC471	This study
MC630	HB101 pRK24 pMC472	This study
MC665	HB101 pRK24 pMC482	This study
MC667	HB101 pRK24 pMC483	This study
MC692	HB101 pRK24 pMC491	This study
MC693	HB101 pRK24 pMC492	This study
MC699	HB101 pRK24 pMC493	This study
MC700	HB101 pRK24 pMC495	This study
MC706	HB101 pRK24 pMC500	This study
MC707	HB101 pRK24 pMC501	This study
C. difficile		
630	Clinical isolate	(70)
630Δ*erm*	Erm^S derivative of strain 630	N. Minton (71)
JIR8094	Erm^S derivative of strain 630	C. Ellermeier (21, 72)
TCD20	JIR8094 *sigV::ermB*	C. Ellermeier (21)
R20291	Clinical isolate	(73)
MC282	630Δ*erm* pMC211	(33)
MC319	630Δ*erm dltD::ermB*	This study
MC361	630Δ*erm sigV::ermB*	This study
MC383	630Δ*erm sigT::ermB*	This study
MC448	630Δ*erm* pMC358	(31)
MC450	MC361 pMC360	This study

MC494	630Δ*erm* pMC364	This study
MC495	630Δ*erm* pMC362	This study
MC497	630Δ*erm* pMC373	This study
MC499	630Δ*erm* pMC375	(31)
MC500	630Δ*erm* pMC376	This study
MC510	MC361 pMC211	This study
MC512	MC361 pMC358	This study
MC513	MC361 pMC364	This study
MC514	MC361 pMC362	This study
MC515	MC361 pMC373	This study
MC519	MC361 pMC375	This study
MC520	MC361 pMC376	This study
MC551	630Δ*erm* pMC390	This study
MC552	MC361 pMC390	This study
RT1075	630Δ*erm sigD::ermB*	R. Tamayo (45)
MC582	630Δ*erm* pMC455	This study
MC583	630Δ*erm* pMC456	This study
MC584	MC361 pMC455	This study
MC585	MC361 pMC456	This study
MC619	630Δ*erm* pMC467	This study
MC620	630Δ*erm* pMC468	This study
MC632	630Δ*erm* pMC470	This study
MC633	630Δ*erm* pMC471	This study
MC634	630Δ*erm* pMC472	This study
MC635	MC361 pMC470	This study
MC636	MC361 pMC471	This study
MC637	MC361 pMC472	This study
MC668	630Δ*erm* pMC482	This study
MC669	MC361 pMC482	This study
MC682	630Δ*erm* pMC483	This study
MC683	MC361 pMC483	This study
MC695	630Δ*erm* pMC491	This study
MC696	630Δ*erm* pMC492	This study
MC697	MC361 pMC491	This study
MC698	MC361 pMC492	This study
MC701	MC361 pMC493	This study
MC702	MC361 pMC495	This study
MC703	630Δ*erm* pMC493	This study
MC704	630Δ*erm* pMC495	This study
MC714	630Δ*erm* pMC500	This study
MC710	630Δ*erm* pMC501	This study
MC711	MC361 pMC500	This study
MC712	MC361 pMC501	This study
MC744	630Δ*erm* pMC523	This study
MC745	MC361 pMC523	This study
MC746	630Δ*erm* pMC524	This study

MC747	MC361 pMC524	This study
Plasmids		
pRK24	Tra$^+$, Mob$^+$; *bla, tet*	(74)
pCR2.1	*bla, kan*	Invitrogen
pUC19	Cloning vector; *bla*	(75)
pCE240	*C. difficile* TargeTron® construct based on pJIR750ai (group II intron, *ermB::*RAM, *ltrA*); *catP*	C. Ellermeier; (30)
pSMB47	Tn*916* integrational vector; CmR, ErmR	(76)
pMC123	*E. coli-C. difficile* shuttle vector; *bla, catP*	(36)
pMC111	pCE240 with *dltD*-targeted intron	(12)
pMC211	pMC123 P*cprA*	(33)
pMC235	pMC123 with *dltD*-targeted intron (at nt 367), *ermB:*RAM *ltrA catP*	This study
pMC276	pCE240 with *sigV*-targeted intron	This study
pMC286	pMC123 with *sigV*-targeted intron (at nt 380), *ermB::*RAM *ltrA catP*	This study
pMC312	pCR2.1 with *sigT*-targeted intron	This study
pMC314	pCE240 with *sigT*-targeted intron	This study
pMC316	pMC123 with *sigT*-targeted intron (at nt 537), *ermB::*RAM *ltrA catP*	This study
pMC358	pMC123 *phoZ*	(31)
pMC360	pMC123 P*cprA::sigV*	This study
pMC362	pMC123 P$dltD_{200}$*::phoZ*	This study
pMC364	pMC123 P$dltD_{100}$*::phoZ*	This study
pMC373	pMC123 P$dltD_{300\ (630\Delta erm)}$*::phoZ*	This study
pMC375	pMC123 P$dltD_{600\ (630\Delta erm)}$*::phoZ*	(31)
pMC376	pMC123 P$dltD_{600\ (R20291)}$*::phoZ*	This study
pMC390	pMC123 P$dltD_{112}$*::phoZ*	This study
pMC455	pMC123 P$dltD_{119}$*::phoZ*	This study
pMC456	pMC123 P$dltD_{170}$*::phoZ*	This study
pMC467	pMC123 P$dltD_{25}$*::phoZ*	This study
pMC468	pMC123 P$dltD_{50}$*::phoZ*	This study
pMC470	pMC123 P$dltD_{140}$*::phoZ*	This study
pMC471	pMC123 P$dltD_{150}$*::phoZ*	This study
pMC472	pMC123 P$dltD_{160}$*::phoZ*	This study
pMC482	pMC123 P$dltD_{130}$*::phoZ*	This study
pMC483	pMC123 P$dltD_{75}$*::phoZ*	This study
pMC491	pMC123 P$dltD_{T43C}$*::phoZ*	This study
pMC492	pMC123 P$dltD_{T51C}$*::phoZ*	This study
pMC493	pMC123 P$dltD_{130\text{-}75}$*::phoZ*	This study
pMC495	pMC123 P$dltD_{G95A}$*::phoZ*	This study
pMC500	pMC123 P$dltD_{C93A}$*::phoZ*	This study
pMC501	pMC123 P$dltD_{G92A}$*::phoZ*	This study
pMC523	pMC123 P$dltD_{A38C}$*::phoZ*	This study
pMC534	pMC123 P$dltD_{T48C}$*::phoZ*	This study

Table 2. Oligonucleotides

Primer	Sequence[a] (5'→3')	Purpose, source or reference
oMC38	5'-AAAGACGGAGTCACAAGTCACC-3'	*dltD* qPCR (CD2154) (12)
oMC39	5'-CTGCTTTATACTCGTCACTTCCC-3'	*dltD* qPCR (CD2154) (12)
oMC44	5'-CTAGCTGCTCCTATGTCTCACATC-3'	*rpoC* qPCR (CD0067) (12)
oMC45	5'-CCAGTCTCTCCTGGATCAACTA-3'	*rpoC* qPCR (CD0067) (12)
oMC74	5'-AAAAGCTTTTGCAACCCACGTCGATCGTGAAAAAGTTG TCTTGGTGCGCCCAGATAGGGTG -3'	*dltD* intron retargeting (12)
oMC75	5'-CAGATTGTACAAATGTGGTGATAACAGATAAGTCGTCTT GTTTAACTTACCTTTCTTTGT -3'	*dltD* intron retargeting (12)
oMC76	5'-CGCAAGTTTCTAATTTCGGTTACTTTTCGATAG AGGAAAGTGTCT -3'	*dltD* intron retargeting (12)
oMC193	5'-TGTATAAGGCACTATACTCAGTGG-3'	*sigV* qPCR (CD1558)
oMC194	5'-ACTCTCCAGTCTCATCTATAAGGTC-3'	*sigV* qPCR (CD1558)
oMC447	5'-GGCGTAGTATTTTTATTTGGGTTAG-3'	*dltD*::Targetron screening
oMC547	5'-TGGATAGGTGGAGAAGTCAGT-3'	*tcdA* qPCR (CD0663) (33)
oMC548	5'-GCTGTAATGCTTCAGTGGTAGA-3'	*tcdA* qPCR (CD0663) (33)
oMC703	5'-AAAAGCTTTTGCAACCCACGTCGATCGTGAA AGAGCTTTGGAAGTGCGCCCAGATAGGGTG-3'	*sigV* (CD1558) intron retargeting
oMC704	5'-CAGATTGTACAAATGTGGTGATAACAGATAAGTC TTGGA AGATAACTTACCTTTCTTTGT-3'	*sigV* (CD1558) intron retargeting
oMC705	5'-CGCAAGTTTCTAATTTCGGTTGCTCTTCGATAGAG GAAA GTGTCT-3'	*sigV* (CD1558) intron retargeting
oMC731	5'- GCTACTTCTTCAATCTTTAAATCTTC-3'	*sigV*::Targetron screening
oMC800	5'-AAAAGCTTTTGCAACCCACGTCGATCGTGAA	*sigT* (CD0677)

	TCTGTTCTGATTGTGCGCCCAGATAGGGTG-3'	intron retargeting
oMC801	5'-CAGATTGTACAAATGTGGTGATAACAGATAAGTCCTGATTCATAACTTACCTTTCTTTGT-3'	*sigT* (CD0677) intron retargeting
oMC802	5'-CGCAAGTTTCTAATTTCGGTTACAGATCGATAGAGGAAAGTGTCT-3'	*sigT* (CD0677) intron retargeting
oMC815	5'-TGGATTCTCTTAAGGAAGAACAATACTTTA-3'	*sigT* qPCR (CD0677)
oMC816	5'- CCTTAACTTCATCTACTGAATAACCTTCA-3'	*sigT* qPCR (CD0677)
oMC817	5'- GCGCTACGATTTGCATAGAAGG-3'	*sigT::*Targetron screening
oMC818	5'-GCTCATATGATTACCTCCGTGTTTTC-3'	*sigT::*Targetron screening
oMC823	5'-GCCGGATCCATTTTCTCTCCTCTAAAAATATTCAAA-3'	P*dlt* cloning (31)
oMC826	5'-GCGGAATTCTGATAGTATATAGTTTATATTAGAAAA TATAAG-3'	Pdlt_{300} cloning (630Δ*erm*-specific)
oMC827	5'-GCGGAATTCGTTAAAATGTCAAATTATAAGTATGAAAAAG-3'	Pdlt_{200} cloning
oMC828	5'-GCGGAATTCGTTTTGACGATTTTATTACAATTTTG-3'	Pdlt_{100} cloning
oMC850	5'-GCGGAATTCTTCTTATATACCATCTGAAATACAGG-3'	Pdlt_{600} cloning (630Δ*erm*-specific) (31)
oMC851	5'-CGCGGATCCGGAGGGAGATTTTACAGGAATG-3'	*sigV* + RBS cloning
oMC852	5'- GCCTGCAGGTCATTCTTTTTATCCCTACTCTTC-3'	*sigV* cloning
oMC853	5'-GCGGAATTCTTCTTATATACCATCTGAAATACAAG-3'	Pdlt_{600} cloning (R20291-specific)
oMC901	5'-CTGAAGCGAAGGCAACTGAA-3'	*phoZ* qPCR (31)
oMC902	5'-GCTTGCTGTCCGACCAAATA-3'	*phoZ* qPCR (31)
oMC977	5'-GCGGAATTCGTATCAAAAAAAGTTTTG-3'	Pdlt_{112} cloning
oMC1023	5'-TTGTTGAATTACTAAGTTCTGATGACCC-3'	P*dlt* 5' RACE (SP1)
oMC1024	5'-TCTCCCTCAAAAGTTCATCAGTTTTAG-3'	P*dlt* 5' RACE (SP2)
oMC1028	5'-GCGGAATTCTGTAACAGTATCAAAAAAAG-3'	Pdlt_{119} cloning
oMC1029	5'-GCGGAATTCGTGCTAAAAAGAAATTTATTTTTG-	Pdlt_{170} cloning

	3’	
oMC1067	5’-AATTCTGAATATTTTTAGAGGAGAGAAAATG-3’	P*dlt*$_{25}$ cloning
oMC1068	5’-GATCCATTTTCTCTCCTCTAAAAATATTCAG-3’	P*dlt*$_{25}$ cloning
oMC1069	5’AATTCAATATGATTAATAATAACATAAATTTGAATATTTTTAGAGGAGAGAAAATg-3’	P*dlt*$_{50}$ cloning
oMC1070	5’GATCCATTTTCTCTCCTCTAAAAATATTCAAATTTATGTTATTATTAATCATATTg-3’	P*dlt*$_{50}$ cloning
oMC1071	5’-GCGGAATTCTTTTCTTTTTTTTTACAA-3’	P*dlt*$_{140}$ cloning
oMC1072	5’-GCGGAATTCTTTGGCGTTTTTTTC-3’	P*dlt*$_{150}$ cloning
oMC1073	5’-GCGGAATTCGAAATTTATTTTTGG-3’	P*dlt*$_{160}$ cloning
oMC1079	5’-GCGGAATTCGTA GTT GAA TAT AC-3’	P*dlt*$_{75}$ cloning
oMC1080	5’-GCGGAATTCTTTTACAATTTTGTAAC-3’	P*dlt*$_{130}$ cloning
oMC1107	5’-GCGGAATTCATTTTCTCTCCTCTCAAAATTGTAATAAA ATCGTC-3’	P*dlt*$_{130\text{-}75}$ cloning
oMC1108	5’-CAAAAAAAGTTTTAACGATTTTATTAC-3’	SDM of P*dlt* (G-95A)
oMC1109	5’-GTAATAAAATCGTTAAAACTTTTTTTG-3’	SDM of P*dlt* (G-95A)
oMC1110	5’-CAAAAAAAGTTTTGAAGATTTTATTAC-3’	SDM of P*dlt* (C-93A)
oMC1112	5’-CAAAAAAAGTTTTGACAATTTTATTAC-3’	SDM of P*dlt* (G-92A)
oMC1114	5’-ACATATCAAAACCAATATGATTAATAATAACA-3’	SDM of P*dlt* (T-51C)
oMC1115	5’-TGTTATTATTAATCATATTGGTTTTGATATGT-3’	SDM of P*dlt* (T-51C)
oMC1116	5’–CAAAACTAATATGACTAATAATAACATAAATTTG-3’	SDM of P*dlt* (T-43C)
oMC1117	5’-CAAATTTATGTTATTATTAGTCATATTAGTTTTG -3’	SDM of P*dlt* (T-43C)
oMC1124	5’-GTAATAAAATCTTCAAAACTTTTTTTG-3’	SDM of P*dlt* (C-93A)
oMC1125	5’-GTAATAAAATTGTCAAAACTTTTTTTG-3’	SDM of P*dlt* (G-92A)
oMC1141	5’-CATATCAAAACTAACATGATTAATAATAAC-3’	SDM of P*dlt* (T-

7		48C)
oMC114	5’-GTTATTATTAATCATGTTAGTTTTGATATG-3’	SDM of P*dlt* (T-
8		48C)
oMC114	5’-CTAATATGATTAATVATAAVATAAATTTG-3’	SDM of P*dlt* (A-
9		38C)
oMC115	5’-CAAATTTATGTTATGATTAATCATATTAG-3’	SDM of P*dlt* (A-
0		38C)

[a]underlined sequences denote restriction sites or intron retarget sites

Table 3. Alkaline phosphatase activity from P*dlt*::*phoZ* fusions

	630Δ*erm*[a]		***sigV*[a]**	
Reporter fusion	BHIS	+Lys[b]	BHIS	+Lys[c]
phoZ	2 ± 0	2 ± 0	2 ± 0	2 ± 0
Pdlt_{75}::*phoZ*	2 ± 0	2 ± 0	2 ± 0	2 ± 0
Pdlt_{100}::*phoZ*	17 ± 4	23 ± 3	23 ± 7	19 ± 1
Pdlt_{112}::*phoZ*	9 ± 1	21 ± 2	8 ± 1	8 ± 2
Pdlt_{119}::*phoZ*	8 ± 1	26 ± 1	7 ± 0	8 ± 1
Pdlt_{130}::*phoZ*	30 ± 1	**124** ± 10	15 ± 3	**36** ± 4
Pdlt_{140}::*phoZ*	29 ± 7	**116** ± 20	22 ± 3	**30** ± 7
Pdlt_{150}::*phoZ*	31 ± 5	**122** ± 17	26 ± 5	**31** ± 5
Pdlt_{160}::*phoZ*	58 ± 15	**174** ± 31	26 ± 2	**36** ± 3
Pdlt_{170}::*phoZ*	79 ± 4	**197** ± 8	69 ± 0	**63** ± 15
Pdlt_{200}::*phoZ*	44 ± 8	**144** ± 18	49 ± 6	**46** ± 1
Pdlt_{300}::*phoZ*	32 ± 2	**135** ± 10	42 ± 7	**38** ± 3
Pdlt_{600}::*phoZ*	59 ± 6	**173** ± 9	49 ± 8	**32** ± 4
Pdlt_{600}::*phoZ* (R20291)	54 ± 8	**146** ± 23	48 ± 3	**42** ± 14

[a]630Δ*erm* and *sigV* (MC361) with *dlt* promoter::*phoZ* fusions plasmids were grown in BHIS alone or with 1 mg/ml lysozyme and assayed for AP activity as described in Methods. Results are the means of calculated AP units ± SEM of at least three biological replicates. All biological replicates were performed as technical duplicates.

[b]Data were analyzed by a two-way analysis of variance with Sidak's multiple comparisons tests, comparing to the same strain and fusion in BHIS. Bold text indicates $p < 0.05$.

[c]Data were analyzed by a two-way analysis of variance and Sidak's multiple comparisons tests, comparing to the same fusion in strain 630Δ*erm* grown in lysozyme. Bold text indicates $p < 0.05$.

Table 4. Alkaline phosphatase activity from P*dlt*::*phoZ* fusions with site-directed mutagenesis

	630Δ*erm*[a, b]		***sigV*** **[a, b]**	
Reporter fusion	BHIS	+Lys	BHIS	+Lys
Pdlt_{300}::*phoZ*	32 ± 2	135 ± 10	42 ± 7	38 ± 3
Pdlt_{300}A-38C::*phoZ*	18 ± 1	102 ± 4	19 ± 3	24 ± 3
Pdlt_{300}T-43C::*phoZ*	**2** ± 0	**2** ± 0	2 ± 0	**3** ± 0
Pdlt_{300}T-48C::*phoZ*	**2** ± 0	**3** ± 0	2 ± 0	**3** ± 0
Pdlt_{300}T-51C::*phoZ*	42 ± 14	145 ± 18	33 ± 5	32 ± 4
Pdlt_{300}G-92A::*phoZ*	31 ± 3	126 ± 4	27 ± 3	43 ± 7
Pdlt_{300}C-93A::*phoZ*	31 ± 5	123 ± 9	48 ± 7	54 ± 7
Pdlt_{300}G-95A::*phoZ*	45 ± 13	149 ± 20	50 ± 7	61 ± 9
Pdlt_{130}::*phoZ*	30 ± 1	124 ± 10	15 ± 3	36 ± 4
P$dlt_{130\text{-}75}$::*phoZ*[c]	**2** ± 0	**2** ± 0	1 ± 0	**2** ± 0

[a]630Δ*erm* and *sigV* (MC361) with *dlt* promoter::*phoZ* fusions plasmids were grown in BHIS alone or with 1 mg/ml lysozyme and assayed for AP activity as described in Methods. Results are the means of calculated AP units ± SEM of at least three biological replicates. All biological replicates were performed as technical duplicates.

[b]The activities from SDM constructs were compared to the native-sequence Pdlt_{300}::*phoZ* in the same conditions by the Student's two-tailed *t*-test with correction for multiple comparisons by the Holm-Sidak method. Bold text indicates $p \leq 0.05$.

[c]AP activity compared to activity from the full-length Pdlt_{130}::*phoZ* construct in the same strain and conditions.

FIGURES

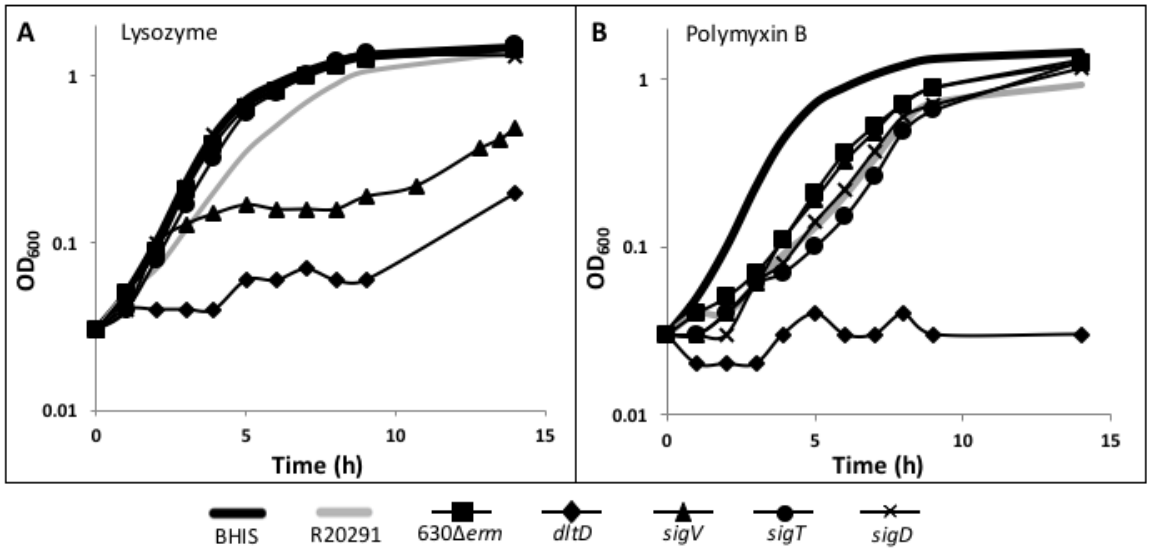

Figure 1. *dlt* and *sigV* mutants have attenuated growth in lysozyme, and a *dlt* mutant has attenuated growth in polymyxin B. Active cultures of strains 630Δ*erm*, R20291, *dltD* (MC319), *sigV* (MC361), *sigT* (MC383), and *sigD* (RT1074) were diluted an to OD_{600} of 0.05 in BHIS supplemented with (**A**) 1 mg/ml lysozyme, or (**B**) 200 μg/ml polymyxin B. All strains grew similarly in BHIS alone, as depicted with the solid black line on each graph. Graphs are representative growth curves from three biological replicates.

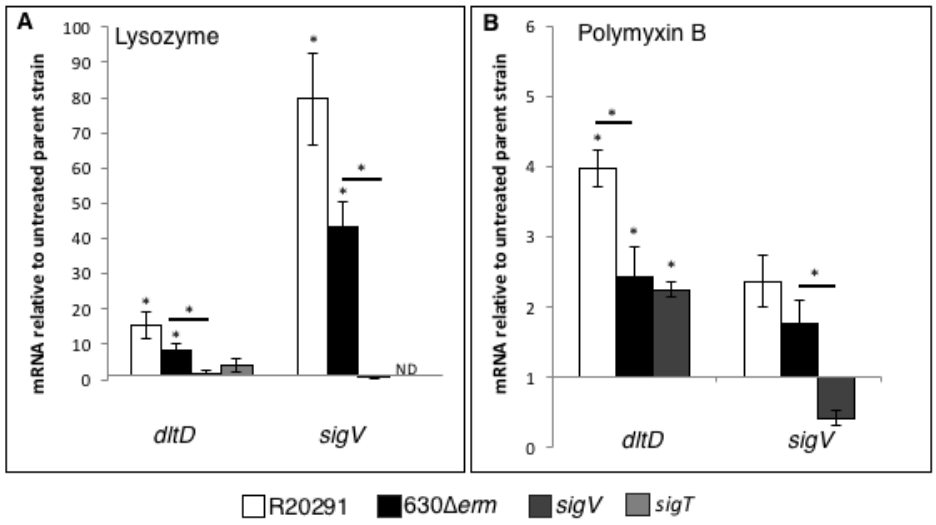

Figure 2. *dltD* and *sigV* expression are induced in lysozyme. qRT-PCR analysis of *dltD* and *sigV* expression in R20291, 630Δ*erm*, *sigV* (MC361*)*, *sigT* (MC383), and *dltD* (MC319) grown in BHIS supplemented with 1 mg/ml lysozyme (**A**) or 200 μg/ml polymyxin B (**B**) as described in Methods. mRNA levels in 630Δ*erm* and the mutant derivatives of this strain (*sigV, sigT, dltD)* are normalized to 630Δ*erm* in BHIS alone. mRNA levels in R20291 are normalized to expression levels in R20291 in BHIS alone. ND indicates not determined. The *sigT* mutant was not assessed in polymyxin B. The means and SEM of three biological replicates are shown. Data were analyzed by a two-way analysis of variance with Sidak's multiple comparison tests. * indicates $p < 0.05$ compared to the untreated parent strain, unless otherwise noted by a bar between the compared strains.

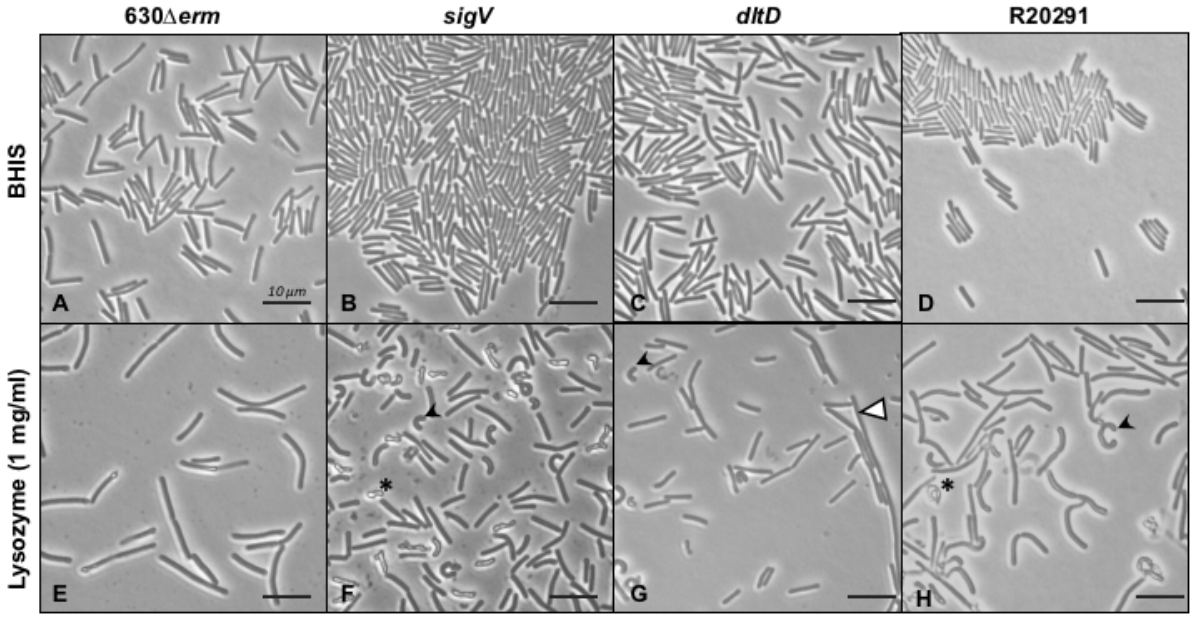

Figure 3. *dlt* and *sigV* mutants have altered cell morphology in lysozyme. Representative phase contrast micrographs of 630Δ*erm*, *sigV* mutant (MC361), *dltD* mutant (MC319), and R20291 were grown in BHIS alone (**A-D**) or BHIS supplemented with 1 mg/ml lysozyme to mid-log phase (**F-H**). Black arrowheads indicate examples of curved morphology, * indicates examples of lysed cells and the white arrowhead indicates an example of an elongated cell.

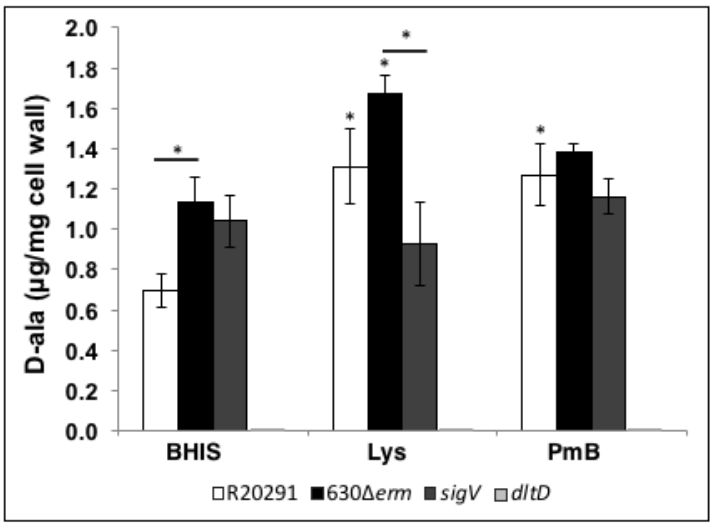

Figure 4. A *sigV* mutant does not increase D-alanine cell wall content in lysozyme. R20291, 630Δ*erm*, *sigV* (MC361), and *dltD* (MC319) were grown in BHIS alone or in BHIS supplemented with either 0.6 mg/ml lysozyme (Lys) or 150 μg/ml polymyxin B (PmB). Results are presented as the means and SEM from at least three biological replicates, each performed as technical duplicates. Data were analyzed by a two-way analysis of variance with Dunnett's multiple comparison tests. *indicates $p < 0.05$ compared to the untreated parent strain, except where indicated by a bar between the compared strains.

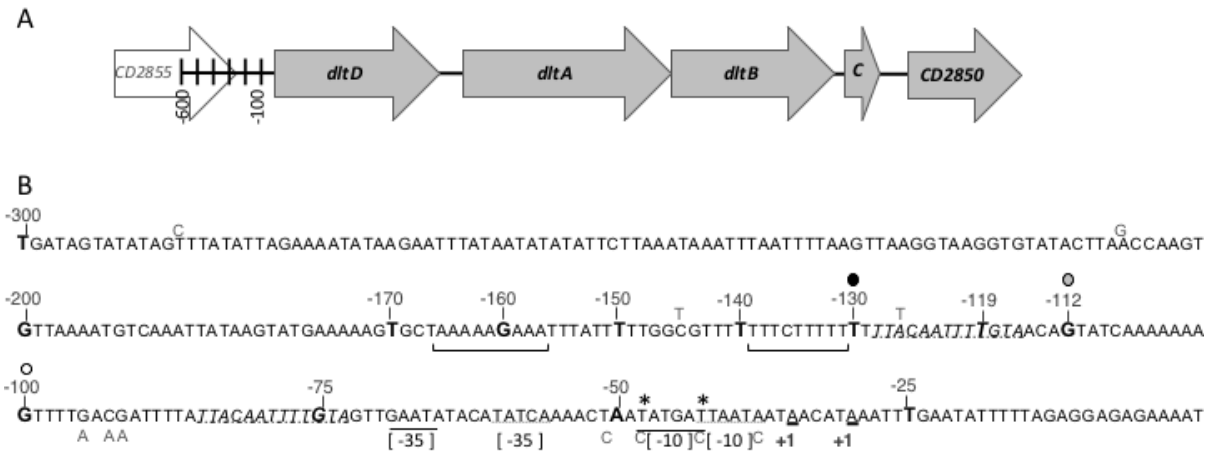

Figure 5. The *dlt* promoter region. (**A**) Schematic of the *dlt* operon and the upstream region used in promoter fusion constructs. The *dlt* operon consists of four genes, *dltDABC*. CD2850 encodes a putative DeoR-type regulator, is co-transcribed with the *dltDABC* operon, and is not required for expression or function of the Dlt pathway (12). CD2855 lies 288 bp upstream of *dltD* and is not part of the operon (12). Promoter fusion constructs were made with segments of the upstream region included. (**B**) DNA sequence from strain 630Δ*erm* from 300 bp upstream of the predicted *dltD* translational start site. Sequence differences in strain R20291 are shown above the sequence. Promoter fusions were created of the indicated sizes marked by bolded nucleotides. The transcriptional start sites identified by 5' RACE analysis are underlined and identified by +1. Identified tandem direct repeat sequences are denoted by italics with black dashed underline. Identified complementary regions are denoted by black brackets above the sequence. Possible spacing for the -10 and -35 of a putative weak σ^A promoter are marked with gray dashed underlines, and possible spacing for the -10 and -35 of a stronger σ^A promoter and overlapping σ^V-dependent promoter are marked with a solid black underline. Base pairs altered by site-directed mutagenesis are indicated below the sequence. * marks the nucleotides that when mutated abolished promoter activity. White

circle denotes minimum required for promoter activity, gray circle denotes region required for lysozyme-dependent activity, and black circle denotes region required for full level of activity.

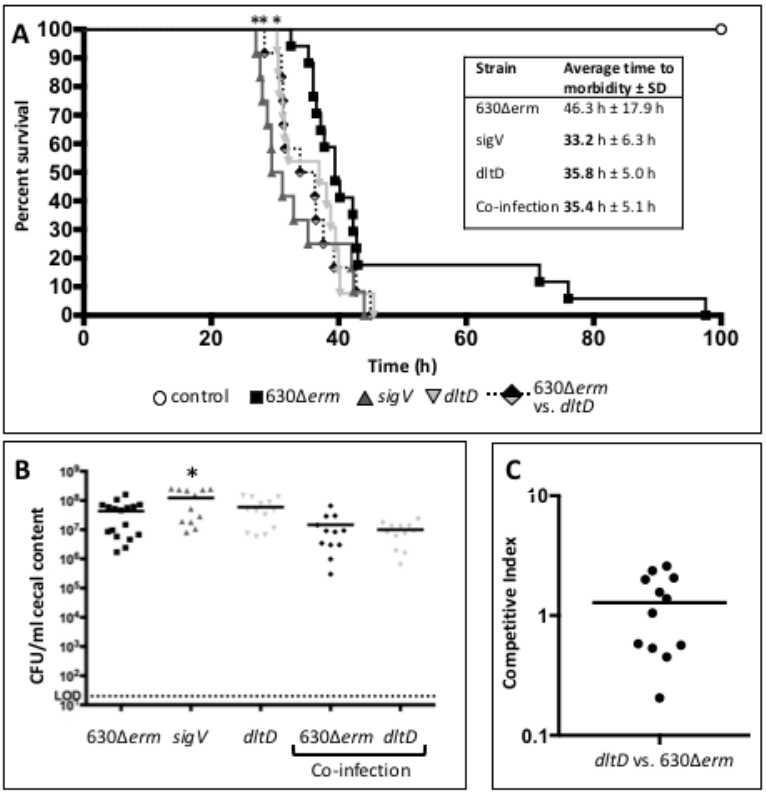

Figure 6. *dlt* and *sigV* mutants are more virulent than the parent strain in a hamster model of infection. Syrian golden hamsters were inoculated with approximately 5000 spores of 630Δ*erm* (n = 17), *dltD* (MC319; n = 13), *sigV* (MC361; n = 12), or a 1:1 mixture of 630Δ*erm* and MC319 (630Δ*erm* vs. *dltD;* n = 12). (**A**) Kaplan-Meier survival curve depicting time to morbidity. * indicates $p \leq 0.05$ by log-rank test. The inset table lists the average time to morbidity for each strain ± SD with bold text indicating $p \leq 0.05$ by log-rank test. (**B**) Total number of *C. difficile* CFU recovered from cecal contents collected post-mortem. Dotted line demarcates limit of detection. Solid black line marks the mean. Numbers of CFU are compared to 630Δ*erm* by a one-way analysis of variance with Dunnett's multiple comparisons tests (* indicates $p < 0.05$). (**C**) Competive index (CI) of the *dlt* mutant for each hamster co-infected with 630Δ*erm* and the *dlt* mutant is shown. CI = 1 indicates no fitness

advantage. CI < 1 indicates reduced fitness of the *dlt* mutant. CI > 1 indicates increased fitness of the *dlt* mutant.

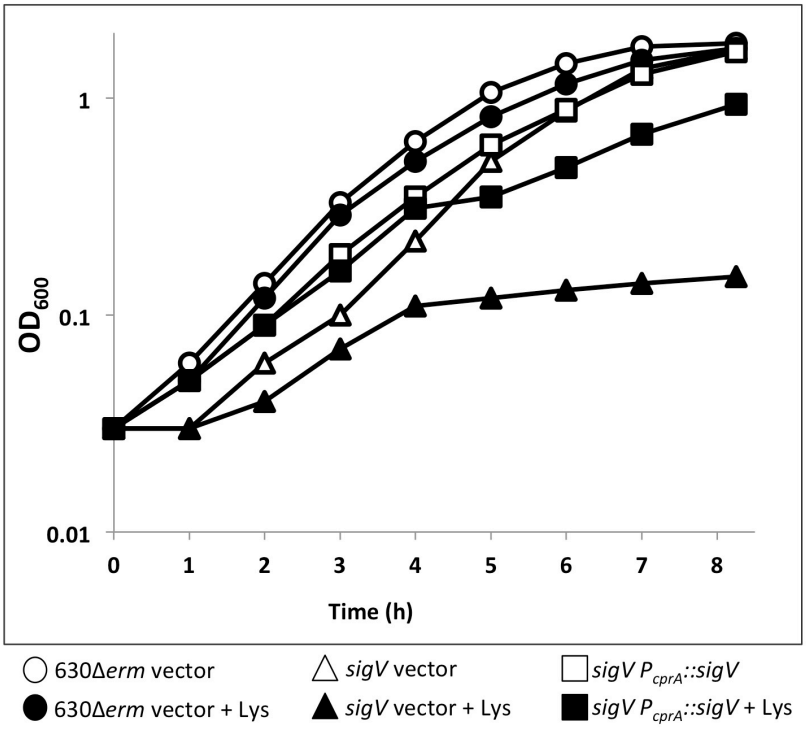

Figure S1. Growth phenotype of the *sigV* mutant can be complemented by σ^V expressed from a plasmid. Active cultures of strains MC282 (630Δ*erm* vector), MC510 (*sigV* vector), and MC450 (*sigV* P_{cprA}::*sigV*) were diluted to an OD_{600} of 0.05 in BHIS with or without 1 mg/ml lysozyme. All cultures were supplemented with 2 μg/ml thiamphenicol to maintain the plasmid and 0.5 μg/ml nisin to induce expression from the *cpr* promoter. Representative growth curve shown from three biological replicates.

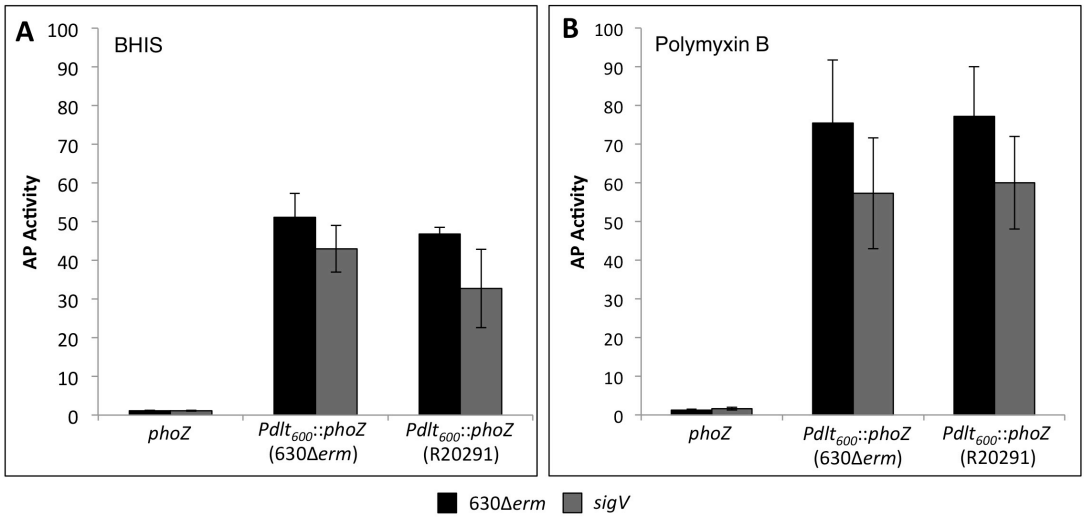

Figure S2. Expression from the *dlt* promoter in polymyxin B is not affected by differences in 630Δ*erm* or R20291 sequences. Strains MC499 (630Δ*erm* Pdlt_{600}::*phoZ* (630Δ*erm*)), MC500 (630Δ*erm* Pdlt_{600}::*phoZ* (R20291)), MC519 (*sigV* Pdlt_{600}::*phoZ* (630Δ*erm*)), and MC520 (*sigV* Pdlt_{600}::*phoZ* (R20291)) were grown in BHIS alone (**A**) or in BHIS supplemented with 200 μg/ml polymyxin B (**B**). Strains MC448 and MC512 containing a plasmid with promoterless *phoZ* (*phoZ*) served as negative controls. Samples were collected during mid-log and assayed for AP activity as described in Methods. Results are the means of calculated AP activity and SEM from three biological replicates, each performed as technical duplicates.

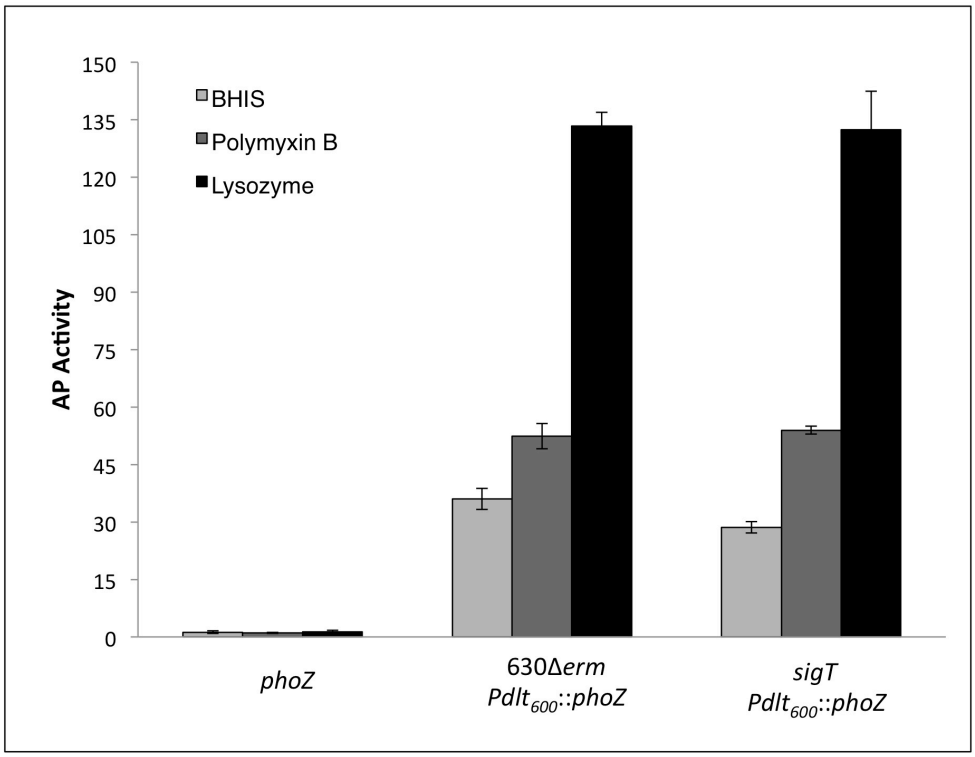

Figure S3. SigT is not required for *dlt* expression in lysozyme or polymyxin B. MC499 (630Δ*erm* Pdlt_{600}::*phoZ*) and MC526 (*sigT* Pdlt_{600}::*phoZ*) were grown in BHIS alone (light gray bars), BHIS supplemented with 200 μg/ml polymyxin B (dark gray bars), or in BHIS supplemented with 1 mg/ml lysozyme (black bars). A plasmid with promoterless *phoZ* (*phoZ*) served as a negative control. Samples were collected during mid-log and assayed for AP activity as described in Methods. Results are the means of calculated AP activity and SEM from three biological replicates, performed as technical duplicates.

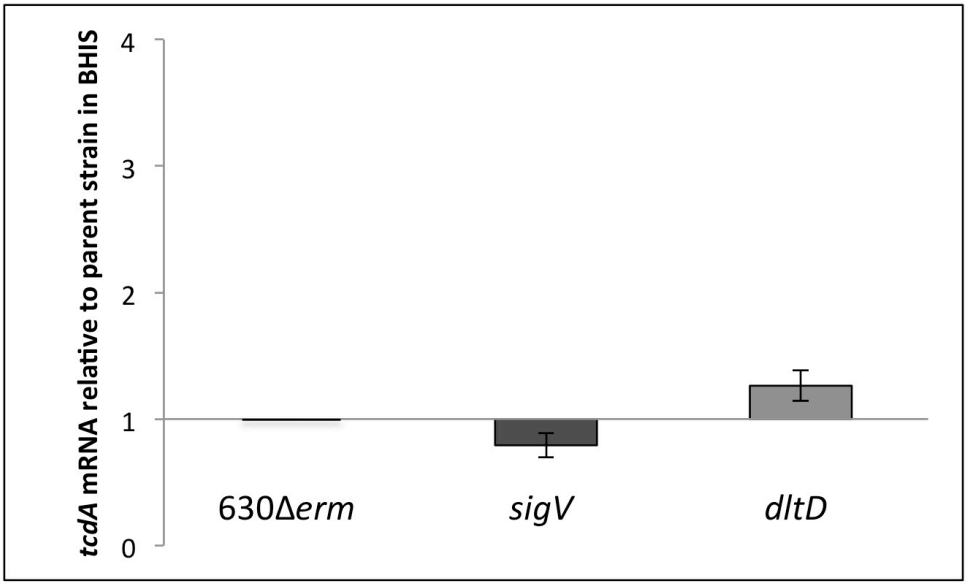

Figure S4. *sigV* and *dlt* mutants have comparable levels of *tcdA* expression as the parent strain. qRT-PCR analysis of *tcdA* expression in 630Δ*erm*, *sigV* (MC361), and *dltD* (MC319) grown in BHIS, as described in the Materials and Methods. mRNA levels are normalized to 630Δ*erm*. The means and standard error of the means of three biological replicates are shown.

References

1. **Lessa FC, Mu Y, Bamberg WM, Beldavs ZG, Dumyati GK, Dunn JR, Farley MM, Holzbauer SM, Meek JI, Phipps EC, Wilson LE, Winston LG, Cohen JA, Limbago BM, Fridkin SK, Gerding DN, McDonald LC.** 2015. Burden of *Clostridium difficile* infection in the United States. N Engl J Med **372:**825-834.
2. **Eckmann L.** 2005. Defence molecules in intestinal innate immunity against bacterial infections. Curr Opin Gastroen **21:**147-151.
3. **Wah J, Wellek A, Frankenberger M, Unterberger P, Welsch U, Bals R.** 2006. Antimicrobial peptides are present in immune and host defense cells of the human respiratory and gastrointestinal tracts. Cell Tissue Res **324:**449-456.
4. **Tollin M, Bergman P, Svenberg T, Jornvall H, Gudmundsson GH, Agerberth B.** 2003. Antimicrobial peptides in the first line defence of human colon mucosa. Peptides **24:**523-530.
5. **Lakshminarayanan B, Guinane CM, O'Connor PM, Coakley M, Hill C, Stanton C, O'Toole PW, Ross RP.** 2013. Isolation and characterization of bacteriocin-producing bacteria from the intestinal microbiota of elderly Irish subjects. J Appl Microbiol **114:**886-898.
6. **Drissi F, Buffet S, Raoult D, Merhej V.** 2015. Common occurrence of antibacterial agents in human intestinal microbiota. Front Microbiol **6:**441.
7. **Muller CA, Autenrieth IB, Peschel A.** 2005. Innate defenses of the intestinal epithelial barrier. Cell Mol Life Sci **62:**1297-1307.
8. **Dommett R, Zilbauer M, George JT, Bajaj-Elliott M.** 2005. Innate immune defence in the human gastrointestinal tract. Mol Immunol **42:**903-912.

9. **Mason DY, Taylor CR.** 1975. The distribution of muramidase (lysozyme) in human tissues. J Clin Pathol **28:**124-132.

10. **Nizet V.** 2006. Antimicrobial peptide resistance mechanisms of human bacterial pathogens. Curr Issues Mol Biol **8:**11-26.

11. **Nawrocki KL, Crispell EK, McBride SM.** 2014. Antimicrobial peptide resistance mechanisms of Gram-positive bacteria. Antibiotics **3:**461-492.

12. **McBride SM, Sonenshein AL.** 2011. The *dlt* operon confers resistance to cationic antimicrobial peptides in *Clostridium difficile*. Microbiology **157:**1457-1465.

13. **Neuhaus FC, Baddiley J.** 2003. A continuum of anionic charge: structures and functions of D-alanyl-teichoic acids in gram-positive bacteria. Microbiol Mol Biol Rev **67:**686-723.

14. **Le Jeune A, Torelli R, Sanguinetti M, Giard JC, Hartke A, Auffray Y, Benachour A.** 2010. The extracytoplasmic function sigma factor SigV plays a key role in the original model of lysozyme resistance and virulence of *Enterococcus faecalis*. PLoS One **5:**e9658.

15. **Guariglia-Oropeza V, Helmann JD.** 2011. *Bacillus subtilis* Sigma(V) confers lysozyme resistance by activation of two cell wall modification pathways, peptidoglycan O-acetylation and D-alanylation of teichoic acids. J Bacteriol **193:**6223-6232.

16. **Antunes A, Camiade E, Monot M, Courtois E, Barbut F, Sernova NV, Rodionov DA, Martin-Verstraete I, Dupuy B.** 2012. Global transcriptional control by glucose and carbon regulator CcpA in *Clostridium difficile*. Nucleic Acids Res **40:**10701-10718.

17. **Cao M, Helmann JD.** 2004. The *Bacillus subtilis* extracytoplasmic-function sigmaX factor regulates modification of the cell envelope and resistance to cationic antimicrobial peptides. J Bacteriol **186:**1136-1146.

18. **Estacio W, Anna-Arriola SS, Adedipe M, Marquez-Magana LM.** 1998. Dual promoters are responsible for transcription initiation of the *fla/che* operon in *Bacillus subtilis*. J Bacteriol **180:**3548-3555.

19. **Perego M, Glaser P, Minutello A, Strauch MA, Leopold K, Fischer W.** 1995. Incorporation of D-alanine into lipoteichoic acid and wall teichoic acid in *Bacillus subtilis*: identification of genes and regulation. J Biol Chem **270:**15598-15606.

20. **Helmann JD.** 2002. The extracytoplasmic function (ECF) sigma factors. Adv Microb Physiol **46:**47-110.

21. **Ho TD, Williams KB, Chen Y, Helm RF, Popham DL, Ellermeier CD.** 2014. *Clostridium difficile* extracytoplasmic function σ factor σ V regulates lysozyme resistance and is necessary for pathogenesis in the hamster model of infection. Infect Immun **82:**2345-2355.

22. **Hastie JL, Williams KB, Sepulveda C, Houtman JC, Forest KT, Ellermeier CD.** 2014. Evidence of a bacterial receptor for lysozyme: binding of lysozyme to the anti-sigma factor RsiV controls activation of the ECF sigma factor sigmaV. PLoS Genetics **10:**e1004643.

23. **Luria SE, Burrous JW.** 1957. Hybridization between *Escherichia coli* and *Shigella*. J Bacteriol **74:**461-476.

24. **Smith CJ, Markowitz SM, Macrina FL.** 1981. Transferable tetracycline resistance in *Clostridium difficile*. Antimicrob Agents Chemother **19:**997-1003.

25. **Bouillaut L, McBride SM, Sorg JA.** 2011. Genetic manipulation of *Clostridium difficile*. Curr Protoc Microbiol **Chapter 9:**Unit 9A 2.

26. **Edwards AN, Suarez JM, McBride SM.** 2013. Culturing and maintaining *Clostridium difficile* in an anaerobic environment. J Vis Exp doi:10.3791/50787**:**e50787.

27. **Sorg JA, Dineen SS.** 2009. Laboratory maintenance of *Clostridium difficile*. Curr Protoc Microbiol **Chapter 9:**Unit9A 1.

28. **Heap JT, Pennington OJ, Cartman ST, Carter GP, Minton NP.** 2007. The ClosTron: a universal gene knock-out system for the genus *Clostridium*. J Microbiol Methods **70:**452-464.

29. **Karberg M, Guo H, Zhong J, Coon R, Perutka J, Lambowitz AM.** 2001. Group II introns as controllable gene targeting vectors for genetic manipulation of bacteria. Nat Biotechnol **19:**1162-1167.

30. **Ho TD, Ellermeier CD.** 2011. PrsW is required for colonization, resistance to antimicrobial peptides, and expression of extracytoplasmic function sigma factors in *Clostridium difficile*. Infect Immun **79:**3229-3238.

31. **Edwards AN, Pascual RA, Childress KO, Nawrocki KL, Woods EC, McBride SM.** 2015. An alkaline phosphatase reporter for use in *Clostridium difficile*. Anaerobe **32C:**98-104.

32. **Dineen SS, Villapakkam AC, Nordman JT, Sonenshein AL.** 2007. Repression of *Clostridium difficile* toxin gene expression by CodY. Mol Microbiol **66:**206-219.

33. **Edwards AN, Nawrocki KL, McBride SM.** 2014. Conserved oligopeptide permeases modulate sporulation initiation in *Clostridium difficile*. Infect Immun **82:**4276-4291.

34. **Purcell EB, McKee RW, McBride SM, Waters CM, Tamayo R.** 2012. Cyclic diguanylate inversely regulates motility and aggregation in *Clostridium difficile*. J Bacteriol **194:**3307-3316.

35. **Putnam EE, Nock AM, Lawley TD, Shen A.** 2013. SpoIVA and SipL are *Clostridium difficile* spore morphogenetic proteins. J Bacteriol **195:**1214-1225.

36. **McBride SM, Sonenshein AL.** 2011. Identification of a genetic locus responsible for antimicrobial peptide resistance in *Clostridium difficile*. Infect Immun **79:**167-176.

37. **Dineen SS, McBride SM, Sonenshein AL.** 2010. Integration of metabolism and virulence by *Clostridium difficile* CodY. J Bacteriol **192:**5350-5362.

38. **Suarez JM, Edwards AN, McBride SM.** 2013. The *Clostridium difficile cpr* locus is regulated by a noncontiguous two-component system in response to type A and B lantibiotics. J Bacteriol **195:**2621-2631.

39. **Hyyrylainen HL, Vitikainen M, Thwaite J, Wu H, Sarvas M, Harwood CR, Kontinen VP, Stephenson K.** 2000. D-Alanine substitution of teichoic acids as a modulator of protein folding and stability at the cytoplasmic membrane/cell wall interface of *Bacillus subtilis*. J Biol Chem **275:**26696-26703.

40. **Fisher N, Shetron-Rama L, Herring-Palmer A, Heffernan B, Bergman N, Hanna P.** 2006. The *dltABCD* operon of *Bacillus anthracis sterne* is required for virulence and resistance to peptide, enzymatic, and cellular mediators of innate immunity. J Bacteriol **188:**1301-1309.

41. **Bartlett JG, Onderdonk AB, Cisneros RL, Kasper DL.** 1977. Clindamycin-associated colitis due to a toxin-producing species of *Clostridium* in hamsters. J Infect Dis **136:**701-705.

42. **Chang TW, Bartlett JG, Gorbach SL, Onderdonk AB.** 1978. Clindamycin-induced enterocolitis in hamsters as a model of pseudomembranous colitis in patients. Infect Immun **20:**526-529.

43. **Wilson KH, Silva J, Fekety FR.** 1981. Suppression of *Clostridium difficile* by normal hamster cecal flora and prevention of antibiotic-associated cecitis. Infect Immun **34:**626-628.

44. **George WL, Sutter VL, Citron D, Finegold SM.** 1979. Selective and differential medium for isolation of *Clostridium difficile*. J Clin Microbiol **9:**214-219.

45. **Bordeleau E, Purcell EB, Lafontaine DA, Fortier LC, Tamayo R, Burrus V.** 2015. Cyclic di-GMP riboswitch-regulated type IV pili contribute to aggregation of *Clostridium difficile*. J Bacteriol **197:**819-832.

46. **McKee RW, Mangalea MR, Purcell EB, Borchardt EK, Tamayo R.** 2013. The second messenger cyclic Di-GMP regulates *Clostridium difficile* toxin production by controlling expression of *sigD*. J Bacteriol **195:**5174-5185.

47. **Lyras D, O'Connor JR, Howarth PM, Sambol SP, Carter GP, Phumoonna T, Poon R, Adams V, Vedantam G, Johnson S, Gerding DN, Rood JI.** 2009. Toxin B is essential for virulence of *Clostridium difficile*. Nature **458:**1176-1179.

48. **Kuehne SA, Cartman ST, Heap JT, Kelly ML, Cockayne A, Minton NP.** 2010. The role of toxin A and toxin B in *Clostridium difficile* infection. Nature **467:**711-713.

49. **Goulding D, Thompson H, Emerson J, Fairweather NF, Dougan G, Douce GR.** 2009. Distinctive profiles of infection and pathology in hamsters infected with *Clostridium difficile* strains 630 and B1. Infect Immun **77:**5478-5485.

50. **Viswanathan VK.** 2014. Memories of a virulent past. Gut Microbes **5:**143-145.

51. **Wu X, Hurdle JG.** 2014. The *Clostridium difficile* proline racemase is not essential for early logarithmic growth and infection. Can J Microbiol **60:**251-254.

52. **Hancock RE, Diamond G.** 2000. The role of cationic antimicrobial peptides in innate host defences. Trends Microbiol **8:**402-410.

53. **Peschel A.** 2002. How do bacteria resist human antimicrobial peptides? Trends Microbiol **10:**179-186.

54. **Kelly CP, Becker S, Linevsky JK, Joshi MA, O'Keane JC, Dickey BF, LaMont JT, Pothoulakis C.** 1994. Neutrophil recruitment in *Clostridium difficile* toxin A enteritis in the rabbit. J Clin Invest **93:**1257-1265.

55. **Kelly CP, Kyne L.** 2011. The host immune response to *Clostridium difficile*. J Med Microbiol **60:**1070-1079.

56. **Redelings MD, Sorvillo F, Mascola L.** 2007. Increase in *Clostridium difficile*-related mortality rates, United States, 1999-2004. Emerg Infect Dis **13:**1417-1419.

57. **McDonald LC, Killgore GE, Thompson A, Owens RC, Jr., Kazakova SV, Sambol SP, Johnson S, Gerding DN.** 2005. An epidemic, toxin gene-variant strain of *Clostridium difficile*. N Engl J Med **353:**2433-2441.

58. **Warny M, Pepin J, Fang A, Killgore G, Thompson A, Brazier J, Frost E, McDonald LC.** 2005. Toxin production by an emerging strain of *Clostridium difficile*

associated with outbreaks of severe disease in North America and Europe. Lancet **366:**1079-1084.

59. **Sebaihia M, Wren BW, Mullany P, Fairweather NF, Minton N, Stabler R, Thomson NR, Roberts AP, Cerdeno-Tarraga AM, Wang H, Holden MT, Wright A, Churcher C, Quail MA, Baker S, Bason N, Brooks K, Chillingworth T, Cronin A, Davis P, Dowd L, Fraser A, Feltwell T, Hance Z, Holroyd S, Jagels K, Moule S, Mungall K, Price C, Rabbinowitsch E, Sharp S, Simmonds M, Stevens K, Unwin L, Whithead S, Dupuy B, Dougan G, Barrell B, Parkhill J.** 2006. The multidrug-resistant human pathogen *Clostridium difficile* has a highly mobile, mosaic genome. Nat Genet **38:**779-786.

60. **Opitz B, Schroder NW, Spreitzer I, Michelsen KS, Kirschning CJ, Hallatschek W, Zahringer U, Hartung T, Gobel UB, Schumann RR.** 2001. Toll-like receptor-2 mediates Treponema glycolipid and lipoteichoic acid-induced NF-kappaB translocation. J Biol Chem **276:**22041-22047.

61. **Schroder NW, Morath S, Alexander C, Hamann L, Hartung T, Zahringer U, Gobel UB, Weber JR, Schumann RR.** 2003. Lipoteichoic acid (LTA) of *Streptococcus pneumoniae* and *Staphylococcus aureus* activates immune cells via Toll-like receptor (TLR)-2, lipopolysaccharide-binding protein (LBP), and CD14, whereas TLR-4 and MD-2 are not involved. J Biol Chem **278:**15587-15594.

62. **Cox KH, Ruiz-Bustos E, Courtney HS, Dale JB, Pence MA, Nizet V, Aziz RK, Gerling I, Price SM, Hasty DL.** 2009. Inactivation of DltA modulates virulence factor expression in *Streptococcus pyogenes*. PLoS One **4:**e5366.

63. **Morath S, Geyer A, Hartung T.** 2001. Structure–function relationship of cytokine induction by lipoteichoic acid from *Staphylococcus aureus*. The Journal of Experimental Medicine **193:**393-398.

64. **Grangette C, Nutten S, Palumbo E, Morath S, Hermann C, Dewulf J, Pot B, Hartung T, Hols P, Mercenier A.** 2005. Enhanced antiinflammatory capacity of a *Lactobacillus plantarum* mutant synthesizing modified teichoic acids. Proc Natl Acad Sci U S A **102:**10321-10326.

65. **Tabuchi Y, Shiratsuchi A, Kurokawa K, Gong JH, Sekimizu K, Lee BL, Nakanishi Y.** 2010. Inhibitory role for D-alanylation of wall teichoic acid in activation of insect Toll pathway by peptidoglycan of *Staphylococcus aureus*. J Immunol **185:**2424-2431.

66. **Savidge TC, Pan WH, Newman P, O'Brien M, Anton PM, Pothoulakis C.** 2003. *Clostridium difficile* toxin B is an inflammatory enterotoxin in human intestine. Gastroenterology **125:**413-420.

67. **Kim H, Rhee SH, Kokkotou E, Na X, Savidge T, Moyer MP, Pothoulakis C, LaMont JT.** 2005. *Clostridium difficile* toxin A regulates inducible cyclooxygenase-2 and prostaglandin E2 synthesis in colonocytes via reactive oxygen species and activation of p38 MAPK. J Biol Chem **280:**21237-21245.

68. **Le Jeune A, Torelli R, Sanguinetti M, Giard J-C, Hartke A, Auffray Y, Benachour A.** 2010. The extracytoplasmic function sigma factor SigV plays a key role in the original model of lysozyme resistance and virulence of *Enterococcus faecalis*. PLoS One **5:**e9658.

69. **Stevenson E, Minton NP, Kuehne SA.** 2015. The role of flagella in *Clostridium difficile* pathogenicity. Trends Microbiol **23:**275-282.

70. **Wust J, Hardegger U.** 1983. Transferable resistance to clindamycin, erythromycin, and tetracycline in *Clostridium difficile*. Antimicrob Agents Chemother **23:**784-786.

71. **Hussain HA, Roberts AP, Mullany P.** 2005. Generation of an erythromycin-sensitive derivative of *Clostridium difficile* strain 630 (630Deltaerm) and demonstration that the conjugative transposon Tn916DeltaE enters the genome of this strain at multiple sites. J Med Microbiol **54:**137-141.

72. **O'Connor JR, Lyras D, Farrow KA, Adams V, Powell DR, Hinds J, Cheung JK, Rood JI.** 2006. Construction and analysis of chromosomal *Clostridium difficile* mutants. Mol Microbiol **61:**1335-1351.

73. **Stabler RA, He M, Dawson L, Martin M, Valiente E, Corton C, Lawley TD, Sebaihia M, Quail MA, Rose G, Gerding DN, Gibert M, Popoff MR, Parkhill J, Dougan G, Wren BW.** 2009. Comparative genome and phenotypic analysis of *Clostridium difficile* 027 strains provides insight into the evolution of a hypervirulent bacterium. Genome Biol **10:**R102.

74. **Thomas CM, Smith CA.** 1987. Incompatibility group P plasmids: genetics, evolution, and use in genetic manipulation. Annu Rev Microbiol **41:**77-101.

75. **Yanisch-Perron C, Vieira J, Messing J.** 1985. Improved M13 phage cloning vectors and host strains: nucleotide sequences of the M13mp18 and pUC19 vectors. Gene **33:**103-119.

76. **Manganelli R, Provvedi R, Berneri C, Oggioni MR, Pozzi G.** 1998. Insertion vectors for construction of recombinant conjugative transposons in *Bacillus subtilis* and *Enterococcus faecalis*. FEMS Microbiol Lett **168:**259-268.

Chapter 3: The *Clostridium difficile clnRAB* operon initiates adaptations to the intestinal environment in response to host LL-37

Emily C. Woods,[1] Adrianne N. Edwards[1], and Shonna M. McBride[1]

[1]Department of Microbiology and Immunology, Emory Antibiotic Resistance Center, Emory University School of Medicine, Atlanta, Georgia, USA

In submission

E.C.W. designed and performed experiments and wrote and edited the manuscript.

A.N.E. designed experiments and edited the manuscript.

S.M.M. designed and performed experiments and wrote and edited the manuscript.

SUMMARY

To cause disease, *Clostridioides* (*Clostridium*) *difficile* must resist killing by innate immune effectors in the intestine, including the host antimicrobial peptide, cathelicidin (LL-37). The mechanisms that enable *C. difficile* to adapt to the intestine in the presence of antimicrobial peptides are unknown. Expression analyses revealed an operon, *CD630_16170-CD630_16190* (*clnRAB*), which is highly induced by LL-37 and is not expressed in response to other cell-surface active antimicrobials. This operon encodes a predicted transcriptional regulator (*clnR*) and an ABC transporter system (*clnAB*), all of which are required for function. Analyses of a *clnR* mutant indicate that ClnR is a pleiotropic regulator that controls the LL-37-dependent expression of numerous genes, including many involved in metabolism, cellular transport, signaling, gene regulation, and pathogenesis. The data suggest that ClnRAB is a novel regulatory mechanism that senses LL-37 as a host signal and regulates gene expression to adapt to the host intestinal environment during infection.

INTRODUCTION

Clostridioides difficile (formerly *Clostridium difficile*) poses a serious, ongoing, public health threat. *C. difficile* infections result in mild to severe diarrhea and lead to approximately 29,000 deaths each year in the United States (1). Patients are typically infected after treatment with antibiotics, which disrupt the intestinal microbiota that provide colonization resistance against *C. difficile* infections (CDI) by competition and release of antimicrobial peptides (AMPs) (1, 2).

The host innate immune system also plays an important role in the prevention of infections. A critical feature of this defense is the production of AMPs, including defensins, cathelicidin (LL-37), and lysozyme (3, 4). To colonize the intestine and cause disease, *C. difficile* must resist killing by host-produced AMPs (5-8). LL-37, a cationic AMP, is of particular importance in CDI because it is not only produced constitutively in the colon by the colonic epithelium, but is also released in high levels from neutrophils, which are a key component of the initial immune response to CDI (9). LL-37 forms an amphipathic alpha-helical structure that can insert into bacterial membranes and cause bacterial cell death (10-12). Common bacterial resistance mechanisms to LL-37 include cell surface modifications that prevent LL-37 access to the bacterial surface, efflux pumps that eliminate LL-37 that enters the bacteria, secreted proteases that degrade LL-37, and modulation of host production of LL-37 (9).

C. difficile demonstrates inducible resistance to LL-37, and current epidemic ribotypes have higher levels of resistance to LL-37 than other ribotypes (13). Although *C. difficile* resistance to LL-37 is documented, no clear homologs of known resistance mechanisms are apparent in the genome and no additional LL-37 resistance mechanisms

have been identified. Moreover, the mechanisms by which *C. difficile* responds to this and other innate immune factors are poorly understood. We hypothesized that *C. difficile* responds to LL-37 and that this response occurs, at least in part, at the level of transcription.

In this study, we determined the transcriptional response of *C. difficile* to the host LL-37 peptide. We identified an operon, *CD630_16170-CD630_16190* (herein named *clnRAB*), that was highly induced by LL-37 and was not expressed in response to other cell-surface active antimicrobials. This operon encodes a predicted GntR-family transcriptional regulator (*clnR*) and an ABC transporter system (*clnAB*). We determined that the ClnR regulator represses *clnRAB* expression, and is also necessary for LL-37 dependent induction of *clnRAB* transcription. Transcriptional analyses of a *clnR* mutant indicated that ClnR is a global regulator that controls the expression of numerous genes including toxins, alternative metabolism pathways, transporters, and transcriptional regulators. Growth analyses revealed that exposure to LL-37 modifies the metabolism of *C. difficile* and that this response occurs through ClnR. In addition, we observed that both a *clnR* and a *clnAB* mutant are more virulent in the hamster model of infection and that ClnR impacts growth of *C. difficile* in the host. Further, *in vitro* analyses confirmed that ClnR is a DNA-binding transcriptional regulator that directly controls expression of the *cln* operon and other ClnR-regulated genes. Based on these data, we propose that LL-37 acts as a host signal that is transmitted through ClnRAB, enabling *C. difficile* to regulate global gene expression to adapt to the intestinal environment during infection.

Discovery of an operon that is highly induced by LL-37.

To test the hypothesis that *C. difficile* responds to LL-37 through changes in gene transcription, we performed RNA-seq analysis on bacteria grown with or without sub-MIC levels (1/10 MIC) of LL-37 to determine which genes were differentially expressed. RNA-seq analysis revealed 228 genes that were differentially expressed at least 2-fold and with $P < 0.05$, including 107 genes that were induced and 121 genes that were down-regulated in the presence of LL-37 (**Table S1**). Genes differentially expressed in LL-37 include loci predicted to encode metabolic pathway components, nutrient acquisition mechanisms, transcriptional regulators, multidrug transporters, antibiotic resistance factors, conjugation-associated proteins, and genes of unknown function. Notably, several of these loci were previously investigated in *C. difficile* and found to contribute to growth, antimicrobial resistance or virulence, including genes involved in succinate, glucose, fructose, mannitol, ethanolamine, butyrate, acetyl-CoA and amino acid metabolism, oligopeptide permeases, elongation factor (EF-G), ferredoxin oxidoreductase, and ECF sigma factors (14-23).

Of the differentially regulated genes identified, the most highly induced by LL-37 were three genes comprising an apparent operon: *CD630_16170-16190*. These genes encode a putative GntR-family transcriptional regulator (*CD630_16170, clnR*) and a downstream ABC transporter system composed of an ATP-binding component (*CD630_16180, clnA*) and a permease (*CD630_16190, clnB*). The results of the RNA-seq analyses for *clnRAB* were verified by qRT-PCR in the 630Δ*erm* strain and for the epidemic 027 ribotype strain, R20291 (**Fig. 1**). Based on the induction of these genes and their resemblance to antimicrobial response systems, we pursued the function of this operon further. Transcriptional analysis of strains grown in increasing concentrations of

LL-37 demonstrated that expression of each of these genes increased in a dose-dependent manner for both strains, illustrating that these genes are similarly expressed and regulated in diverse *C. difficile* isolates (**Fig. 1**). Using nested PCR from *C. difficile* cDNA templates, we also confirmed that the *CD630_16170-16190* genes are transcribed as an operon (**Fig. S1**).

The *cln* operon does not contribute significantly to LL-37 resistance

Given the high level of induction of the *clnRAB* operon in LL-37, and because transporters are common antimicrobial resistance mechanisms, we hypothesized that ClnAB may confer resistance to LL-37. To test this, we generated insertional disruptions in the *CD630_16170* (*clnR*) and *CD630_16180* (*clnA*) coding sequences (**Fig. S2**), and analyzed the ability of the mutants to grow in the presence of LL-37 (**Fig. 2**). Although the *clnR* mutant has a minor growth defect when grown in BHIS alone, both the *clnR* and *clnA* mutants grew slightly better than the parent strain in 2.5 μg LL-37 ml^{-1}. Evaluation of the minimum inhibitory concentrations (MICs) and minimum bactericidal concentrations (MBCs) for LL-37 in these strains revealed no observable differences in either the MIC or MBC for the *clnR* or *clnA* mutant in comparison to the parent strain (**Table S2**). Considering that some antimicrobial transporter mechanisms are activated by and confer resistance to multiple classes of antimicrobials, we investigated the resistance of both mutants to other cell-surface acting compounds. Neither the *clnR* nor the *clnA* mutant had altered MIC values for any other cell surface-active antimicrobial tested (**Table S3**). These findings indicate that the *cln* operon does not play a significant role in resistance to LL-37 or most other cell-surface active antimicrobials.

Induction of *clnRAB* is specific to LL-37-like cathelicidins

The induction of the *cln* operon suggested that this locus was responsive to LL-37; however, antimicrobials may induce changes in bacterial gene expression as a general stress response or due to disruptions in cellular processes (24, 25). To determine whether the induction of this operon is specific to LL-37 or a general response to cellular stress, we evaluated the expression of *clnR* in the presence of a variety of other antimicrobial compounds (**Table 1**). Transcription of *clnR* was also induced when *C. difficile* was exposed to the mouse cathelicidin, mCRAMP, but *clnR* was not induced in the presence of sequence-scrambled LL-37 or with the sheep cathelicidin, SMAP-29, which is less similar to LL-37 than mCRAMP (**Fig. S3**) (26-28). Similarly, none of the other cell-surface-active antimicrobials tested (lysozyme, ampicillin, vancomycin, nisin, or polymyxin B) induced *clnR* expression (**Table 1**). These results indicate that induction of the *clnRAB* operon is dependent on the specific sequence of LL-37 and is not induced by antimicrobial-caused cell-surface stress. Accordingly, we named this operon *clnRAB* to reflect the specificity of the induction in response to LL-37 and similar **C**athe**l**icidi**n**s.

ClnR is a global regulator of gene expression in *C. difficile*

As antimicrobial resistance did not explain the changes in growth for the *clnR* and *clnA* mutants in LL-37, we hypothesized that there were changes in the expression of genes other than *clnRAB* in the *cln* mutants. To test this, we examined gene expression by RNA-seq for the *clnR* mutant grown with and without LL-37, compared to that of the parent strain (**Table S4**). This analysis revealed that 178 genes were differentially

expressed at least 2-fold in the *clnR* mutant. Notably, the *clnR* mutant demonstrated negative and positive effects on transcription, with many genes exhibiting additional conditional regulation by LL-37. In the absence of LL-37, the *clnR* mutant exhibited increased expression of 14 genes and decreased expression of 32 genes. Disruption of *clnR* had an even greater impact on expression in the presence of LL-37, resulting in increased expression of 29 genes and decreased expression of 103 genes. Of the genes differentially regulated by LL-37 (**Table S1**), 56 were also influenced by *clnR* (**Table S5**). These results indicate that ClnR acts as both a repressor and inducer of gene expression, and that this regulatory potential is largely dependent on LL-37. The 178 genes regulated by ClnR fell into many different functional classes, with the most common ClnR-dependent genes encoding proteins with predicted metabolic functions (**Fig. 3**). These results support the premise that ClnR acts as a global regulator in response to LL-37.

RNA-seq results from the *clnR* mutant and parent strain were validated by qRT-PCR for several apparent ClnR-dependent genes, including analysis of expression in the *clnA* mutant (**Table S6**). Comparisons of *clnR* and *clnA* mutant expression revealed that the regulator and transporter disruptions resulted in disparate effects on the transcription of some genes, including genes predicted to function in antimicrobial resistance, *vanZ1*, *csfU, csfT, and cdd4,* and the metabolic genes *mtlA, iorA, grdA,* and *CD0284* (**Table S6**). These disparate effects are most prominent in the presence of LL-37, highlighting that ClnR activity is dependent on LL-37. In some cases, the *clnR* and *clnA* mutants had similar levels of expression, suggesting that the ClnAB transporter function is important for the activation of ClnR, whereas in other cases expression diverged in the *clnR* and *clnA* mutants, suggesting a role for the ClnAB transporter in the regulation of some LL-

37-dependent genes, independent of ClnR. These complex gene regulatory patterns suggest that multiple factors are involved in the transcription of some ClnR-regulated genes, and that ClnR has both direct and indirect effects on the expression of some loci.

ClnR conditionally represses and induces *clnRAB* in response to LL-37

To understand the molecular mechanism of ClnR function, we further explored regulation of the *clnRAB* locus. ClnR is annotated as a GntR-family transcriptional regulator, and protein sequence comparisons suggest that it is a member of the YtrA sub-family of GntR regulators (**Fig. S4**). GntR-family regulators are most common among bacteria that inhabit complex environmental niches (29). The YtrA sub-family regulators are often found in conjunction with ABC-transporters and are typically autoregulatory (30). We examined the impact of *clnR* or *clnA* disruption on expression of the *clnRAB* operon to determine if ClnR regulates expression of itself and *clnAB*. qRT-PCR analysis of *clnR* expression revealed that transcription of *clnR* and *clnA* are increased in the *clnR* mutant grown without LL-37 (**Fig. 4**), suggesting that ClnR auto-represses the *cln* operon. However, in the presence of LL-37, *clnR* and *clnA* expression are no longer induced in the *clnR* mutant, demonstrating that ClnR also conditionally regulates the c*ln* operon in response to LL-37. Conversely, the *clnA* mutant displays lower *clnR* and *clnA* expression during growth with or without LL-37 (**Fig. 4**). The expression phenotypes of both mutants were restored upon complementation with the *cln* operon (**Fig. 4**). These results provide further evidence that the ClnAB transporter contributes to regulation of the *cln* operon, and the ability of ClnR to respond to LL-37.

ClnR regulates the metabolism of different nutrient sources in *C. difficile*

Based on the evident changes in metabolic gene expression in the *clnR* mutant and the impact of LL-37 on ClnR-dependent transcription, we investigated the impact of ClnR and LL-37 on the growth of *C. difficile* with relevant metabolites. To this end, we grew the *clnR* mutant and the parent strain in minimal medium supplemented with glucose, fructose, mannose, mannitol, N-acetylglucosamine, or ethanolamine, with and without LL-37 (**Fig. S5**). We observed that for the first 2-3 h, growth of the *clnR* mutant and the parent strain were indistinguishable in the presence or absence of LL-37, regardless of the supplemented carbon source (**Fig. S5**). Other groups have also observed preferential utilization of peptides by *C. difficile*, as amino acids are a preferred energy source for this bacterium (31-33). As anticipated, the addition of each of the examined carbon sources to minimal medium resulted in shorter doubling times (i.e. faster growth) and a higher final cell density for the parent strain cultures (630Δ*erm*) than in the base minimal medium (**Table 2,** column one). However, the addition of nutrients provided less advantage to the *clnR* mutant, compared to the parent strain, suggesting that ClnR is important for the utilization of a variety of nutrients. When a low concentration of LL-37 (0.5 μg/ml; 1/30 MIC) was added to the growth medium, the rate of *C. difficile* growth in the presence of added nutrients diminished considerably (**Table 2**, rows). In contrast, the *clnR* mutant demonstrated no significant changes in nutrient utilization when LL-37 was present. These results indicate that the lengthening of doubling times observed with low levels of LL-37 are due to changes in ClnR-dependent bacterial metabolism, rather than the antimicrobial activity of LL-37. Moreover, the data strongly suggest that the

reductions in growth rates and metabolism observed in LL-37 are mediated by ClnR through repression and activation of metabolic gene expression (**Tables S4, S5**).

ClnRAB modulates growth and virulence *in vivo*

As LL-37 is a host-produced antimicrobial and *C. difficile* inhabits the gastrointestinal tract, the natural consequences of ClnR-LL-37–dependent gene regulation would appear during the growth of the pathogen in the host intestine. To examine the effects of *cln* mutants *in vivo*, we used the hamster model of *C. difficile* infection (CDI). Syrian golden hamsters are acutely susceptible to infection by *C. difficile*, and hamsters produce a cathelicidin very similar to that of mice and humans (**Fig. S3**). Animals were infected with spores of the *clnA, clnR* or 630Δ*erm* strains, and monitored for symptoms of infection as described in the Methods. Hamsters infected with either the *clnA* or *clnR* mutant strains succumbed to infection more rapidly than animals inoculated with the parent strain, indicating that the *clnR* and *clnA* mutants are more virulent (mean time to morbidity: 46.0 ± 12.2 h for 630Δ*erm*, 32.5 ± 5.8 h for *clnR* (P = 0.0003), 35.2 ± 6.1 h for *clnA* (P = 0.0045); **Fig. 5A**).

To assess *C. difficile* colonization by the different strains, fecal samples were taken at 12 h post-infection and plated onto selective medium. *C. difficile* was recovered from fecal samples in significantly more animals infected with the the *clnR* strain than in the 630Δ*erm*-infected group, suggesting that the *clnR* mutant colonizes the intestine more rapidly (**Fig. 5B**). In addition, the *clnR* mutant reached a higher bacterial burden at the time of morbidity (1.2 x 10^7 CFU/ml for 630Δ*erm*, 2.7 x 10^7 CFU/ml for *clnR*; **Fig. 5C**). These results illustrate that the *clnRAB* operon plays a significant role in colonization

dynamics and virulence of *C. difficile* during infection. In the future, competitive infections could provide additional information about the fitness differences of these mutants *in vivo*.

C. difficile disease is mediated by the two primary toxins, TcdA and TcdB. To determine whether the increased virulence of the *cln* strains was related to increased toxin levels, we extracted RNA from cecal samples collected from animals at the time of morbidity and performed digital droplet PCR for absolute quantification of *tcdA* and *tcdB* expression (**Fig. S6**). Although statistical significance was not achieved, animals infected with the *clnR* mutant trended towards having higher levels of both *tcdA* and *tcdB* detected in their cecum at the time of morbidity. Because only one timepoint could be assessed, the results do not resolve whether the *clnR* and *clnA* mutants have altered toxin expression during the course of infection. But, the time from infection to morbidity for *clnR* and *clnA* infections indicate that these mutants produce toxin earlier in the course of infection, resulting in earlier symptoms of disease and morbidity.

Considering that differences in either sporulation or germination rates can also influence virulence and bacterial burden i*n vivo,* we assessed sporulation and germination for the *clnR* and *clnA* mutants for defects in either process. No significant difference in sporulation or germination rates was observed for either mutant (**Fig. S7**).

ClnRAB and LL-37 promote toxin production

Since toxin production is the primary virulence factor leading to *C. difficile* symptoms, we further investigated the effects of LL-37 and ClnRAB on toxin production under more controlled conditions *in vitro*. qRT-PCR analysis of *tcdA* and *tcdB*

transcription was assessed for the *cln* mutants and parent strain during logarithmic growth in BHIS medium, with or without added LL-37. As shown in **Fig. S8**, LL-37 exposure resulted in increased expression of *tcdA* (4.6-fold) and *tcdB* (2.2-fold) in wild-type cells. In contrast, the *clnR* and *clnA* mutants demonstrated lower expression of toxins, suggesting that ClnRAB is partially responsible for LL-37-dependent regulation of toxin expression. Toxin expression is known to be controlled by several regulatory factors, many of which respond to low nutrient availability and/or the transition to stationary phase growth (34). To determine which of the toxin regulators may be influenced by LL-37, we examined expression of regulators and regulator-dependent factors, including *tcdR, sigD, ilcV* (as an indication of CodY activity), and *CD0341* (as an indication of CcpA activity) (**Table S7**). Of these, only *ilvC* expression is statistically altered in LL-37; however, the increase in *ilvC* expression is far more modest (2.2-fold increase) than would be expected with robust CodY activation.

Because toxin production is typically low at mid-logarithmic phase in BHIS medium, we also examined toxin expression after 24 h growth in TY medium. Western blot analysis indicated that TcdA levels were lower in the *clnR* and *clnA* mutants in TY medium, relative to the parent strain. When cells were grown in medium supplemented with LL-37, final TcdA levels decreased about 3-fold in the parent strain. (**Fig. S8C**). In comparison, TcdA levels did not change for the *clnR* and *clnA* mutants in LL-37. While these findings contradict the induction of *tcdA* expression observed at log-phase in BHIS medium, the data support the observation that LL-37 and ClnRAB influence toxin expression, and that the outcome of this regulation on toxin production is dependent on growth conditions. These observations provide further evidence that the ClnRAB system

is involved in toxin production and that this system is necessary for the influence of LL-37 on toxin production.

ClnR acts as a DNA-binding regulator that binds multiple promoters

As a predicted GntR-family transcriptional regulator, we hypothesized that ClnR binds DNA. Because we had found that ClnR is autoregulatory (**Fig. 4**), we initially tested whether ClnR directly regulates its own promoter. We produced recombinant His-tagged ClnR and performed gel shifts with fluorescein-labeled DNA of the 84 bp upstream of the *clnR* transcriptional start site. This DNA fragment was selected because it encompasses a predicted σ^A-dependent promoter with -10 (at -52 to -47 bp) and -35 (at -73 to -68 bp) consensus sequences and a tandem repeat sequence (at -46 to -16 bp) that includes a possible ClnR-binding site (**Fig. S9**). Incubation of His-ClnR with this DNA fragment resulted in a shift visible after electrophoresis, both with and without LL-37 (**Fig. 6A**). This interaction was specific, as indicated by continued binding in the presence of 100x nonspecific DNA (**Fig. 6A**). The apparent K_d value for this interaction was calculated to be 118 nM (± 40 nM) without LL-37 and 39 nM (± 17 nM) with LL-37, indicating that the affinity of ClnR for this DNA sequence increases in the presence of LL-37.

Additional ClnR-regulated promoters were examined for direct binding, including predicted upstream promoter elements for the metabolic operons *grd* (CD630_23540), *mtl* (CD630_23340), and *ior* (CD630_23810); genes involved in antimicrobial resistance, including *vanZ* (CD630_12400) and *CD630_06680* (response regulator of *cdd* lantibiotic transporter); toxin (*tcdA*) *CD630_06630*; and other transcriptional regulators, including

sigU (*csfU, CD630_18870*) and *CD630_16060*. ClnR bound to all of these promoter sequences, but exhibited specificity for P*vanZ*, P*CD1606*, and P*sigU*, with or without LL-37 (**Fig. 6B-D**). Binding was not specific for P*grd,* P*mtl,* P*ior,* P*tcdA,* and *CD630_06680* (**Fig. S10**). The calculated apparent K_d for P*vanZ* was 141 nM (± 59 nM) without LL-37 and 139 nM (± 33 nM) with LL-37, the apparent K_d for P*CD630_16060* was 1.9 μM (± 0.2 μM) without LL-37 and 2.6 μM (± 0.5 μM) with LL-37, and the apparent K_d for P*sigU* was 2.5 μM (± 0.2 μM) without LL-37 and 4.2 μM (± 3.4 μM) with LL-37 (**Fig. 6**). Because the apparent K_d values for these targets are similar both with and without LL-37, it does not appear that LL-37 influences ClnR regulation of these targets in these *in vitro* binding conditions.

DISCUSSION

Many bacteria encode signaling systems for detecting conditions within the host environment, allowing for activation of genes that are necessary for survival within the host. LL-37 acts as a signal for many pathogens to adapt to the host, though most of the mechanisms that have been investigated are implicated in bacterial virulence and antimicrobial resistance. (35-41). Little is known about the molecular mechanisms that *C. difficile* uses to adapt and survive in the host intestinal environment. Our results have revealed that LL-37 alters global gene expression in *C. difficile* through the previously unknown regulator and ABC-transporter system, ClnRAB. Moreover, the activation of ClnRAB is specific to LL-37 and independent of the antimicrobial effects of this host peptide.

Many of the genes regulated by LL-37 and ClnRAB function in metabolism and

energy production (**Table S4, Fig. 3**). The regulation of metabolic pathways in response to LL-37 was previously observed in other pathogens, including *S. pyogenes*, *E. coli, P. aeruginosa*, and *S. pneumonia*e, but their role in the bacterial response to LL-37 has not been clear (37, 40-42). Our data indicate that the regulation of genes by LL-37/ClnRAB *in vivo* has robust effects on *C. difficile* colonization and virulence (**Fig. 5**). The animal infection results suggest that disruption of ClnRAB results in dysregulation of metabolism that initially allows for greater growth and proliferation of *C. difficile*, but quickly progresses to nutrient deprivation and toxin production. These effects are not unexpected, given that nutrient deprivation is demonstrably the primary factor driving *C. difficile* toxin expression (21, 32, 34, 43-48). *C. difficile* possesses an unusual metabolic repertoire for energy generation, including solventogenic fermentation (49, 50), Stickland (amino acid) fermentation (31), and autotrophic growth via the Wood-Ljungdahl pathway (51). However, the importance of most of these individual metabolic pathways for growth and virulence *in vivo* has not been determined. Because ClnR is a global regulator that negatively and positively influences the expression of multiple metabolic pathways, many of which are constitutively expressed in a *clnR* mutant, we cannot infer which of these pathways are most influential for host pathogenesis. Determining how and which ClnR-controlled pathways and mechanisms influence disease could expose potential vulnerabilities of *C. difficile* that may be exploited to prevent infections.

Overall our results indicate that ClnRAB responds specifically to LL-37 without conferring LL-37 resistance and suggest that ClnR responds to LL-37 as an indicator of the host environment. The *clnRAB* locus is highly conserved in *C. difficile,* with representation at ≥ 99% amino acid sequence identity in over 500 strains at the time of

this publication (NCBI, BLASTp). The data strongly suggest that ClnR acts as a pleiotropic regulator in *C. difficile* that controls the expression of genes involved in metabolism and virulence, in response to the host peptide, LL-37. To our knowledge this finding is the first report of a global regulator in *C. difficile* that responds to a specific host environment signal. Further study of the activation and downstream impacts of this regulatory pathway will contribute greatly to our understanding of how *C. difficile* adapts to the host environment and causes disease.

Author Contributions

E.W. and S.M. designed and conducted experiments and wrote the paper. A.E. designed experiments and edited the manuscript.

Acknowledgements

The authors would like to thank the members of the McBride lab for useful feedback on this manuscript and Graeme Conn for advice on apparent K_d calculations. In addition, the authors would like to thank Mike Billingsley, Gregory Tharp, Nirav Patel, and Steven Bosinger of the Yerkes Genomics Core Laboratory for assistance with the next-generation sequencing experiments and data analysis. The authors are also grateful to Anice Lowen for allowing use of her ddPCR machine.

Funding Information

This work was supported by the U.S. National Institutes of Health through research grants DK087763, DK101870, and AI109526 to SMM, and GM008169 to ECW.

The content of this manuscript is solely the responsibility of the authors and does not necessarily reflect the views of the National Institutes of Health. The Genomics Core receives financial support from P51 OD011132 "Support of the Yerkes National Primate Research Center."

METHODS

Bacterial strains and growth conditions

Table S8 lists the bacterial strains and plasmids used in this study. *Escherichia coli* was grown aerobically in LB medium (Teknova) at 37˚C (52). As needed, cultures were supplemented with 20 μg chloramphenicol ml^{-1} (Sigma-Aldrich) or 100 μg ampicillin ml^{-1} (Cayman Chemical Company). *C. difficile* was grown at 37˚C in an anaerobic chamber containing 10% H_2, 5% CO_2 and 85% N_2 (Coy Laboratory Products) in brain heart infusion medium supplemented with 2% yeast extract (BHIS; Becton, Dickinson, and Company), TY broth (45), or 70:30 sporulation agar (53), as previously described (54). As needed, *C. difficile* cultures were supplemented with LL-37 (Anaspec) at the concentrations stated in the text, or 2 μg thiamphenicol ml^{-1} (Sigma-Aldrich) for plasmid selection.

Strain and plasmid construction

Table S9 lists the oligonucleotides used in this study. *C. difficile* strain 630 (GenBank accession NC_009089.1) served as the reference for primer design and cloning. PCR amplification was performed using genomic DNA from strain 630Δ*erm* as a template.

PCR, cloning, and plasmid DNA isolation were performed according to standard protocols (54-56). Plasmids were confirmed by sequencing (Eurofins MWG Operon).

Null mutations in *C. difficile* genes were introduced by re-targeting the group II intron of pCE240 using the primers listed in **Table S2,** as previously described (17, 55). Plasmids were introduced into *E. coli* strain HB101 pRK24 via transformation. *E. coli* strains were then conjugated with *C. difficile* for plasmid transfer. Transconjugants were exposed to 50 μg kanamycin ml^{-1} to select against *E. coli*, 10 μg thiamphenicol ml^{-1} to select for plasmids, and subsequently, 5 μg erythromycin ml^{-1} to select for insertion of the group II intron into the chromosome. Insertion of the group II intron into erythromycin resistant clones was confirmed by PCR using the primers listed in **Table S9**.

The *clnRAB* coding sequence and apparent promoter (pMC649) were introduced into the *Tn*916 transposon of BS49 as MC951 (21). MC951 was then mated with *C. difficile* strains MC885 and MC935 to generate MC950 and MC953, respectively. Transconjugants were exposed to 50 μg kanamycin ml^{-1} to select against *B. subtilis* and 5 μg erythromycin ml^{-1} to select for integration of the transposon. Insertion of the genes was confirmed by PCR using the primers listed in **Table S9**. Complete information on plasmid construction is available in the supplemental materials (**Table S10**).

RNA sequencing (RNA-seq)

Active cultures of 630Δ*erm* or the *clnR* mutant were diluted to approximately OD_{600} 0.05 in BHIS alone or with 2 μg LL-37 ml^{-1} and grown to OD_{600} 0.5 for harvesting. RNA was extracted and DNase I treated as previously described (19, 57). rRNA was depleted from the total RNA using the Bacterial Ribo-Zero™ rRNA Removal Kit (EpiCentre, Madison,

USA) following the manufacturer's instructions. cDNA libraries were prepared with the ScriptSeq v2 RNA-Seq library preparation kit (Epicentre, Madison, USA). Briefly, the rRNA depleted sample was fragmented using an RNA fragmentation solution prior to cDNA synthesis. The fragmented RNA was further reverse transcribed using random hexamer primers containing a tagging sequence at their 5′ ends, 3′ tagging was accomplished using the Terminal-Tagging Oligo (TTO). The di-tagged cDNA was purified using the AMPure™ XP (Agencourt, Beckmann-Coulter, USA). The di-tagged cDNA was further PCR amplified to add index and sequencing adapters, the amplified final library was purified using AmpureXP beads. The final pooled libraries were sequenced on the Illumina HiSeq3000 system in a Single-end (SE) 150 cycle format, each sample was sequenced to approximate depth of 8-12 million reads. Sequenced reads were aligned to the CD630Derm (GenBank Accession GCA_000953275.1) genome reference for the 630Derm strain of *C. difficile* using the STAR Aligner (version 2.4.0g1; (58)). Counts of reads that uniquely map to genes in the reference genome annotation were accumulated using htseq-count (HTSeq 0.6.1p1; (59)). Samples from two independent experiments were library size normalized separately in DESeq2 (60) and the resulting normalized gene read counts were used as the gene abundance estimation and imported into Excel for gene expression comparisons. Gene abundances from the two experiments were averaged, and data were analyzed using the Student's two-tailed t-test. Cluster of orthologous genes (COG) designations were assigned according to the NCBI COG database (2014 updated version) (61). Sample preparation and analyses were performed by the Yerkes Nonhuman Primate Genomics Core (Emory University). Raw data files are available in the NCBI-SRA database under accession number (pending).

Quantitative reverse transcription PCR analysis (qRT-PCR)

Active cultures were diluted to an OD_{600} of approximately 0.05 in BHIS alone or BHIS with antimicrobials. The antimicrobials used included: LL-37 (Anaspec), scrambled LL-37 (Anaspec), mCRAMP (Anaspec), SMAP-29 (Anaspec), ampicillin (Cayman Chemicals), vancomycin (Sigma Aldrich), nisin (MP Biomedicals), or polymyxin B (Sigma Aldrich). Cultures were harvested at an OD_{600} of 0.5, mixed with 1:1 ethanol:acetone on ice and stored at -80˚C. RNA was extracted, DNase I treated, and used to generate cDNA as described above for RNA sequencing. qRT-PCR reactions were performed using the Bioline Sensi-Fast SYBR and Fluroescein kit on a Roche LightCycler 96 instrument. Primers were designed with the assistance of the IDT PrimerQuest tool (Integrated DNA Technologies) and are listed in **Table S9**. Each qRT-PCR reaction was performed as technical triplicates for at least three biological replicates. The $\Delta\Delta C_t$ method was used to normalize expression to *rpoC,* an internal control transcript, for relative quantification (62). Statistical analysis of the results was performed using GraphPad Prism version 7 for Macintosh (GraphPad Software, La Jolla, GA) to perform either one- or two-way analysis of variance (ANOVA) with Dunnett's or Sidak's multiple-comparison test, as indicated.

Droplet Digital PCR (ddPCR)

RNA was extracted from cecal samples as previously described (23). RNA was subsequently DNase I treated and used to generate cDNA as described above for qRT-PCR. cDNA was diluted to a final concentration of 5 ng/μl RNA equivalent. Samples

were prepared in duplicate with 1.25 ng/μl cDNA, 70 nM each of forward and reverse primers (as listed in **Table S9**), and 1x QX200 ddPCR EvaGreen Supermix (Bio-Rad). 20 μl of each sample was loaded into a Bio-rad DG8 cartridge for droplet generation in a Bio-Rad QX200 Droplet Generator with 70 μl Droplet Generation Oil for EvaGreen (Bio-Rad) per sample. Droplets were transferred to an Eppendorf Twin-Tech 96-well plate, which was sealed with foil prior to PCR on a C1000 Touch thermal cycler with the following reaction parameters: 5 min at 95˚C, 40 rounds of 30 s at 95˚C and 1 min at 53˚C, 5 min at 4˚C, 5 min at 90˚C (all steps with 2˚C/s ramp). Droplets were then read on the Bio-Rad QX200 Droplet Reader. Samples without reverse transcriptase were run as a negative control and were used as reference to manually set the threshold values for positive calls in the QuantaSoft analysis software. Samples were only analyzed for *tcdA* and *tcdB* expression if *rpoC* transcripts were detected (as a housekeeping gene, the detection of *rpoC* indicates sufficient *C. difficile* genomic material was present in the sample). Statistical analysis of the results using GraphPad Prism version 7 for Macintosh (GraphPad Software, La Jolla, GA) to perform two-way ANOVA with Dunnett's multiple-comparison test.

Minimum inhibitory concentration (MIC) and minimum bactericidal concentration (MBC)

Minimum inhibitory concentrations (MIC) were determined as previously described (63). MICs were determined for LL-37 (Anaspec), ampicillin (Cayman Chemicals), vancomycin (Sigma Aldrich), nisin (MP Biomedicals), and polymyxin B (Sigma Aldrich). Briefly, overnight cultures of *C. difficile* strains were diluted 1:50 in Mueller-Hinton

Broth (Difco) and grown to OD_{600} of 0.45 (~5 x 10^7 CFU/ml). Cultures were then diluted 1:10 in MHB and seeded at a further 1:10 dilution in a round-bottom 96-well plate prepared with serial dilutions of antimicrobials for a starting concentration of ~5 x 10^5 CFU/ml. Plates were incubated for 24 h at 37°C in the anaerobic chamber. The MIC was determined as the lowest concentration of antimicrobial at which no growth was visible after 24 h. For MBC determination, the full volume of wells at concentrations at and above the MIC were transferred as a 1:10 dilution into BHIS and incubated for 24 h at 37°C in the anaerobic chamber. The minimum bactericidal concentration (MBC) was determined as the lowest concentration of antimicrobial at which no growth was visible after 24 h.

Western blots

C. difficile strains were grown in BHIS medium containing 0.2% fructose and 0.1% taurocholate, as previously described (21). Cultures were diluted into BHIS medium and grown to OD_{600} of ~0.5, then diluted 1:10 into TY medium with or without 2 μg LL-37 ml^{-1} and grown for 24 h at 37°C. Cells were harvested by centrifugation, resuspended in SDS-PAGE loading buffer (without dye) and mechanically disrupted as previously described (20, 64). Protein concentrations were assessed using a micro BCA assay (Thermo Scientific) and 8 μg of whole cell protein was loaded onto a 12% polyacrylamide gel (Bio-Rad). Proteins were subsequently transferred from the SDS-PAGE gel onto nitrocellulose membranes (0.45 μM; Bio-Rad), and probed with mouse anti-TcdA antibody (Novus Biologicals). Membranes were then washed and probed with goat anti-mouse secondary Alexa Fluor 488 antibody (Life Technologies). Imaging and

densitometry analyses were performed using a ChemiDoc MP and Image Lab Software (Bio-Rad). Three biological replicates were analyzed for each strain and condition. Statistical analyses were performed using a two-way ANOVA, followed by a Dunnett's multiple-comparison test.

Electrophoretic mobility shift assays (EMSAs)

Recombinant N-terminally His-tagged ClnR was produced by GenScript (Piscataway, NJ). Gene transcription in the *clnR* mutant complemented with His-tagged ClnR confirmed the functionality of this protein (**Table S11**). 5'-fluorescein-labeled DNA (10 ng per reaction; purified by extraction from a 4-20% TGX polyacrylamide gel) was incubated for 30 min at 37˚C with His-ClnR (0 – 8 μM) with 10 mM Tris, pH 7.4, 10 mM $MgCl_2$, 100 mM KCl, 7.5% glycerol, and 2mM DTT. 50 ng of salmon sperm DNA was added to each reaction as a noncompetitive inhibitor. In competition experiments, either 100 ng (10x) or 1 μg (100x) unlabeled target DNA (specific) or unlabeled P*spo0A* (nonspecific) DNA was incubated with His-ClnR (125 nM for P*cln* reactions, 8 μM for other targets) for 20 min at 37˚C prior to the addition of labeled P*clnR* DNA for a further 10 min incubation. Reactions were loaded onto a pre-run 4-20% TGX polyacrylamide gel (Bio-Rad) and imaged on a Typhoon phosphoimager (GE Lifesciences) using the 520 BP fluorescence channel. Images from at least three replicates were analyzed in ImageLab (Bio-Rad) to determine the density of signal in bound and unbound fractions. Using GraphPad Prism, apparent K_d values were calculated by non-linear regression using an equation for cooperative binding of $Y = F_{max}*((x/K_d)^n)/(1+(x/K_d)^n)$, where Y = the fraction of bound DNA, x = the concentration of ClnR, F_{max} = the saturation level of bound DNA,

K_d = the concentration of ClnR when half of the DNA is bound, and n = cooperativity coefficient (65).

Growth curves in minimal medium

Growth curves were performed using a minimal medium based on a previously described complete defined minimal media (CDMM), but lacking D-glucose as used by Cartman *et al*. and adjusted to pH 7.4 (33, 66). The base medium was supplemented with 10 mM D-glucose (Sigma-Aldrich), 10 mM D-fructose (Fisher), 10 mM D-mannose (BD Difco), 20 mM D-mannitol (Amresco), 20 mM N-acetylglucosamine (Chem-Impex), or 20 mM ethanolamine-HCl (Sigma-Aldrich), as noted. Growth curves in minimal medium (MM) were carried out as follows: log-phase cultures were grown to an OD_{600} of 0.5 in BHIS medium, then diluted 10-fold into MM. Diluted cultures were then used to inoculate minimal medium broth for growth assays at a starting OD_{600} of ~0.01 (2 ml into 23 ml of MM).

Animal studies

The Emory University Institutional Animal Care and Use Committee (IUCAC) approved all animal studies in advance. Male (n=6 per condition) and female (n=6 per condition) Syrian golden hamsters (*Mesocricetus auratus;* Charles River Laboratories) were housed individually in sterile cages within a biosafety level 2 facility in the Emory University Division of Animal Resources. Sterile water and rodent feed pellets were available for the animals to consume *ad libitum*. Hamsters were administered 30 mg/kg body weight clindamycin (Hospira) by oral gavage 7 days prior to inoculation with *C. difficile*, to

promote susceptibility to infection (20, 64). Spores were prepared as previously described (67, 68), stored in phosphate-buffered saline (PBS) with 1% bovine serum albumin. Spores were heated for 20 minutes at 60˚C and cooled to room temperature prior to inoculating hamsters. Hamsters were administered approximately 5,000 spores of strains 630Δ*erm, clnR* (MC885), or *clnA* (MC935) by oral gavage and monitored for signs of disease. Hamsters were considered moribund after ≥ 15% weight loss from maximum body weight or when lethargic, with or without concurrent diarrhea and wet tail. Hamsters were euthanized once reaching either of these criteria. Fecal samples were collected daily, and cecal samples were collected post-mortem at the time of morbidity. Colony forming units (CFU) in fecal and cecal samples were plated on TCCFA medium as described previously (21). Differences in CFU counts were analyzed using one-way ANOVA with Dunnett's multiple-comparison test, and differences in survival were analyzed using log-rank regression. Fisher's exact test was performed to examine differences in the numbers of animals with detectable CFU at 12 h.p.i. These statistical analyses were performed using GraphPad Prism version 7 for Macintosh (GraphPad Software, La Jolla, CA).

Germination assays

Spores were purified as described previously, with some modifications (20, 69). *C. difficile* strains were grown on 4-6 70:30 sporulation agar plates for 72 h to induce spore formation and allow for vegetative cell lysis. Cells were then scraped from the agar plates, resuspended in sterile water, briefly frozen at -80˚C, thawed at 37˚C, and left overnight at room temperature. Spore preparations were pelleted at 3200 x g for 20 min, washed in 10

ml of spore stock solution (1x PBS, 1% BSA), pelleted, and resuspended in 1 ml of spore stock solution. The spore suspension was then applied to a 12 ml, 50% sucrose solution and centrifuged at 3200 x g for 20 min. Following centrifugation, the supernatant was decanted and the spore pellet was checked by phase contrast microscopy to verify the elimination of vegetative cells. Sucrose purification was repeated, if necessary, to achieve >95% spore purity. Purified spores were diluted in spore stock solution to a stock concentration of OD_{600} = 3.0. Spores were heat activated for 30 min at 60˚C immediately prior to germination assessments. Activated spores were then diluted 1:10 into 800 μl BHIS with either 100 μl of 50 mM taurocholic acid or 100 μl dH_2O as a negative control, and the OD_{600} was then recorded every 2 min for 20 min. The percentage decrease in optical density was determined based on the starting OD_{600}. Assays were performed with spores from three independent spore preparations. Data from the three replicates was averaged and analyzed by a one-way ANOVA for each time point.

Sporulation assays

Sporulation efficiency was assessed as previously described (70). Briefly, mid-log *C. difficile* cultures at OD_{600} = 0.05 were plated on 70:30 plates and incubated anaerobically at 37˚C for 24 hours. Cells were scraped from the plate, resuspended in BHIS, and imaged on a Nikon Eclipse Ci-L microscope with an X100 Ph3 oil-immersion objective. At least 1,000 cells from at least 2 fields of view were assessed per strain and experiment. The percentage of spores was calculated as the number of spores divided by the total number of cells, multiplied by 100. The mean percentage of spores and the standard error

of the mean were calculated from three independent experiments and analyzed by two-way ANOVA.

Accession numbers.

C. difficile strain 630 (GenBank accession NC_009089.1); *C. difficile* strain R20291 (NC_013316.1). The locus tags for individual genes mentioned in the text are listed in **Table S8**.

Table 1. Induction of *clnR* is specific to LL-37-like cathelicidins

Antimicrobial[a]	**Relative *clnR* expression**[b, c]
LL-37	**530.1** ± 110.5
scrambled LL-37	1.7 ± 0.8
mCRAMP	**111.4** ± 27.3
SMAP-29	0.7 ± 0.1
Lysozyme	1.1 ± 0.3
Ampicillin	0.9 ± 0.2
Vancomycin	0.9 ± 0.1
Nisin	1.1 ± 0.4
Polymyxin B	1.2 ± 0.2

[a]Concentrations of antimicrobials used: LL-37 2 μg/ml, scrambled LL-37 2 μg/ml, mCRAMP 2 μg/ml, SMAP-29 0.35 μg/ml, lysozyme 1 mg/ml, ampicillin 4 μg/ml, vancomycin 0.5 μg/ml, nisin 7.5 μg/ml, polymyxin B 200 μg/ml

[b]Relative expression determined by qRT-PCR and normalized to 630Δ*erm* grown in BHIS without antimicrobials. Values are the mean of three replicates ± standard error of the mean.

[c]Bolded values indicate significant difference (adjusted P value < 0.05) from 630Δ*erm* grown in BHIS without antimicrobials and analyzed by one-way ANOVA and Dunnett's test for multiple comparisons.

Table 2. Doubling times of 630Δ*erm* and the *clnR* mutant in minimal media supplemented with metabolites, with or without LL-37

MM+[a]	strain	No LL-37	LL-37[c]
		Doubling time (h)[b]	**Doubling time (h)[b]**
--	630Δ*erm*	1.18 ± 0.04	§1.69 ± 0.23
	clnR	1.21 ± 0.13	*1.31 ± 0.10
Glucose	630Δ*erm*	0.96 ± 0.02	§1.20 ± 0.14
	clnR	*1.11 ± 0.07	1.16 ± 0.02
Fructose	630Δ*erm*	1.01 ± 0.03	1.25 ± 0.19
	clnR	1.12 ± 0.07	1.18 ± 0.02
Mannose	630Δ*erm*	0.99 ± 0.01	§1.15 ± 0.06
	clnR	*1.13 ± 0.08	1.14 ± 0.02
NAG	630Δ*erm*	1.07 ± 0.04	§1.62 ± 0.34
	clnR	1.25 ± 0.11	1.57 ± 0.18
Mannitol	630Δ*erm*	0.93 ± 0.14	1.15 ± 0.06
	clnR	1.02 ± 0.06	1.09 ± 0.02
EA	630Δ*erm*	1.10 ± 0.17	1.66 ± 0.49
	clnR	1.44 ± 0.31	1.76 ± 0.37

[a]Strains were grown in MM with additional nutrients as listed: 10mM glucose, 10 mM fructose, 10 mM mannose, 20 mM N-acetylglucosamine (NAG), 20 mM mannitol, 20 mM ethanolamine (EA)

[b]Doubling time was calculated during the period of maximal growth (hours 4-6 post-inoculation), where $t_d = \ln(2)/\mu$, where $\mu = (\ln(OD_{t2}) - \ln(OD_{t1}))/(t_2 - t_1)$ (71, 72). Values shown are the average of at least three independent experiments ± standard deviation. Data were analyzed by Student's unpaired t-test; * indicates $P < 0.05$ comparing 630Δ*erm* to *clnR* in the same substrate (columns). § indicates $P < 0.05$ comparing either 630Δ*erm* or *clnR* in the same substrate, with or without LL-37 (rows).

[c]LL-37, 0.5 μg/ml

Table S1. Genes differentially expressed in LL-37

Gene[a]	Fold change in LL-37[b]	Product	COG[c]	*p*[d]
Induced in LL-37				
CD630_16180 (clnA)	202.99	ABC-type transport system multidrug-family ATP-binding protein	V	0.02
CD630_16190 (clnB)	192.16	ABC-type transport system multidrug-family permease	-	0.00
CD630_16170 (clnR)	186.82	Transcriptional regulator GntR family	K	0.00
CD630_16100	64.45	conserved hypothetical protein	-	0.00
CD630_16110	34.77	conserved hypothetical protein	-	0.03
CD630_16090	30.62	conserved hypothetical protein	-	0.03
CD630_16070	30.25	ABC-type transport system multidrug-family ATP-binding protein	V	0.01
CD630_12400 (vanZ)	28.43	Teicoplanin resistance protein	V	0.01
CD630_23410 (abfD)	14.81	Gamma-aminobutyrate metabolism dehydratase/isomerase	Q	0.00
CD630_23820	13.76	putative pyridoxal phosphate-dependent transferase	E	0.05
CD630_23810 (iorA)	13.66	Indole pyruvate ferredoxin/flavodoxin oxidoreductase	C	0.01
CD630_23390 (cat2)	13.27	4-hydroxybutyrate CoA transferase	C	0.02
CD630_23400	13.14	uncharacterised protein	-	0.05
CD630_23380 (4hbD)	12.95	4-hydroxybutyrate dehydrogenase	C	0.01
CD630_23420 (sucD)	12.71	Succinate-semialdehyde dehydrogenase	C	0.01
CD630_23430 (cat1)	11.85	Succinyl-CoA:coenzyme A transferase	C	0.01
CD630_23440	10.85	putative membrane protein (butyrate conversion)	R	0.01
CD630_23800 (iorB)	10.81	Indole pyruvate ferredoxin/flavodoxin oxidoreductase	C	0.01
CD630_12382	5.60	Fragment of conserved hypothetical protein	-	0.00
CD630_05500	5.52	putative membrane protein	-	0.05
CD630_18870 (csfU)	5.34	Extracytoplasmic function (ECF) sigma factor	K	0.00
CD630_05490	4.74	conserved hypothetical protein	-	0.05
CD630_18890	4.54	ABC-type transport system multidrug-family ATP-binding protein	V	0.00
CD630_25560	4.24	PTS system fructose/mannitol-family IIAB component	GT	0.02
CD630_16990 (ribE)	4.23	Riboflavin synthase alpha subunit	H	0.03
CD630_04900	4.13	putative sugar-phosphate dehydrogenase	ER	0.05
CD630_04980	4.13	putative cell-division FtsK/SpoIIIE-family protein	D	0.01

		Tn5397 CTn3-Orf21		
CD630_04960	4.13	putative conjugative transposon protein DUF961 family Tn5397 CTn3-Orf23	-	0.04
CD630_33740	3.92	putative conjugative transposon protein Tn916-like CTn7-Orf8	-	0.01
CD630_04970	3.86	putative conjugative transposon protein DUF961 family Tn5397 CTn3-Orf22	-	0.01
CD630_18880 (rsiU)	3.69	Extracytoplasmic function (ECF) anti-sigma factor	-	0.00
CD630_17000 (ribD)	3.65	Riboflavin biosynthesis protein	H	0.02
CD630_05000	3.61	putative antirestriction protein Tn5397 CTn3-Orf18	-	0.01
CD630_18900	3.60	ABC-type transport system multidrug-family permease	-	0.01
CD630_10590 (thlA1)	3.56	Acetoacetyl-CoA thiolase 1	I	0.04
CD630_05060	3.54	Reverse transcriptase/maturase/endonuclease Group II intron	V	0.00
CD630_10580 (hbd)	3.51	3-hydroxybutyryl-CoA dehydrogenase	I	0.05
CD630_04670	3.43	putative hydrolase HAD superfamily subfamily IIB	HR	0.00
CD630_04780 (spaF)	3.43	ABC-type transport system lantibiotic/multidrug-family ATP-binding protein	V	0.02
CD630_33730 (mgtA)	3.39	Magnesium-transporting ATPase P-type Tn916-like CTn7-Orf7	P	0.04
CD630_03580	3.38	putative conjugative transposon protein Tn916-like CTn1-Orf3	-	0.02
CD630_05102	3.35	Fragment of putative conjugative transposon protein Tn5397 CTn3-Orf5	-	0.00
CD630_05101	3.31	putative conjugative transposon protein Tn5397 CTn3-Orf8	-	0.00
CD630_15510 (hisH)	3.29	Imidazole glycerol phosphate synthase subunit	E	0.00
CD630_05103	3.27	putative conjugative transposon protein Tn5397 CTn3-Orf4	-	0.03
CD630_02910	3.25	putative peptidase M20A family	E	0.01
CD630_10560 (etfA3)	3.22	Electron transfer flavoprotein subunit alpha	C	0.03
CD630_16120	3.18	putative amidohydrolase	Q	0.01
CD630_23790 (buk2)	3.13	Butyrate kinase	C	0.01
CD630_15500 (hisB)	3.12	Imidazoleglycerol-phosphate dehydratase	E	0.00
CD630_15540 (hisI)	3.10	Histidine biosynthesis bifunctional protein	E	0.02
CD630_10550 (etfB3)	3.07	Electron transfer flavoproteins subunit beta	C	0.02
CD630_05100	3.07	putative RNA polymerase sigma factor Tn5397 CTn3-Orf7	K	0.00

CD630_18020	3.05	putative hydrolase metallo-beta-lactamase superfamily	R	0.04
CD630_08530 (oppB)	3.02	ABC-type transport system oligopeptide-family permease	EP	0.04
CD630_10570 (crt2)	2.97	3-hydroxybutyryl-CoA dehydratase (Crotonase)	I	0.03
CD630_14240	2.97	conserved hypothetical protein	-	0.00
CD630_05770	2.96	conserved hypothetical protein	R	0.01
CD630_33750 (mgtC)	2.96	Magnesium-transporting ATPase protein Tn916-like CTn7-Orf10	S	0.00
CD630_21640 (ldh)	2.95	L-lactate dehydrogenase	C	0.00
CD630_10540 (bcd2)	2.94	Butyryl-CoA dehydrogenase	I	0.02
CD630_15470 (hisZ)	2.92	ATP phosphoribosyltransferase regulatory subunit	E	0.04
CD630_20140 (ilvD)	2.90	Dihydroxy-acid dehydratase	EG	0.00
CD630_08570 (oppF)	2.88	Fragment of ABC-type transport system oligopeptide-family ATP-binding protein	-	0.03
CD630_15490 (hisC)	2.86	Histidinol-phosphate aminotransferase	E	0.05
CD630_15520 (hisA)	2.80	1-(5-phosphoribosyl)-5-[(5-phosphoribosylamino)m ethylideneamino]imidazole-4-carboxamide isomerase	E	0.04
CD630_16590	2.69	Cation-transporting ATPase	P	0.00
CD630_20270	2.69	N-carbamoyl-L-amino acid hydrolase	E	0.05
CD630_33911	2.66	conserved hypothetical protein	-	0.02
CD630_16310 (sodA)	2.59	spore coat protein-superoxide dismutase (Mn)	P	0.01
CD630_03830	2.58	putative cell-division FtsK/SpoIIIE-family protein Tn916-like CTn1-Orf28	D	0.01
CD630_10860	2.54	putative peptidase M20D family	R	0.03
CD630_21930 (cwp24)	2.54	putative cell wall-binding protein	-	0.05
CD630_20910	2.49	putative xanthine/uracil permease	F	0.01
CD630_17880	2.48	putative membrane protein	-	0.03
CD630_16740	2.47	putative NADPH-dependent FMN reductase	R	0.00
CD630_22330 (asrA)	2.43	Anaerobic sulfite reductase subunit A	C	0.04
CD630_17021 (thiS)	2.41	Thiamine biosynthesis protein	H	0.01
CD630_20280 (racX)	2.39	putative aspartate racemase	M	0.00
CD630_27090	2.37	putative oxidoreductase	I	0.01
CD630_09260	2.36	putative phage protein	-	0.05
CD630_13900	2.35	conserved hypothetical protein DUF819 family	S	0.00
CD630_21270	2.34	putative exported protein	-	0.04
CD630_27840 (cwp6)	2.30	putative N-acetylmuramoyl-L-alanineamidase autolysin	M	0.01

CD630_23090	2.29	conserved hypothetical protein	-	0.01
CD630_04800 (spaG)	2.29	ABC-type transport system lantibiotic/multidrug-family permease	S	0.04
CD630_04890	2.26	putative phosphoribosylaminoimidazole-succinocarb oxamide synthetase	F	0.00
CD630_17151	2.24	conserved hypothetical protein	-	0.02
CD630_15100	2.24	conserved hypothetical protein	-	0.01
CD630_07290 (gcvH)	2.23	Glycine cleavage system H protein	E	0.04
CD630_20751	2.21	conserved hypothetical protein	-	0.02
CD630_16130 (cotA)	2.18	spore coat assembly protein	-	0.02
CD630_10980	2.17	Two-component sensor histidine kinase Tn1549-like CTn4-Orf27	T	0.00
CD630_10850	2.17	putative membrane protein	E	0.02
CD630_15560	2.16	putative polysaccharide deacetylase	G	0.00
CD630_15120 (panC)	2.15	Pantothenate synthetase	H	0.02
CD630_16200	2.15	Transporter Major Facilitator Superfamily (MFS)	G	0.00
CD630_33790	2.14	putative conjugative transposon proteinTn916-like CTn7-Orf15	-	0.01
CD630_29620	2.13	conserved hypothetical protein	-	0.00
CD630_04440 (ortB)	2.09	2-amino-4-ketopentanoate thiolase beta subunit	E	0.01
CD630_17170	2.07	uncharacterised protein	S	0.04
CD630_27250	2.07	putative monogalactosyldiacylglycerol synthase	M	0.02
CD630_25171	2.04	putative phage protein	-	0.00
CD630_19440	2.03	Fragment of conserved hypothetical protein	-	0.00
CD630_26820 (pfo)	2.03	Pyruvate-ferredoxin oxidoreductase	C	0.02
CD630_15660 (ilvB)	2.01	Acetolactate synthase large subunit	EH	0.04
CD630_19670	2.01	uncharacterised protein	-	0.00
Reduced in LL-37				
CD630_23310 (mtlD)	0.12	Mannitol-1-phosphate 5-dehydrogenase	G	0.00
CD630_26140	0.12	uncharacterised protein DegV family	S	0.00
CD630_23320 (mtlF)	0.12	PTS system mannitol-specific EIIA component	G	0.00
CD630_23330 (mtlR)	0.14	Transcription antiterminator PTS operonregulator	K	0.00
CD630_23340 (mtlA)	0.15	PTS system mannitol-specific IICB component	G	0.00
CD630_19120 (eutA)	0.20	Ethanolamine reactivating factor for ammonialyase eutBC	E	0.02
CD630_19150 (eutL)	0.21	Ethanolamine carboxysome structural protein	E	0.00
CD630_31750 (cggR)	0.22	Transcriptional regulator SorC family	K	0.05
CD630_01631	0.22	conserved hypothetical protein	-	0.00
CD630_09950	0.23	putative D-3-phosphoglycerate dehydrogenase	HE	0.01

(serA)				
CD630_24291	0.23	putative 4Fe-4S ferredoxin iron-sulfur binding domain protein	C	0.02
CD630_09080	0.23	putative phage protein	-	0.00
CD630_09960	0.24	conserved hypothetical protein	S	0.01
CD630_30270	0.25	PTS system glucose-like IIA component	G	0.02
CD630_19220 *(eutN)*	0.25	Ethanolamine carboxysome structural protein	QC	0.02
CD630_20160	0.26	conserved hypothetical protein	-	0.03
23S_rRNA	0.27	23S ribosomal RNA	-	0.03
CD630_09360	0.28	putative phage endodeoxyribonuclease RusA-like	L	0.01
CD630_29341	0.29	putative phage protein	-	0.05
CD630_29470	0.30	putative phage protein	-	0.02
CD630_29320	0.30	putative phage protein	-	0.03
CD630_28780 *(fhuD)*	0.30	ABC-type transport system ferrichrome-specific extracellular solute-binding protein	P	0.00
CD630_14890 *(metN)*	0.32	ABC-type transport system methionine-specific ATP-binding protein	P	0.03
CD630_14900 *(met I)*	0.32	ABC-type transport system methionine-specific permease	P	0.03
CD630_16632	0.32	conserved hypothetical protein	-	0.02
CD630_17452	0.34	conserved hypothetical protein	R	0.03
CD630_21710	0.34	Fragment of putative sodium:dicarboxylate symporter	-	0.01
CD630_31360 *(bglA7)*	0.35	6-phospho-beta-glucosidase	G	0.00
CD630_26640 *(murE)*	0.35	UDP-N-acetylmuramyl-tripeptide synthetase	M	0.00
CD630_28770 *(fhuB)*	0.35	ABC-type transport system ferrichrome-specific permease	P	0.00
CD630_36010	0.35	D-alanyl-D-alanine carboxypeptidase M15 family	M	0.01
CD630_31000	0.36	putative C4-dicarboxylate anaerobic carrier Dcu family	S	0.05
CD630_18470	0.36	putative conjugative transposon protein Tn1549-like CTn5-Orf3	-	0.00
CD630_31150 *(bglA4)*	0.37	6-phospho-beta-glucosidase	G	0.00
CD630_13610	0.37	putative phage protein	-	0.00
CD630_32570	0.37	putative polysaccharide deacetylase	G	0.02
CD630_30340	0.38	Transcriptional regulator TrmB family	K	0.01
CD630_27491	0.38	Autoinducer prepeptide	-	0.00
CD630_25150	0.38	putative L-aspartate-beta-decarboxylase	E	0.04
CD630_27640	0.38	putative hydrolase HAD superfamily IIB subfamily	R	0.00
CD630_26710	0.38	ABC-type transport system ATP-binding protein putative oligopeptide transport system	EP	0.03
CD630_33440	0.39	putative cell-division FtsK/SpoIIIE-family protein Tn916-like CTn6-Orf22	D	0.01
CD630_09340	0.39	putative phage protein	-	0.01
CD630_35370 *(phnH)*	0.39	putative phosphonate metabolism protein	P	0.01
CD630_31370 *(bglF5)*	0.39	PTS system beta-glucoside-specific IIAB component	G	0.02
CD630_30360	0.39	Transporter Major Facilitator Superfamily (MFS)	E	0.02

CD630_08450	0.40	putative nuclease	-	0.03
CD630_22010	0.40	Transporter Major Facilitator Superfamily (MFS)	G	0.05
CD630_25090	0.40	putative glycoside hydrolase family 4	G	0.02
CD630_23710 (nadB)	0.40	L-aspartate oxidase (Quinolinate synthetase B)	H	0.00
CD630_23720 (nadA)	0.40	Quinolinate synthetase A	H	0.00
CD630_13640	0.40	putative phage XkdM-like protein	-	0.00
CD630_19180 (eutK)	0.40	Ethanolamine carboxysome strutural protein	QC	0.04
CD630_11540	0.40	Transcriptional regulator PadR family	K	0.02
CD630_03270 (cbiO)	0.40	ABC-type transport system cobalt-specific ATP-binding protein	P	0.00
CD630_05790	0.40	Transcriptional regulator TetR family	K	0.03
CD630_30990	0.40	putative amidohydrolase M20D family	R	0.03
CD630_03260 (cbiQ1)	0.41	ABC-type transport system cobalt-specific permease	P	0.00
CD630_18860	0.41	Transcriptional regulator PadR family	K	0.01
CD630_30720	0.41	conserved hypothetical protein	S	0.02
CD630_03140	0.41	putative membrane protein	S	0.02
CD630_26860	0.41	putative membrane protein	-	0.01
CD630_24620 (grpE)	0.41	HSP-70 cofactor	O	0.00
CD630_29420	0.41	putative phage resolvase/integrase	-	0.00
CD630_11261	0.42	Transcriptional regulator HTH-type	K	0.00
CD630_29400	0.42	putative phage protein	-	0.04
CD630_17540	0.42	ABC-type transport system multidrug-family permease	-	0.02
CD630_03240 (cbiM)	0.42	Cobalamin biosynthesis protein	P	0.01
CD630_23700 (nadC)	0.42	Nicotinate-nucleotide pyrophosphorylase	H	0.00
CD630_06140	0.43	conserved hypothetical protein	-	0.03
CD630_26700	0.43	ABC-type transport system ATP-binding protein putative oligopeptide transport system	E	0.02
CD630_01060 (cwlD)	0.43	Germination-specific N-acetylmuramoyl-L-alanineamidase Autolysin	M	0.01
CD630_26650	0.43	Transcriptional regulator AraC family	K	0.01
CD630_26660 (ptsG-A)	0.43	PTS system glucose-specific IIA component	G	0.05
CD630_03901	0.43	conserved hypothetical protein	-	0.02
CD630_25160 (ansB)	0.44	L-asparaginase	EJ	0.03
CD630_29360	0.44	putative phage protein	-	0.01
CD630_05670	0.44	uncharacterised protein DegV family	S	0.03
CD630_01250	0.44	putative cell wall endopeptidase	M	0.05
CD630_04090	0.44	putative replication initiation protein Tn1549-like CTn2-Orf2	-	0.03
CD630_29440	0.44	putative phage essential recombination functionprotein	-	0.04
CD630_12700	0.45	Two-component sensor histidine kinase	T	0.00
CD630_30260	0.45	conserved hypothetical protein	TK	0.00
CD630_11710 (etfB4)	0.45	Electron transfer flavoprotein subunit alpha	C	0.01

CD630_29430	0.45	putative phage replication protein	L	0.01
CD630_09170	0.45	putative phage recombination protein Bet	-	0.00
CD630_06240	0.45	putative transcriptional regulator activator	S	0.00
CD630_29310	0.45	putative phage endodeoxyribonuclease RusA-like	-	0.05
CD630_29710 (bioY)	0.45	Biotin synthase	R	0.01
CD630_01930 (groS)	0.46	chaperonin	O	0.00
CD630_20451	0.46	conserved hypothetical protein	-	0.00
CD630_13450	0.46	Transcriptional regulator PadR family	K	0.00
CD630_26870	0.46	conserved hypothetical protein	-	0.01
CD630_29490	0.46	Transcriptional regulator Phage-type	-	0.00
CD630_05780	0.47	Transporter Major Facilitator Superfamily (MFS)	-	0.00
CD630_18270	0.47	Transcriptional regulator MarR family	K	0.03
CD630_30250	0.47	putative ferredoxin iron-sulphur domain-containing protein	C	0.01
CD630_32090	0.47	Transcriptional regulator PadR family	K	0.01
CD630_00470 (ispD)	0.48	2-C-methyl-D-erythritol 4-phosphatecytidylyltransferase	I	0.03
CD630_21430	0.48	Transcriptional regulator HTH-type	-	0.02
CD630_24610 (dnaK)	0.48	Chaperone protein dnaK (Heat shock protein 70)	O	0.01
CD630_25110	0.48	Transcription antiterminator PTS operon regulator	K	0.03
CD630_32100	0.48	conserved hypothetical protein	E	0.03
CD630_32620 (pstA)	0.48	ABC-type transport system phosphate-specific permease	P	0.05
CD630_25100	0.48	PTS system glucose-like IIBC component	G	0.04
CD630_27880	0.48	putative membrane protein GtrA family	S	0.00
CD630_13720	0.48	putative phage XkdT-like protein	-	0.00
CD630_13660	0.48	putative phage tail protein	-	0.05
CD630_19210	0.48	putative ethanolamine utilization protein	-	0.02
CD630_10280	0.48	putative signaling protein	TK	0.03
CD630_21510	0.48	putative membrane protein DUF819 family	S	0.01
CD630_23300 (xpt)	0.49	Xanthine phosphoribosyltransferase (XPRTase)	F	0.04
CD630_15800 (hom2)	0.49	Homoserine dehydrogenase	E	0.01
CD630_24630 (hrcA)	0.49	Transcriptional regulator Heat-inducibler epressor	K	0.01
CD630_32220 (sdaB)	0.49	L-serine dehydratase	E	0.00
CD630_27500 (agrB)	0.49	Accessory gene regulator	OTK	0.00
CD630_32600 (phoU)	0.49	Phosphate uptake regulator	P	0.00
CD630_13460	0.50	conserved hypothetical protein DUF1700	S	0.00
CD630_26691	0.50	putative Na(+)/H(+) antiporter	P	0.01
CD630_29330	0.50	Hypothetical protein	J	0.01
CD630_03250 (cbiN)	0.50	ABC-type transport system cobalt-specific extracellular solute-binding protein	P	0.03

[a]Gene accession numbers are given for strain 630.

[b]Ratio of no LL-37/with LL-37 as determined by RNA sequencing analysis of 630Δ*erm* grown in BHIS alone or BHIS supplemented with 2 μg/ml LL-37 as described in Methods. Genes are included in this list if they had ≥ 2-fold increase or decrease in expression and a *P* value ≤ 0.05 by Student's two-tailed t-test.
[c]COG (classification of gene) designations are based on the 2014 COG database. Letter designations correspond to the categories listed in the table below.
[d]*P*-values determined by Student's two-tailed *t*-test.

A	RNA processing and modification
B	Chromatin Structure and dynamics
C	Energy production and conversion
D	Cell cycle control and mitosis
E	Amino Acid metabolism and transport
F	Nucleotide metabolism and transport
G	Carbohydrate metabolism and transport
H	Coenzyme metabolism
I	Lipid metabolism
J	Translation
K	Transcription
L	Replication and repair
M	Cell wall/membrane/envelop biogenesis
N	Cell motility
O	Post-translational modification, protein turnover, chaperone functions
P	Inorganic ion transport and metabolism
Q	Secondary Structure
T	Signal Transduction
U	Intracellular trafficking and secretion
Y	Nuclear structure
Z	Cytoskeleton
R	General Functional Prediction only
S	Function Unknown
-	Unassigned

Table S2. LL-37 MIC and MBC values for *clnR* and *clnA* mutants

	MIC[a]	MBC[b]
630Δ*erm*	15	20
clnR	15	30
clnA	15	20

[a] Minimum inhibitory concentration of LL-37 (μg/ml).
[b] Minimum bactericidal concentration of LL-37 (μg/ml).

Table S3. MIC values for *clnR* and *clnA* mutants in various antimicrobials

	Van[a]	Amp	PmB	Nis
630Δ*erm*	1	4	500	360
clnR	1	4	500	360
clnA	1	4	500	360

[a]Values shown are μg/ml. Van: vancomycin, Amp: ampicillin, PmB: polymyxin B, Nis: nisin.

Table S4. Genes differentially expressed in a *clnR* mutant in the presence/absence of LL-37

Gene[a]	*clnR*/ WT[b]	Product	COG[c]	*p*[d]
ClnR activates (without LL-37)				
CD630_16632	0.22	conserved hypothetical protein	-	0.00
CD630_23030	0.22	Fragment of putative phage transcriptional repressor	-	0.00
CD630_35370 (phnH)	0.22	putative phosphonate metabolism protein	P	0.00
CD630_19280	0.22	putative membrane protein	D	0.00
CD630_29341	0.23	putative phage protein	-	0.01
CD630_01631	0.24	conserved hypothetical protein	-	0.01
CD630_13700	0.25	putative phage XkdS-like protein	-	0.02
CD630_32770	0.26	PTS system mannose/fructose/sorbose IIC component	G	0.00
CD630_29330	0.32	Hypothetical protein	J	0.01
CD630_04090	0.33	putative replication initiation protein Tn1549-like CTn2-Orf2	-	0.03
CD630_00410	0.33	PTS system galactitol-specific IIA component	GT	0.00
CD630_11980 (spoIIIAG)	0.33	Stage III sporulation protein AG	-	0.00
CD630_07400	0.35	putative pyridoxal phosphate-dependent aminotransferase	E	0.01
CD630_07420	0.37	putative ethanolamine transporter	E	0.00
CD630_36361	0.38	conserved hypothetical protein	-	0.01
CD630_29370	0.39	putative phage protein	-	0.01
CD630_01350	0.41	PTS system lactose/cellobiose-family IIA component	G	0.03
CD630_23260	0.41	PTS system fructose/mannitol family IIBc omponent	G	0.00
CD630_24170	0.42	PTS system Sorbitol-like IIB component	G	0.00
CD630_26870	0.43	conserved hypothetical protein	-	0.00
CD630_01981	0.43	conserved hypothetical protein	-	0.04
CD630_02850	0.44	PTS system mannose/fructose/sorbose IIB component	G	0.00
CD630_29490	0.44	Transcriptional regulator Phage-type	-	0.00
CD630_13630	0.45	putative phage XkdK-like protein	-	0.02
CD630_29360	0.45	putative phage protein	-	0.01
CD630_16490	0.45	ABC-type transport system iron-family ATP-binding protein	P	0.02
CD630_21970	0.46	putative ferredoxin/flavodoxin oxidoreductase	C	0.02
CD630_12332	0.46	conserved hypothetical protein	-	0.03
CD630_26570	0.49	conserved hypothetical protein	-	0.01
CD630_04200	0.49	putative cell surface protein Tn1549-like CTn2-Orf15	R	0.01
CD630_21021	0.49	conserved hypothetical protein	-	0.01
CD630_04880 (orr)	0.50	putative small multidrug resistance SugE-like protein	P	0.04
ClnR represses (without LL-37)				
CD630_16180 (clnA)	57.26	ABC-type transport system multidrug-family ATP-binding protein	V	0.02
CD630_16190	53.69	ABC-type transport system multidrug-family	-	0.00

(clnB)		permease		
CD630_12400	21.50	Teicoplanin resistance protein		0.02
(vanZ)			V	
CD630_33370	3.37	putative membrane protein Tn916-like CTn6-Orf14	B	0.01
CD630_07970	2.96	putative pyruvate carboxyltransferase	E	0.01
CD630_16310	2.70	spore coat protein-superoxide dismutase		0.00
(sodA)			P	
CD630_01820	2.47	conserved hypothetical protein	-	0.02
CD630_18840	2.43	conserved hypothetical protein	-	0.04
CD630_22180	2.43	Fragment of putative integrase		0.04
(int2)			-	
CD630_03710	2.43	putative conjugative transposon protein Tn916-like CTn1-Orf16	-	0.04
CD630_15111	2.26	conserved hypothetical protein	-	0.04
CD630_16680	2.13	putative membrane protein	-	0.00
CD630_27340	2.09	putative Na+/H+ antiporter NhaC family	C	0.00
CD630_12450	2.08	conserved hypothetical protein	-	0.03
ClnR activates (with LL-37)				
CD630_23540	0.06	Betaine reductase component B subunit		0.00
(grdE)			-	
CD630_23520	0.07	Glycine reductase complex selenoprotein A		0.00
(grdA)		(selenocysteine)	-	
CD630_02850	0.07	PTS system mannose/fructose/sorbose IIB component	G	0.00
CD630_02840	0.08	PTS system mannose/fructose/sorbose IIA component	G	0.00
CD630_23550	0.09	Thioredoxin 2		0.01
(trxA2)			O	
CD630_23260	0.09	PTS system fructose/mannitol family IIB component	G	0.01
CD630_02880	0.10	PTS system mannose/fructose/sorbose IIC component	G	0.00
CD630_16080	0.13	ABC-type transport system multidrug-family permease	-	0.00
CD630_02890	0.13	PTS system mannose/fructose/sorbose IID component	G	0.00
CD630_02860	0.13	PTS system mannose/fructose/sorbose IIA component	G	0.01
CD630_16060	0.13	Transcriptional regulator GntR family	K	0.00
CD630_16100	0.13	conserved hypothetical protein	-	0.00
CD630_16110	0.14	conserved hypothetical protein	-	0.00
CD630_02870	0.14	PTS system mannose/fructose/sorbose IIB component	G	0.00
CD630_23570	0.14	putative glycine reductase complex component		0.02
(grdX)			-	
CD630_16090	0.15	conserved hypothetical protein	-	0.00
CD630_23560	0.15	Thioredoxin reductase 3		0.02
(trxB3)			O	
CD630_23490	0.16	Glycine reductase complex component C		0.01
(grdC)			I	
CD630_16070	0.16	ABC-type transport system multidrug-family ATP-	V	0.00

		binding protein		
CD630_20751	0.18	conserved hypothetical protein	-	0.00
CD630_29290	0.18	putative phage protein	-	0.00
CD630_04200	0.20	putative cell surface protein Tn1549-like CTn2-Orf15	R	0.00
CD630_23240	0.21	putative sugar-phosphate dehydrogenase	ER	0.05
CD630_33740	0.21	putative conjugative transposon protein Tn916-like CTn7-Orf8	-	0.00
CD630_23030	0.21	Fragment of putative phage transcriptional repressor	-	0.01
CD630_26000 (cstA)	0.22	Carbon starvation protein	T	0.00
CD630_23810 (iorA)	0.22	Indole pyruvate ferredoxin/flavodoxin oxidoreductase	C	0.00
CD630_04670	0.24	putative hydrolase HAD superfamily subfamily IIB	HR	0.00
CD630_23800 (iorB)	0.24	Indole pyruvate ferredoxin/flavodoxin oxidoreductase	C	0.00
CD630_25990	0.24	putative transcriptional regulator	J	0.04
CD630_02900	0.25	conserved hypothetical protein	-	0.00
CD630_23820	0.26	putative pyridoxal phosphate-dependent transferase	E	0.00
CD630_29410	0.27	putative phage single-strand DNA-binding protein	L	0.04
CD630_16180 (clnA)	0.27	ABC-type transport system multidrug-family ATP-binding protein	V	0.00
CD630_33750 (mgtC)	0.27	Magnesium-transporting ATPase protein Tn916-like CTn7-Orf10	S	0.00
CD630_16190 (clnB)	0.27	ABC-type transport system multidrug-family permease	-	0.01
CD630_33730 (mgtA)	0.27	Magnesium-transporting ATPase P-type Tn916-like CTn7-Orf7	P	0.00
CD630_00330	0.28	putative glycoside hydrolase	G	0.05
CD630_07400	0.28	putative pyridoxal phosphate-dependent aminotransferase	E	0.04
CD630_05490	0.28	conserved hypothetical protein	-	0.00
CD630_33741	0.29	putative conjugative transposon protein Tn916-like CTn7-Orf9	-	0.00
CD630_28130 (garR)	0.30	Tartronate semialdehyde reductase	I	0.04
CD630_29370	0.31	putative phage protein	-	0.00
CD630_00220 (fusA1)	0.31	Elongation factor G	J	0.01
CD630_18570	0.31	putative cell wall hydrolase Tn1549-like CTn5-Orf13	M	0.04
CD630_18880 (rsiU)	0.32	Extracytoplasmic function (ECF) anti-sigma factor	-	0.00
CD630_05000	0.32	putative antirestriction protein Tn5397 CTn3-Orf18	V	0.01
CD630_17970	0.34	Coenzyme A disulfide reductase	R	0.04
CD630_01350	0.34	PTS system lactose/cellobiose-family IIA component	G	0.05
CD630_04960	0.34	putative conjugative transposon protein DUF961 family Tn5397 CTn3-Orf23	-	0.01
CD630_23480 (grdD)	0.34	Glycine reductase complex component C	I	0.01
CD630_04980	0.34	putative cell-division FtsK/SpoIIIE-family protein Tn5397 CTn3-Orf21	D	0.00

CD630_17000 (ribD)	0.35	Riboflavin biosynthesis protein	H	0.01
CD630_00450	0.35	putative sugar-phosphate aldolase	G	0.05
CD630_28620	0.36	putative peptidase M19 family	E	0.02
CD630_18560	0.36	putative hydrolase Tn1549-like CTn5-Orf12	U	0.00
CD630_15970	0.36	conserved hypothetical protein	-	0.00
CD630_28240	0.36	Fragment of putative membrane protein	-	0.02
CD630_33721	0.36	putative conjugative transposon protein Tn916-like CTn7-Orf5	-	0.00
CD630_04970	0.36	putative conjugative transposon protein DUF961 family Tn5397 CTn3-Orf22	-	0.01
CD630_05103	0.37	putative conjugative transposon proteinTn5397%2CCTn3-Orf4	-	0.01
CD630_04990	0.38	putative replication initiation factor Tn5397 CTn3-Orf20	L	0.00
CD630_22820	0.39	PTS system fructose/mannitol family IIA component	GT	0.02
CD630_04991	0.39	putative conjugative transposon protein Tn5397 CTn3-Orf19	-	0.01
CD630_02910	0.40	putative peptidase M20A family	E	0.01
CD630_16980 (ribBA)	0.40	GTP cyclohydrolase-2 Riboflavin biosynthesis protein	H	0.01
CD630_05100	0.40	putative RNA polymerase sigma factor Tn5397 CTn3-Orf7	K	0.00
CD630_17960	0.40	putative nitrite and sulfite reductase subunit	C	0.04
CD630_05102	0.40	Fragment of putative conjugative transposon protein Tn5397 CTn3-Orf5	-	0.00
CD630_05060	0.41	Reverse transcriptase/maturase/endonuclease Group II intron	V	0.00
CD630_33722	0.41	putative conjugative transposon protein Tn916-like CTn7-Orf6	-	0.00
CD630_23790 (buk2)	0.41	Butyrate kinase	C	0.00
CD630_18870 (csfU)	0.41	Extracytoplasmic function (ECF) sigma factor	K	0.00
CD630_28280	0.41	putative pyridoxal phosphate-dependent transferase	E	0.03
CD630_05101	0.41	putative conjugative transposon protein Tn5397 CTn3-Orf8	-	0.00
CD630_07390	0.42	putative exported protein	-	0.00
CD630_15431	0.43	conserved hypothetical protein	-	0.02
CD630_20750 (pbuX)	0.43	putative xanthine permease	F	0.00
CD630_28110	0.43	conserved hypothetical protein	S	0.01
CD630_08650	0.44	putative ADP-ribose binding protein	R	0.01
CD630_06790	0.45	conserved hypothetical protein	R	0.02
CD630_04890	0.45	putative phosphoribosylaminoimidazole-succinocarboxamide synthetase	F	0.00
CD630_23590	0.46	putative hydrolase HAD superfamily subfamily IIB	R	0.00
CD630_28590	0.46	putative D-aminoacylase	Q	0.02
CD630_18890	0.47	ABC-type transport system multidrug-family ATP-binding protein	V	0.00
CD630_06770	0.47	Extracytoplasmic function (ECF) sigma factor	K	0.00

(csfT)				
CD630_21600	0.47	putative membrane protein	V	0.02
CD630_16220	0.47	peptidase propeptide and ypeb domain protein	S	0.03
CD630_24020	0.47	putative cell wall hydrolase phosphatase-associated protein	M	0.01
CD630_18900	0.47	ABC-type transport system multidrug-family permease	O	0.01
CD630_04400 (cwp27)	0.47	putative cell wall binding protein	-	0.00
CD630_07170	0.48	Bifunctional carbon monoxide dehydrogenase/acetyl-CoA synthase accessory protein	D	0.05
CD630_29490	0.48	Transcriptional regulator Phage-type	-	0.00
CD630_27080 (aroE2)	0.48	Shikimate dehydrogenase 2	E	0.00
CD630_09370	0.48	putative phage anti-repressor	K	0.01
CD630_25670	0.49	PTS system mannose-specfic IIB component	G	0.01
CD630_05020	0.49	putative ATPase Tn5397 CTn3-Orf16	L	0.00
CD630_29300	0.49	putative phage anti-repressor protein	K	0.01
CD630_27840 (cwp6)	0.49	putative N-acetylmuramoyl-L-alanineamidase autolysin	M	0.00
CD630_01420	0.49	putative RNA-binding protein	J	0.03
CD630_22490	0.50	putative ATPase	R	0.00
CD630_21910	0.50	putative phosphoesterase	ER	0.01
CD630_23090	0.50	conserved hypothetical protein	-	0.04
ClnR represses (with LL-37)				
CD630_26140	7.62	uncharacterised protein DegV family	S	0.02
CD630_06680	4.19	Two-component response regulator	TK	0.01
CD630_06690	4.01	Two-component sensor histidine kinase	T	0.01
CD630_27491 (agrD)	3.46	Autoinducer prepeptide	-	0.00
CD630_11920	3.10	Stage III sporulation protein AA	S	0.04
CD630_24291	3.10	putative 4Fe-4S ferredoxin iron-sulfur binding domain protein	C	0.04
CD630_28370	2.74	putative membrane protein	S	0.05
CD630_04370	2.74	Fragment of integrase Tn1549-like CTn2	-	0.05
CD630_09780	2.52	Transcriptional regulator beta-lactams repressor Phage-type	-	0.01
CD630_22290	2.49	putative membrane protein	S	0.05
CD630_10950	2.48	ABC-type transport system multidrug-family permease Tn1549-like CTn4-Orf30	-	0.03
CD630_25150	2.45	putative L-aspartate-beta-decarboxylase	E	0.04
CD630_04640	2.45	putative beta-lactamase-like hydrolase	R	0.02
CD630_26640 (murE)	2.42	UDP-N-acetylmuramyl-tripeptide synthetase	M	0.01
CD630_09950 (serA)	2.40	putative D-3-phosphoglycerate dehydrogenase	HE	0.02
CD630_09960	2.34	conserved hypothetical protein	S	0.01
CD630_21510	2.34	putative membrane protein DUF819 family	S	0.01
CD630_33360	2.32	putative cell wall hydrolase Tn916-like CTn6-Orf13	M	0.00
CD630_01260	2.29	Stage III sporulation protein D	-	0.00

(spoIIID)				
CD630_30730	2.24	putative membrane protein	-	0.01
CD630_10970	2.22	ABC-type transport system multidrug-family ATP-binding protein Tn1549-like CTn4-Orf28	V	0.01
CD630_25290	2.18	conserved hypothetical protein	-	0.02
CD630_21710	2.18	Fragment of putative sodium:dicarboxylate symporter	-	0.04
CD630_08220	2.11	ABC-type transport system multidrug-family ATP-binding protein	V	0.02
CD630_26700	2.10	ABC-type transport system ATP-binding protein putative oligopeptide transport system	E	0.03
CD630_25940 (uraA)	2.10	ABC-type transport system uracil-specific permease	F	0.00
CD630_08230	2.05	ABC-type transport system multidrug-family permease	-	0.04
CD630_30230	2.03	conserved hypothetical protein	-	0.03
CD630_23750	2.03	uncharacterised protein	-	0.02

[a]Gene accession numbers are given for strain 630. Gene *CD630_20072 (ermB*) is excluded from these tables because it is an artifact of the insertional disruption used to generate the *clnR* mutant.
[b]Ratio of expression in *clnR* mutant/630Δ*erm*, as determined by RNA sequencing analysis of 630Δ*erm* and *clnR* grown in BHIS alone or BHIS supplemented with 2 μg/ml LL-37 as described in Methods. Fold-change represents the ratio of expression in *clnR*/630Δ*erm* in the condition indicated (with or without LL-37). Genes are included in this list if they had ≥ 2-fold increase or decrease in expression and a *P* value ≤ 0.05 by Student's two-tailed t-test.
[c]COG designations are based on the 2014 COG database. Letter designations correspond to the categories listed in the table associated with Table S1.
[d]*P*-values determined by Student's two-tailed t-test.

Table S5. Genes regulated by both ClnR and LL-37

Gene[a]	Fold change in LL-37[b]	*clnR* /WT[c]	*clnR*/WT (+ LL-37)[d]	Product
CD630_01631	0.22	0.24	1.63	spore coat protein-superoxide dismutase
CD630_02910	3.25	1.32	0.40	putative peptidase M20A family
CD630_04090	0.44	0.33	0.87	putative replication initiation protein Tn1549-like CTn2-Orf2
CD630_04670	3.43	1.44	0.24	putative hydrolase HAD superfamily subfamily IIB
CD630_04890	2.26	1.04	0.45	putative phosphoribosylaminoimidazole-succinocaroxamide synthetase
CD630_04960	4.13	1.19	0.34	putative conjugative transposon protein DUF961 family Tn5397 CTn3-Orf23
CD630_04970	3.86	0.93	0.36	putative conjugative transposon protein DUF961 family Tn5397 CTn3-Orf22
CD630_04980	4.13	0.93	0.34	putative cell-division FtsK/SpoIIIE-family protein Tn5397 CTn3-Orf21
CD630_05000	3.61	1.08	0.32	putative antirestriction protein Tn5397 CTn3-Orf18
CD630_05060	3.54	0.97	0.41	Reverse transcriptase/maturase/endonuclease Group II intron
CD630_05100	3.07	0.79	0.40	putative RNA polymerase sigma factor Tn5397 CTn3-Orf7
CD630_05101	3.31	1.05	0.41	putative conjugative transposon protein Tn5397 CTn3-Orf8
CD630_05102	3.35	0.89	0.40	Fragment of putative conjugative transposon protein Tn5397 CTn3-Orf5
CD630_05103	3.27	1.06	0.37	putative conjugative transposon protein Tn5397 CTn3-Orf4
CD630_05490	4.74	1.15	0.28	conserved hypothetical protein
CD630_05500	5.52	0.81	0.53	putative membrane protein
CD630_09950 (serA)	0.23	1.14	2.40	putative D-3-phosphoglycerate dehydrogenase
CD630_09960	0.24	1.19	2.34	conserved hypothetical protein
CD630_12400 (vanZ)	28.43	21.50	0.74	Teicoplanin resistance protein
CD630_16070	30.25	1.02	0.16	ABC-type transport system multidrug-family ATP-binding protein
CD630_16090	30.62	1.15	0.15	conserved hypothetical protein
CD630_16100	64.45	2.17	0.13	conserved hypothetical protein
CD630_16110	34.77	1.22	0.14	conserved hypothetical protein
CD630_16180 (clnA)	202.99	57.26	0.27	ABC-type transport system multidrug-family ATP-binding protein
CD630_16190 (clnB)	192.16	53.69	0.27	ABC-type transport system multidrug-family permease
CD630_16310 (sodA)	2.59	2.70	0.88	spore coat protein-superoxide dismutase
CD630_16632	0.32	0.22	3.61	conserved hypothetical protein
CD630_17000 (ribD)	3.65	1.11	0.35	Riboflavin biosynthesis protein
CD630_18870	5.34	1.24	0.41	Extracytoplasmic function (ECF) sigma factor

(csfU)				
CD630_18880 (rsiU)	3.69	0.95	0.32	Extracytoplasmic function (ECF) anti-sigma factor
CD630_18890	4.54	1.40	0.47	ABC-type transport system multidrug-family ATP-binding protein
CD630_18900	3.60	1.17	0.47	ABC-type transport system multidrug-family permease
CD630_20140 (ilvD)	2.90	1.02	0.53	Dihydroxy-acid dehydratase
CD630_20751	2.21	0.51	0.18	conserved hypothetical protein
CD630_21510	0.48	1.11	2.34	putative membrane protein DUF819 family
CD630_21710	0.34	1.05	2.18	Fragment of putative sodium:dicarboxylate symporter
CD630_22290	0.51	1.02	2.49	putative membrane protein
CD630_23090	2.29	1.03	0.50	conserved hypothetical protein
CD630_23790 (buk2)	3.13	0.81	0.41	Butyrate kinase
CD630_23800 (iorB)	10.81	0.64	0.24	Indole pyruvate ferredoxin/flavodoxin oxidoreductase
CD630_23810 (iorA)	13.66	0.62	0.22	Indole pyruvate ferredoxin/flavodoxin oxidoreductase
CD630_25150	0.38	1.02	2.45	putative L-aspartate-beta-decarboxylase
CD630_26140	0.12	1.18	7.62	uncharacterised protein DegV family
CD630_26640 (murE)	0.35	1.08	2.42	UDP-N-acetylmuramyl-tripeptide synthetase
CD630_26700	0.43	0.91	2.10	ABC-type transport system ATP-binding protein putative oligopeptide transport system
CD630_26870	0.46	0.43	0.79	conserved hypothetical protein
CD630_27491	0.38	0.92	3.46	Autoinducer prepeptide
CD630_27840 (cwp6)	2.30	0.97	0.49	putative N-acetylmuramoyl-L-alanineamidase autolysin
CD630_29330	0.50	0.32	1.45	Hypothetical protein
CD630_29341	0.29	0.23	1.34	putative phage protein
CD630_29360	0.44	0.45	0.57	putative phage protein
CD630_29490	0.46	0.44	0.48	Transcriptional regulator Phage-type
CD630_33730 (mgtA)	3.39	0.78	0.27	Magnesium-transporting ATPase P-type Tn916-like CTn7-Orf7
CD630_33740	3.92	0.76	0.21	putative conjugative transposon protein Tn916-like CTn7-Orf8
CD630_33750 (mgtC)	2.96	0.57	0.27	Magnesium-transporting ATPase protein Tn916-like CTn7-Orf10
CD630_35370 (phnH)	0.39	0.22	1.96	putative phosphonate metabolism protein

[a]Gene accession numbers are given for strain 630. Genes are included in this list if they had ≥ 2-fold increase or decrease in expression and a *P* value ≤ 0.05 by Student's two-tailed t-test in both 630Δ*erm* in LL-37 and the *clnR* mutant (either with or without LL-37).
[b]Ratio of no LL-37/with LL-37 as determined by RNA sequencing analysis of 630Δ*erm* grown in BHIS alone or BHIS supplemented with 2 μg/ml LL-37 as described in Methods.
[c]Ratio of expression in *clnR* mutant/expression in 630Δ*erm* as determined by RNA sequencing analysis of strains grown in BHIS alone as described in Methods.
[b]Ratio of expression in *clnR* mutant/expression in 630Δ*erm* as determined by RNA sequencing analysis of strains grown in BHIS supplemented with 2 μg/ml LL-37 as described in Methods.

Table S6. Relative expression of selected RNA-seq transcripts in *clnR* and *clnA* mutants

Gene	BHIS			+ LL-37 (2 μg/ml)		
	630Δ*erm*	*clnR*	*clnA*	630Δ*erm*	*clnR*	*clnA*
cdd4 (CD630_06670)	1.0 ± 0.0[a]	0.9 ± 0.1	1.1 ± 0.2	7.1 ± 2.4	**915.0** ± 30.5	**1672.6** ± 357.3
vanZ1 (CD630_12400)	1.0 ± 0.0	**25.2** ± 5.5	0.8 ± 0.1	36.9 ± 6.0	**13.4** ± 5.8	**0.9** ± 0.2
cstA (CD630_26000)	1.0 ± 0.0	0.9 ± 0.2	1.2 ± 0.1	6.7 ± 1.5	**2.3** ± 0.5	**2.9** ± 1.2
sigU (csfU; CD630_18870)	1.0 ± 0.0	0.5 ± 0.2	1.3 ± 0.3	10.5 ± 6.8	**2.0** ± 0.6	3.1 ± 1.4
sigT (csfT; CD630_06770)	1.0 ± 0.0	0.9 ± 0.1	1.0 ± 0.2	3.6 ± 0.1	2.3 ± 1.1	**1.2** ± 0.1
grdA (CD630_23520)	1.0 ± 0.0	0.9 ± 0.1	1.0 ± 0.0	16.5 ± 10.5	1.4 ± 0.1	1.9 ± 0.1
mtlA (CD630_23340)	1.0 ± 0.0	0.9 ± 0.4	3.3 ± 2.1	1.0 ± 0.3	1.2 ± 0.7	5.5 ± 4.3
iorA (CD630_23810)	1.0 ± 0.0	0.5 ± 0.1	0.7 ± 0.1	16.8 ± 8.4	2.1 ± 0.4	20.5 ± 17.3
CD630_02840	1.0 ± 0.0	1.2 ± 0.1	1.1 ± 0.1	29.3 ± 18.8	**2.2** ± 0.5	**2.1** ± 0.2

[a]Relative expression levels were determined by qRT-PCR and are normalized to 630Δ*erm* in BHIS as described in methods. Values shown are the mean of at least 3 biological replicates ± standard error of the mean. Bolded values indicate an adjusted *P* value ≤ 0.05 by two-way ANOVA with Dunnett's multiple comparisons test, comparing to 630Δ*erm* in the same condition.

Table S7. Expression of toxin regulation-associated genes

Gene	Fold-change in expression LL-37[a, b]
sigD	0.95 ± 0.08
tcdR	1.47 ± 0.44
ilvC[c]	**2.21** ± 0.20
CD0341[d]	2.54 ± 0.59

[a]Fold-change determined by qRT-PCR and normalized to 630Δ*erm* grown in BHIS alone. Concentration of LL-37 = 2 μg/ml. Values are the mean of three replicates ± standard error of the mean.
[b]Bolded values indicate significant difference (P value < 0.05) from 630Δ*erm* grown in BHIS without LL-37 and analyzed by Student's two-tailed *t*-test.
[c]*ilvC* indicates CodY activity.
[d]*CD0341* indicates CcpA activity.

Table S8. Plasmids and Strains

Plasmid or Strain		Relevant genotype or features	Source, construction or reference
Strains			
E. coli			
	HB101	F$^-$ *mcrB mrr hsdS20*(r_B^- m_B^-) *recA13 leuB6 ara-14 proA2 lacY1 galK2 xyl-5 mtl-1 rpsL20*	B. Dupuy
	MC101	HB101 pRK24	B. Dupuy
	MC135	HB101 pRK24 pMC123	(73)
	MC881	HB101 pRK24 pMC616	
	MC932	HB101 pRK24 pMC645	
	MC1122	HB101 pRK24 pMC723	
B. subtilis	BS49	*Tn*916	
	MC951	BS49 *Tn*916::*CD1617-1619*	
C. difficile			
	630	Clinical isolate	
	630Δ*erm*	Erm^S derivative of strain 630	N. Minton
	R20291	Clinical isolate	
	MC324	630Δ*erm* pMC123	(21)
	MC885	630Δ*erm CD1617::ermB*	
	MC935	630Δ*erm CD1618::ermB*	
	MC950	MC885 *Tn*916::*CD1617-1619*	
	MC953	MC935 *Tn*916::*CD1617-1619*	
	MC1123	MC885 pMC123	
	MC1131	MC885 pMC723	
Plasmids	pRK24	Tra$^+$, Mob$^+$; *bla, tet*	
	pCR2.1	*bla, kan*	Invitrogen
	pUC19	Cloning vector; *bla*	
	pCE240	*C. difficile* TargeTron® construct based on pJIR750ai (group II intron, *ermB::*RAM, *ltrA*); *catP*	C. Ellermeier;
	pSMB47	Tn*916* integrational vector; CmR, ErmR	
	pMC123	*E. coli-C. difficile* shuttle vector; *bla, catP*	
	pMC577	pCR2.1 with *clnR*-targeted intron	
	pMC602	pCE240 with *clnR*-targeted intron	
	pMC616	pMC123 with *clnR*-targeted intron (~nt 127, *ermB::*RAM *ltrA catP*	
	pMC643	pCE240 with *clnA*-targeted intron	
	pMC645	pMC123 with *clnA*-targeted intron (~nt 217, *ermB*::RAM *ltrA catP*	
	pMC649	pSMB47 Tn*916*::*CD1617-1619*	
	pMC723	pMC123 with P_{clnR}*::*His-*clnRAB*	

Table S9. Oligonucleotides

Primer	Sequence[a]	Purpose, source, or reference[b]
oMC44	CTAGCTGCTCCTATGTCTCACATC	*rpoC* (*CD0067*) qPCR (73)
oMC45	CCAGTCTCTCCTGGATCAACTA	*rpoC* (*CD0067*) qPCR (73)
oMC112	GGCAAATGTAAGATTTCGTACTCA	*tcdB* (*CD0660*) qPCR (21)
oMC113	TCGACTACAGTATTCTCTGAC	*tcdB* (*CD0660*) qPCR (21)
oMC152	GTTATGGAAGTCAAGGACATGCAC	*ilvC (CD1565*) qPCR (19)
oMC153	GCTTCTGCTACACTCTTAACTTCA	*ilvC (CD1565*) qPCR (19)
oMC178	CTTGAGTTAAATCTTGTGCAGTCA	*csfU (CD1887*) qPCR
oMC179	GGTGATAATAGTGAATGATGCTCGG	*csfU (CD1887*) qPCR
oMC189	TGCCTCTTGTAAAGAGTATAGCA	*sigD (CD0266)* qPCR (74)
oMC190	GCATCAATCAATCCAATGACTCCAC	*sigD (CD0266)* qPCR (74)
oMC242	TCCACAAGGAGCTGTATATGGT	*cdd4 (CD0667)* qPCR
oMC243	GTGGGTTTAGCAAGTCCAAGAA	*cdd4 (CD0667)* qPCR
oMC547	TGGATAGGTGGAGAAGTCAGT	*tcdA (CD0663*) qPCR (21)
oMC548	GCTGTAATGCTTCAGTGGTAGA	*tcdA (CD0663*) qPCR (21)
oMC569	AGCAAGAAATAACTCAGTAGATGATT	*tcdR (CD0659*) qPCR (Rita Tamayo)
oMC570	TTATTAAATCTGTTTCTCCCTCTTCA	*tcdR (CD0659*) qPCR (Rita Tamayo)
oMC683	GTATCTGACAACATCAATTGCCTAAA	*CD0341* qPCR (21)
oMC684	TCAGCTTGAGATTCAATTTCTTCATT	*CD0341* qPCR (21)
oMC815	TGGATTCTCTTAAGGAAGAACAATACTTTA	*sigT* (*CD0677*) qPCR (23)
oMC816	CCTTAACTTCATCTACTGAATAACCTTCA	*sigT* (*CD0677*) qPCR (23)
oMC1249	GTCGAGGATCCGATGACAAGTTATTGGAATA CACAG	P*spo0A* amplification
oMC1290	GAATGGGAACTTGATAATAACAAACC	check *CD1617-1618* co-transcription
oMC1291	AAGTTCTGTTAGAGCCTTTTGC	check *CD1616-1617* co-transcription
oMC1292	AGGTGTAAACAAGAGTTATGGAAC	check *CD1618-1619* co-transcription
oMC1293	TCTATGGATGGTTTCATTCCATTTATC	check *CD1617-1618* co-transcription
oMC1294	AAGCAAGTGGAAGAATATTTATACCG	*clnB (CD1619*) qPCR
oMC1295	ACATTAAATAACCTTCATCCCCC	*clnB (CD1619*) qPCR
oMC1297	CACTGCAGTTTTATCCATTTTATAATTC	screening for Targetron insertion in *clnR*
oMC1310	AAAAGCTTTTGCAACCCACGTCGATCGTGAAC CGCATCTTCTGGTGCGCCCAGATAGGGT	*clnR (CD1617)* intron retargeting
oMC1311	CAGATTGTACAAATGTGGTGATAACAGATAA GTCCTTCTGCTTAACTTACCTTTCTTTGT	*clnR (CD1617)* intron retargeting
oMC1312	CGCAAGTTTCTAATTTCGGTTTGCGGTCGATA GAGGAAAGTGTCT	*clnR (CD1617)* intron retargeting
oMC1319	AAAAGCTTTTGCAACCCACGTCGATCGTGAA AAAATAGTTTCAGTGCGCCCAGATAGGGT	*clnA (CD1618)* intron retargeting
oMC1320	CAGATTGTACAAATGTGGTGATAACAGATAA GTCGTTTCATATAACTTACCTTTCTTTGT	*clnA (CD1618)* intron retargeting
oMC1321	CGCAAGTTTCTAATTTCGGTTATTTTTCGATA	*clnA (CD1618)* intron

	GAGGAAAGTGTCT	retargeting
oMC1383	GTAGAAGGAGCAGAGGTTGTTT	*grdA (CD2352*) qPCR
oMC1384	TCAGCAGCATCTTTAACTCTGT	*grdA (CD2352*) qPCR
oMC1393	TGAAACCATGAATCTTAGAAGCATAAAC	*vanZ (CD1240)* qPCR
oMC1394	CACATATATCCCAAATGGTACAAATATAGC	*vanZ (CD1240)* qPCR
oMC1410	GTGGGATCCGCTAAAACTTATTACAG	*clnA (CD1618*) cloning
oMC1416	GTGGGATCCAGAAGAACAGTTTAA	P*clnR* cloning
oMC1427	GTTTGGAAAGCCAATGCCAA	check *CD1616-1617* co-transcription
oMC1467	TAGCAGAAGATGCGGAAGTTAAT	*clnR (CD1617*) qPCR
oMC1473	GTTACAAATCTTCCTTTAGTTCTCTGAC	*clnR (CD1617*) qPCR
oMC1476	GCGCATGCATTACTCAAAAGATAGCT	*clnRAB* cloning
oMC1483	CTGGGTCAACACCACCTATAG	verify *clnA (CD1618)* disruption
oMC1493	GTTAGAAGAGCAAATGAGATGATTAAAAGC	*clnA (CD1618*) qPCR
oMC1614	GTGTACTCCACCAGCAAAGA	*cstA* (*CD2600*) qPCR
oMC1615	GCAGGGTTAGGTCCGATATTT	*cstA* (*CD2600*) qPCR
oMC1684	GCGGAATTCCTAAAAAGTAATTGACATATACTTTG	P*clnR* cloning
oMC1689	GTGGGATCCGGCGCCATGCATCACCATCACCATCACATGGAATGGGAACTTGATAATAAC	*clnR* cloning with His-tag
oMC1690	GTGGGCGCCGTTCATGCCTCCTTATTA	P*clnR* cloning
oMC1691	FAM-CTAAAAAGTAATTGACATATACTTTG	P*clnR* amplification with fluorescein
oMC1692	FAM-CATGCCTCCTTATTATATTATTG	P*clnR* amplification with fluorescein
oMC1700	FAM-AGTTTGTGCAGTTTCTGAA	P*iorA* amplification with fluorescein
oMC1701	FAM-ACTACAATTATTAAATTCATAGATG	P*iorA* amplification with fluorescein
oMC1702	FAM-CTCCAAAATACTACATAAATAA	P*mtlA* amplification with fluorescein
oMC1703	FAM-TATATCGATATGATTCCCTTTTG	P*mtlA* amplification with fluorescein
oMC1704	FAM-CAAATTAAAATAAAGCAATTTATA	P*CD1606* amplification with fluorescein
oMC1705	FAM-CTAGTGTATTAATACGATAGTAC	P*CD1606* amplification with fluorescein
oMC1706	FAM-TTGTTTAAGTATTAATTATGAGT	P*csfU* amplification with fluorescein
oMC1707	FAM-CGTCATTATATATAACGATTTATAC	P*csfU* amplification with fluorescein
oMC1710	FAM-ATGTTTCATCCCCTTTTTTAATC	P*cdd4*/*CD0668* amplification with fluorescein
oMC1711	FAM-CACCCTCCTTTAGTATACC	P*cdd4*/*CD0668* amplification with fluorescein
oMC1712	FAM-CAATATTAATTTATTTTTAAAAAATAG	P*tcdA* amplification with fluorescein
oMC1713	FAM-AGTATTATTATTTTTGATAATAAATC	P*tcdA* amplification with

		fluorescein
oMC1714	FAM-CTTGTAATAAAATAAAGATTTAAGTG	P*grdE* amplification with fluorescein
oMC1715	FAM-CACCTCCTGTTATTTAATTTG	P*grdE* amplification with fluorescein
oMC1716	CACCAATAATTTTATTATTTTGTATTATTG	P*spo0A* amplification
oMC1735	AGAAAGATATGAAATACTACAATAGC	P*vanZ* amplification with fluorescein
oMC1736	TAGATTTCATTTATTACCTCCTTAC	P*vanZ* amplification with fluorescein
oMC1737	AGtGaattcgagctcggtacccggggatccCAGAAGAACAG TTTAAACTTTTAAAAG	P*clnR* Gibson assembly
oMC1738	CATTCCATGTGATGGTGATGGTGATGCATggcg ccTTCATGCCTCCTTATTATATTAttg	P*clnR* Gibson assembly
oMC1739	CTCCAAAATACTACATAAATAA	P*mtlA* amplifciation
oMC1740	TATATCGATATGATTCCCTTTTG	P*mtlA* amplification
oMC1741	CAAATTAAAATAAAGCAATTTATA	P*CD1606* amplification
oMC1742	CTAGTGTATTAATACGATAGTAC	P*CD1606* amplification
oMC1743	TTGTTTAAGTATTAATTATGAGT	P*csfU* amplification
oMC1744	CGTCATTATATATAACGATTTATAC	P*csfU* amplification
oMC1745	ATGTTTCATCCCCTTTTTTAATC	P*cdd4*/*CD0668* amplification
oMC1746	CACCCTCCTTTAGTATACC	P*cdd4*/*CD0668* amplification
oMC1717	TTGAGTACTATAGGTGACCCAATGA	*mtlA (CD2334)* qPCR
oMC1718	CCTCTTTGTCCTGCTATTGCTTTA	*mtlA (CD2334)* qPCR
oMC1719	GGGTAAATGGTGGTATGGTACTTATT	*iorA (CD2381)* qPCR
oMC1720	AGCTTCTTGACTAGTTGATGGTTC	*iorA (CD2381)* qPCR
oMC1754	GGAATAATAGTTATGACTCATGGGAGTT	*CD0284* qPCR
oMC1755	AGTTTAATTGCTGCTGTTCTTTCTG	*CD0284* qPCR

[a] All sequences are listed 5' to 3'. Underlined sequences denote restriction sites or intron retarget sites.
[b] Abbreviations: qPCR, quantitative PCR

Table S10. Plasmid construct details.

pMC602: The group II intron of pCE240 was targeted to *CD1617* at nucleotide 127 bysplicing PCR using primers oMC1310, oMC1311, oMC1312, and EBSu as outlined in the TargeTron users manual (Sigma-Aldrich). The primers for intron retargeting were obtained by using the jpintronator algorithm. The group II *CD1617*-targeted intron was subcloned using the *BsrG*I and *Hind*III sites into pCE240.

pMC616: The 5.45 kb *Sph*I/*Sfo*I fragment from pMC602 was cloned as *Sph*I/*SnaB*I into pMC123.

pMC643: The group II intron of pCE240 was targeted to *CD1618* at nucleotide 217 bysplicing PCR using primers oMC1319, oMC1320, oMC1321, and EBSu as outlined in theTargeTron users manual (Sigma-Aldrich). The primers for intron retargeting were obtained by using the jpintronator algorithm. The group II *CD1618*-targeted intron was subcloned using the *BsrG*I and *Hind*III sites into pCE240.

pMC645: The 5.45 kb *Sph*I/*Sfo*I fragment from pMC645 was cloned as *Sph*I/*SnaB*I into pMC123.

pMC649: The coding sequence of *CD1617-1619* and 300 bp upstream of *CD1617* was amplified using oMC1416 and oMC1476 and cloned into pSMB47 as *Bam*HI/*Sph*I.

pMC687: The coding sequence of *CD1234* was amplified with primers oMC1609 and oMC1610 and cloned into pMC211 as *BamH*I/*Pst*I.

pMC723: The *clnRAB* operon was amplified with an N-terminal 6x His tag using primers oMC1689 and oMC1476 and cloned as *BamH*I/*Sph*I into pMC123. Subsequently, P*clnR* (amplified using primers oMC1737 and oMC1738) was cloned by Gibson assembly as *BamH*I/*Sfo*I.

Table S11. Expression of several ClnR-dependent genes in the *clnR* mutant complemented with His-ClnR.

Gene	BHIS			+ LL-37 (0.5 μg/ml)		
	630Δ*erm* + pMC123	*clnR* + pMC123	*clnR* + pMC123 P*clnR::His-ClnRAB*	630Δ*erm* + pMC123	*clnR* + pMC123	*clnR* + pMC123 P*clnR::His-ClnRAB*
clnA (CD630_16180)	1.0 ± 0.0[a]	37.4 ± 6.6	69.4 ± 20.3	81.6 ± 20.5	44.9 ± 8.0	236.5 ± 22.7
vanZ1 (CD630_12400)	1.0 ± 0.0	17.5 ± 2.4	4.1 ± 1.3	15.4. ± 2.8	21.8 ± 1.8	18.6 ± 2.3

[a]Relative expression levels were determined by qRT-PCR and are normalized to 630Δ*erm* + pMC123 in BHIS as described in methods. Values shown are the mean of 3 biological replicates ± standard error of the mean.

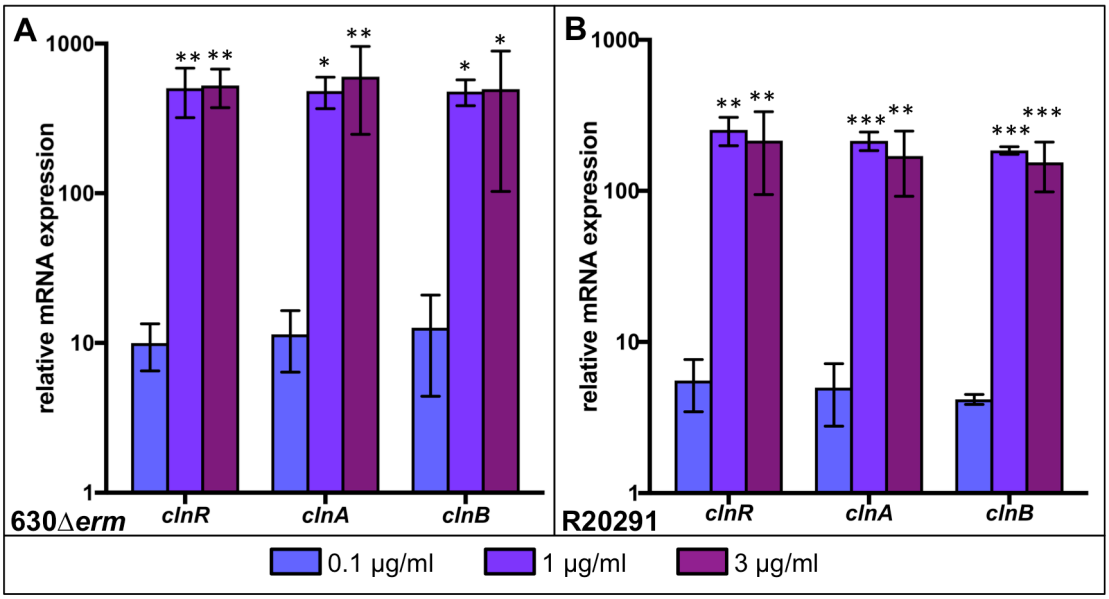

Figure 1. Expression of *CD630_16170-CD630_16190* is induced by LL-37 in a dose-dependent manner. Active cultures of **A)** 630Δ*erm* and **B**) R20291 were grown in BHIS or BHIS with 0.1, 1, or 3 µg/ml LL-37. Samples were harvested, cDNA generated, and qRT-PCR performed as described in Methods. mRNA levels are normalized to expression levels in BHIS alone. Bars represent the mean and standard deviation for at least three biological replicates. Expression levels of each gene were analyzed by one-way ANOVA and Dunnett's test for multiple comparisons, comparing to expression without LL-37. Adjusted P values indicated by * ≤ 0.05, ** ≤ 0.01, *** ≤ 0.001.

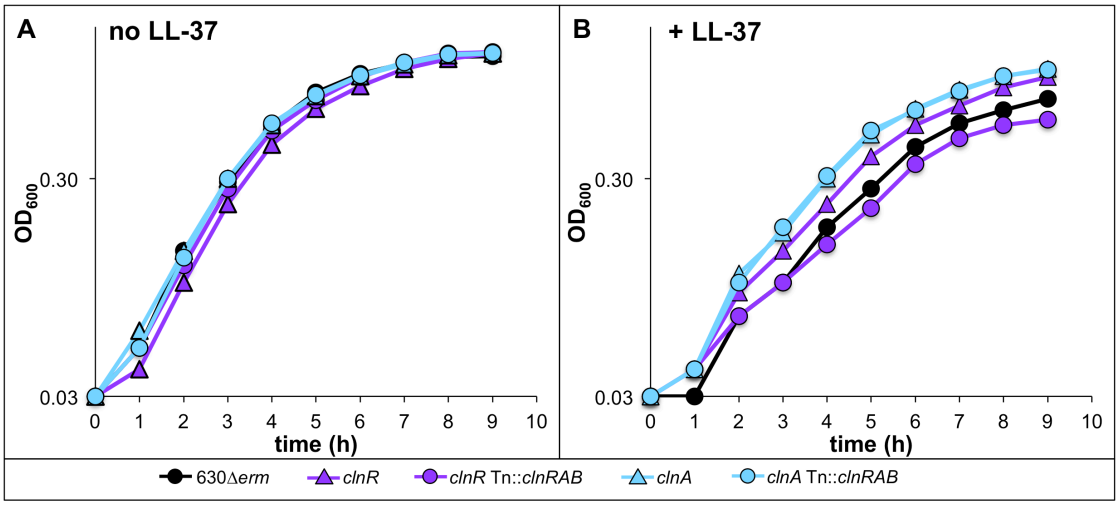

Figure 2. Growth of *clnR* and *clnA* mutants with and without LL-37. Active cultures of 630Δ*erm* (black), *clnR* (MC885; purple triangles), *clnR* Tn::*clnRAB* (MC950; purple circles), *clnA* (MC935; blue triangles), *clnA* Tn::*clnRAB* (MC953; blue circles) were diluted to an OD_{600} 0.05 in **A)** BHIS alone or **B)** BHIS with 2.5 µg/ml LL-37. Graph is representative of three independent replicates.

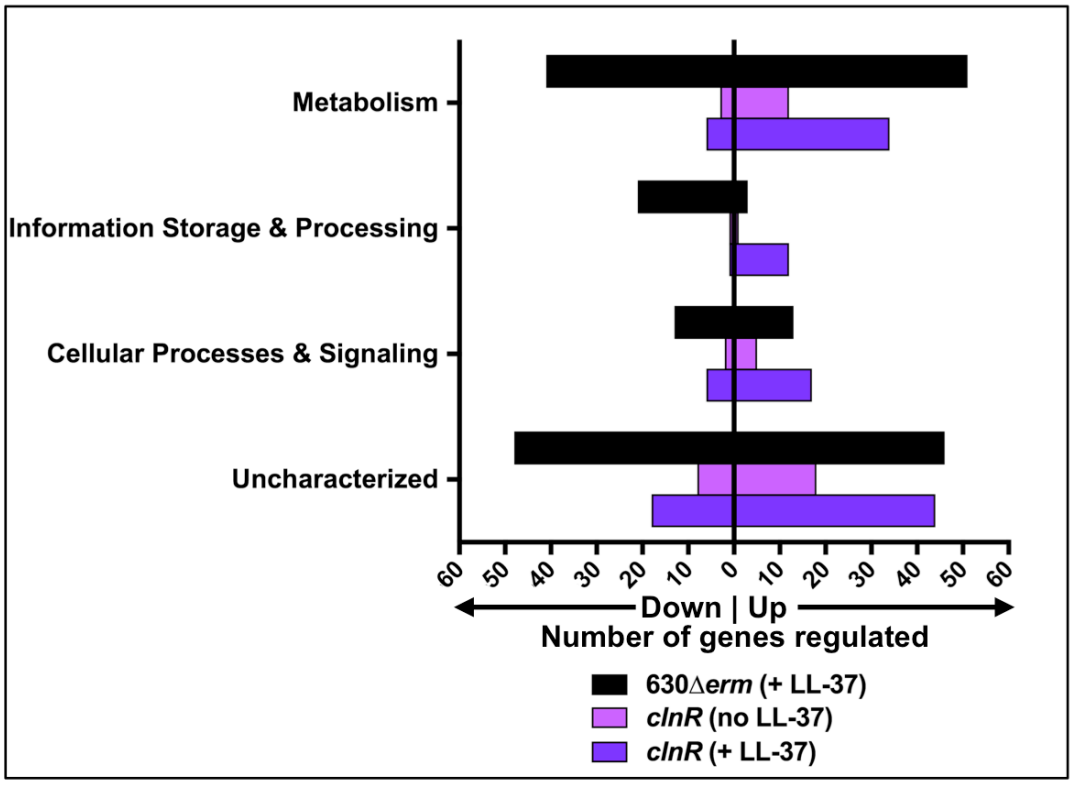

Figure 3. LL-37 and ClnR impact global gene expression. The genes listed in **Table S1** (black) and **Table 2** (light and dark purple) were assigned COG classifications according to the 2014 COG database. COG classifications were then grouped according to broader functions of Metabolism (COG classes C, E, F, G, H, I, P, and Q), Information Storage & Processing (COG classes A, B, J, K, and L), Cellular Processes & Signaling (COG classes D, M, N, O, T, U, V, W, Y, and Z), and Uncharacterized (COG classes R and S or unassigned). Genes with functions that fall within two different groups are represented within both of the groups.

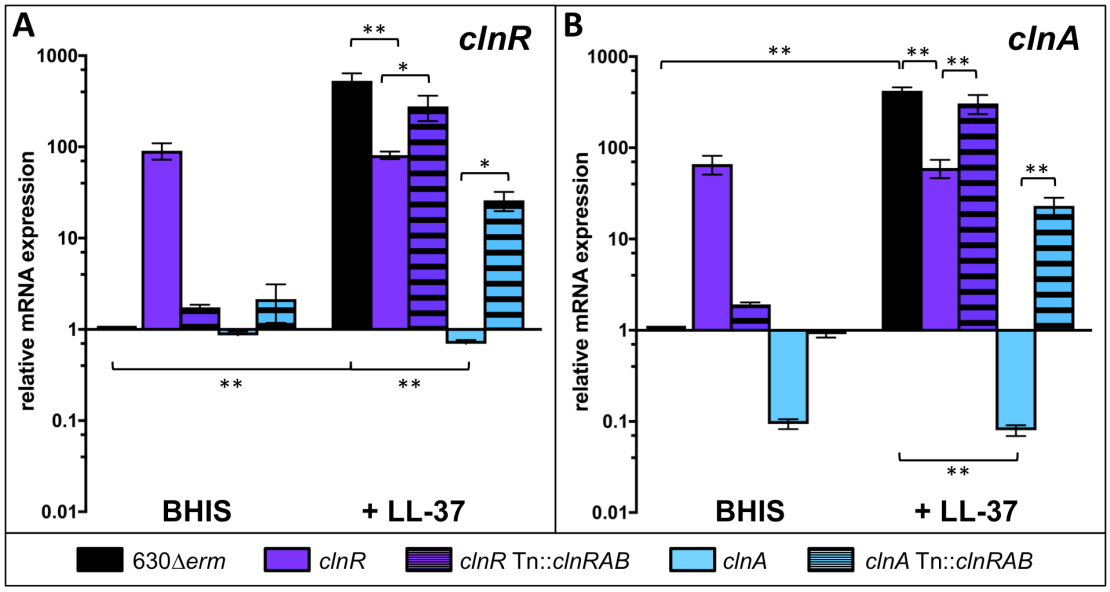

Figure 4. ClnR acts as a conditional repressor and inducer of *clnRAB* expression. Cultures of 630Δ*erm, clnR* (MC885)*, clnR* Tn::*clnRAB* (MC950)*, clnA* (MC935)*,* and *clnA* Tn::*clnRAB* (MC953) were grown in BHIS alone or BHIS with 2 µg/ml LL-37. RNA samples were collected and processed for qRT-PCR analysis as described in Methods. Graphs show the mean mRNA expression levels of **A)** *clnR* and **B)** *clnA* relative to expression in strain 630Δ*erm* in BHIS alone. Error bars represent the standard error of the mean from at least three independent experiments. Data were analyzed by two-way ANOVA and Tukey's multiple comparisons test, with comparisons indicated by brackets. * indicates $P < 0.05$, ** indicates $P \leq 0.0001$.

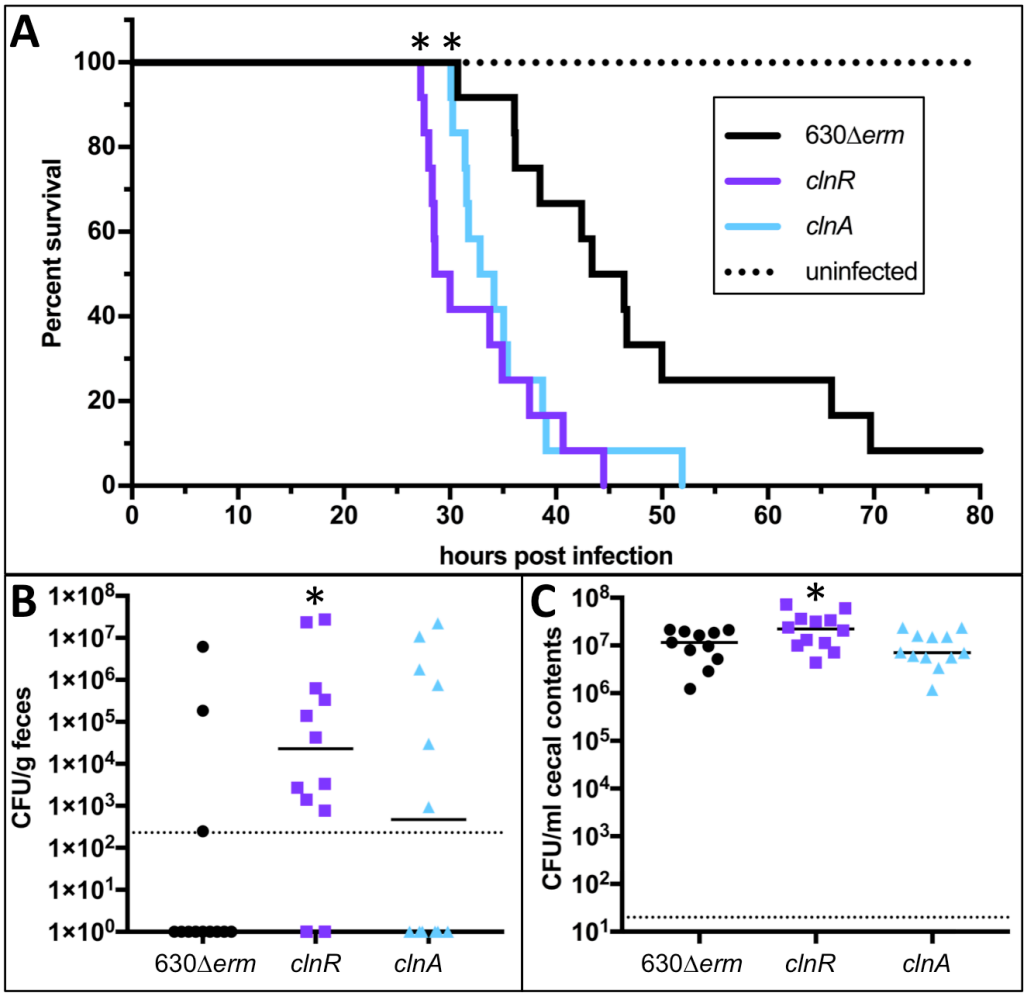

Figure 5. *clnR* and *clnA* mutants are more virulent in a hamster model of infection. Syrian golden hamsters were inoculated with approximately 5000 spores of 630Δ*erm* (n = 12), *clnR* (MC885; n = 12), or *clnA* (MC935; n = 12). **A**) Kaplan-Meier survival curve depicting time to morbidity. Mean times to morbidity were: 630Δ*erm* 46.0 ± 12.2 (n=11); *clnR* 32.5 ± 5.8 (n=12); *clnA* 35.2 ± 6.1 (n=12). * indicates $P \leq 0.01$ by log-rank test. **B**) Total *C. difficile* CFU recovered from fecal samples collected at 12 h.p.i. Dotted line demarcates limit of detection. Solid black line marks the median. Fisher's exact test compared the number of animals without and with detectable CFU compared to 630Δ*erm* (* indicates $P < 0.05$). **C)** Total *C. difficile* CFU recovered from cecal contents collected

post-mortem. Dotted line demarcates lower limit of detection. Solid black line marks the median. Numbers of CFU are compared to 630Δ*erm* by one-way ANOVA with Dunnett's test for multiple comparisons (* indicates $P < 0.05$).

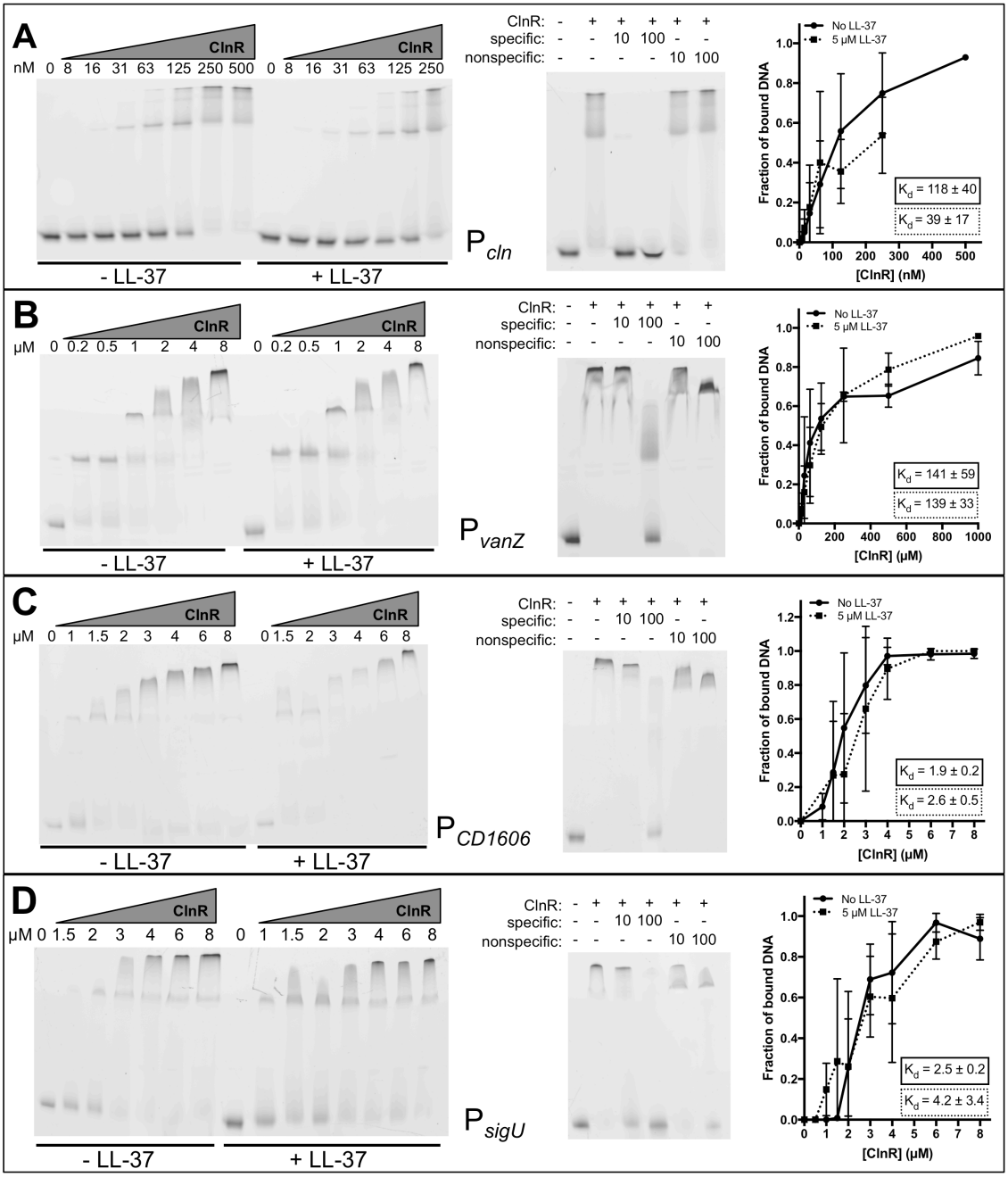

Figure 6. His-ClnR directly and specifically binds several DNA targets.

Electrophoretic mobility shift assays were performed as described in Methods using His-tagged ClnR and fluorescein-labeled DNA encompassing regions upstream of **A**) *clnR,* **B**) *vanZ,* **C**) *CD1606,* or **D**) *sigU*. ClnR was added to reactions at varying concentrations (specified in nM in **A**, in μM elsewhere) either without or with 0.5 μM LL-37 as

indicated. Competitive EMSAs were performed with the addition of unlabeled target DNA (specific) or unlabeled P*spo0A* DNA (nonspecific) at either 10x or 100x the concentration of labeled target DNA. 125 nM ClnR was used for the competitive EMSA for P*cln,* 8 μM for all others. Apparent K_d values were calculated as described in Methods. Graphs are the binding curves showing the mean and standard deviation from three independent replicates.

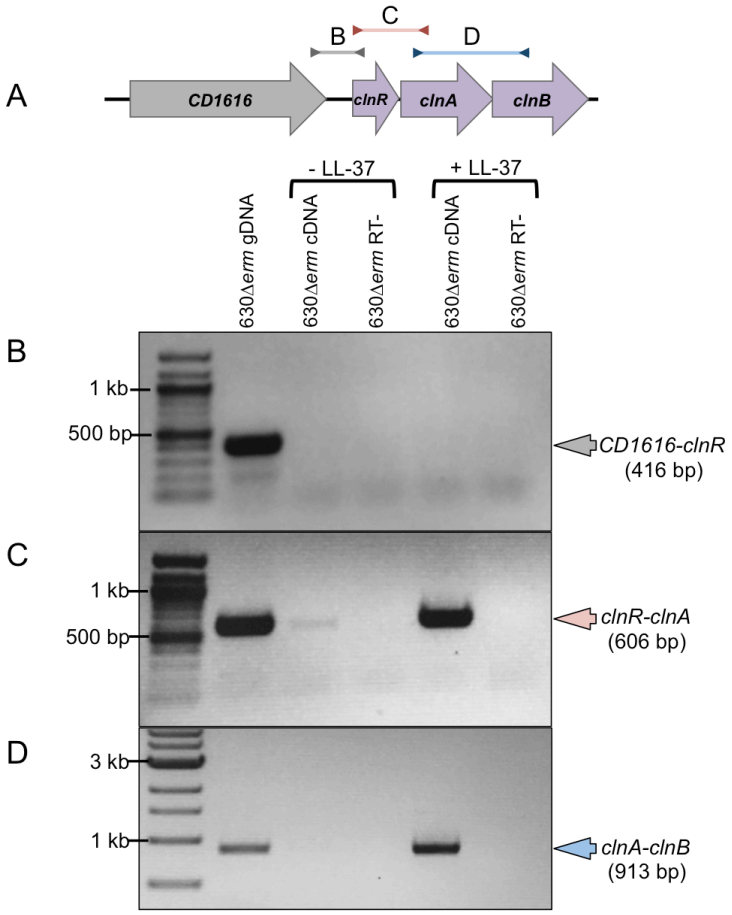

Figure S1. *clnRAB* is transcribed as an operon. A) The organization of *CD630_16160-CD630_16190* (*clnRAB*). Cultures of strain 630Δ*erm* were grown with or without the addition of 1 µg/ml LL-37, samples collected for RNA and cDNA generated as described in Methods. PCR was performed using genomic DNA (gDNA, positive controls), cDNA templates, or cDNA without reverse transcriptase (RT-, negative controls). Products were generated using primers **B)** located at the 3' end of *CD630_16160* (oMC1427) and at the 5' end of *clnR* (oMC1291), **C)** within *clnR* (oMC1290) and at the 5' end of *clnA* (oMC1293), or **D)** within *clnA* (oMC1292) and at the 5' end of *clnB* (oMC1295)**.** 25 cycles of PCR were performed and the product visualized on a 0.7% agarose gel. Arrows indicate the expected product size.

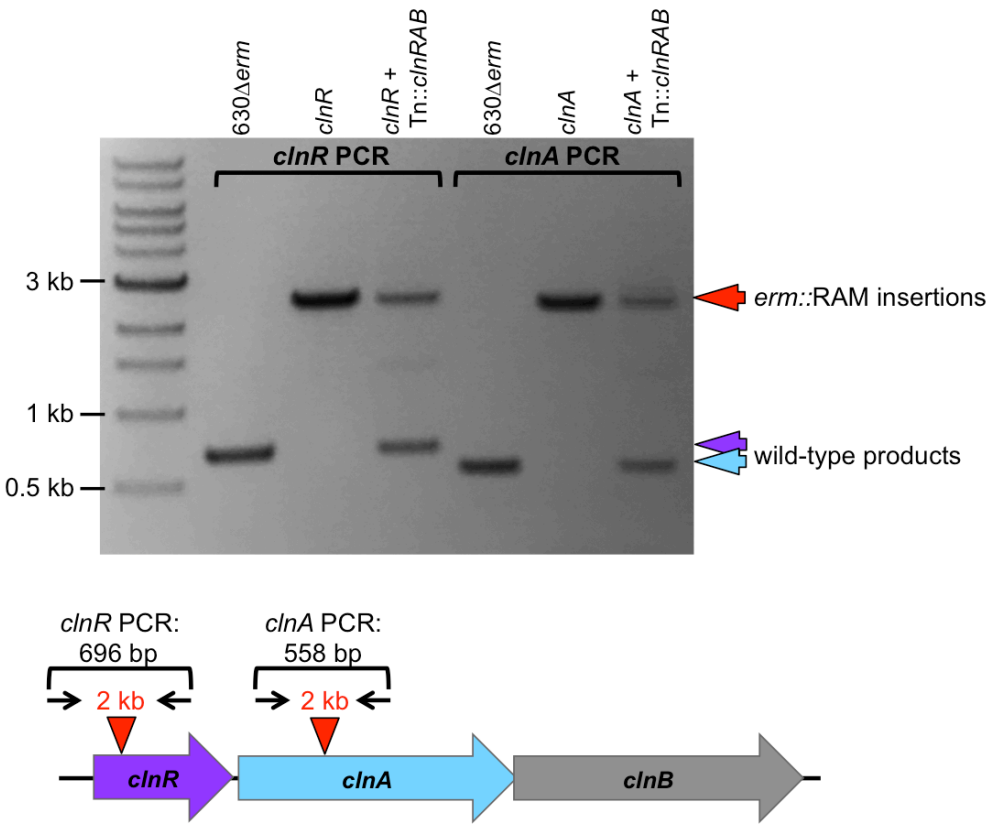

Figure S2. Confirmation of *clnR* and *clnA* mutants, and their complemented strains. PCR products were generated using primers flanking the Targetron *erm::*RAM insertion sites of *clnR* or *clnA*, and genomic DNA from 630Δ*erm* (control), *clnR* (MC885), *clnR* Tn:*clnRAB* (MC950), *clnA* (MC935), or *clnA* Tn:*clnRAB* (MC953) templates. The wild-type PCR product for *clnR* is 696 bp (primers oMC1416/oMC1297), and 558 bp for *clnA* (primers oMC1410/oMC1483). Mutants with intron insertions generate ~2 kb larger product. Complemented strains yield both the wild-type and insertion products.

Figure S3. Alignment of mature cathelicidin sequences. Cathelicidins from humans (LL-37), mice (mCRAMP) and sheep (SMAP-29) were aligned using the CLUSTAL format alignment (MAFFT, V7.310). Residues corresponding to hydrophobic side chains are labeled above the sequence (Wang *et al*. 2008).

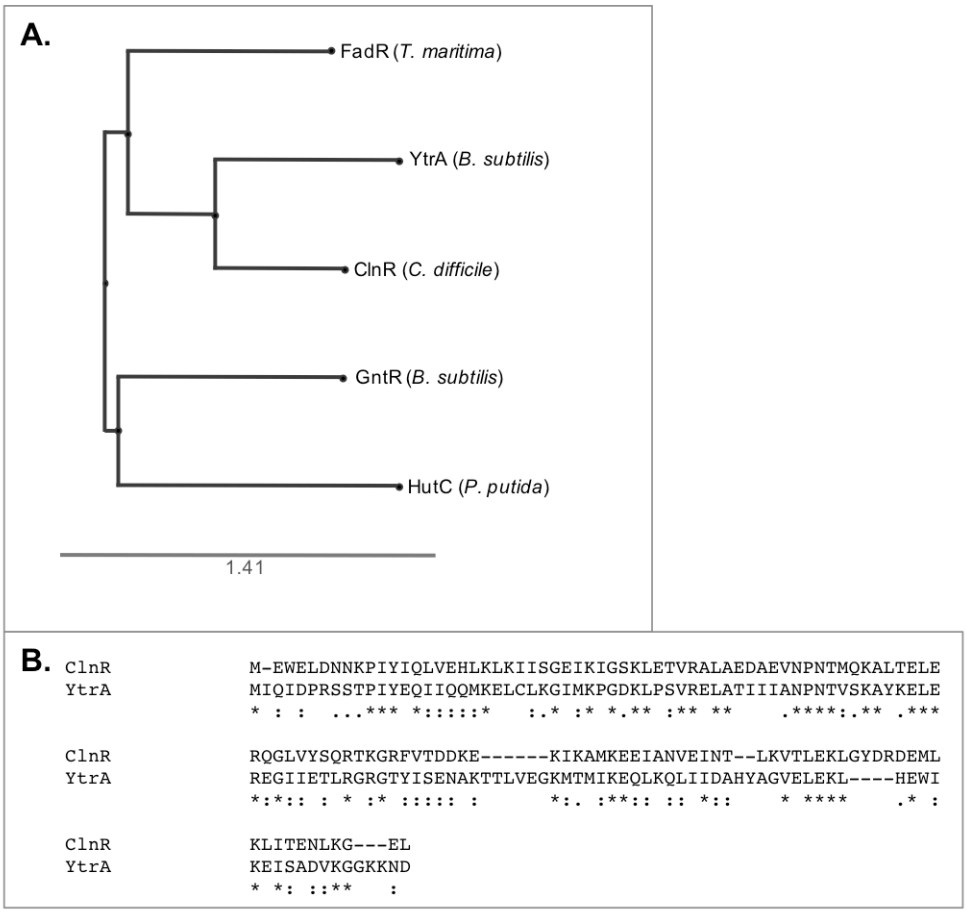

Figure S4. Alignment of ClnR and GntR-family proteins. A) Protein sequences for *C. difficile* ClnR (YP_001088118.1) and *B. subtilis* YtrA (KIX83587.1) were analyzed using MAFFT version 7 (Katoh et al., 2005 Nucl Acids Res). An asterik below the sequence indicates identical residues, colons indicate similar residues, and dots indicate low similarity. **B)** Unrooted phylogenetic tree featuring GntR and sub-family representatives: GntR (*B. subtilis;* CAB16042.1), FadR (*T. maritima*; NP_228249.1), HutC (*P. putida*; ADR62377.1), YtrA (*B. subtilis*; KIX83587.1) and ClnR (*C. difficile*; YP_001088118.1) generated using Phylo.io version 1.0k (http://phylo.io/; Robinson et al., 2016 arXiv:1602.04258).

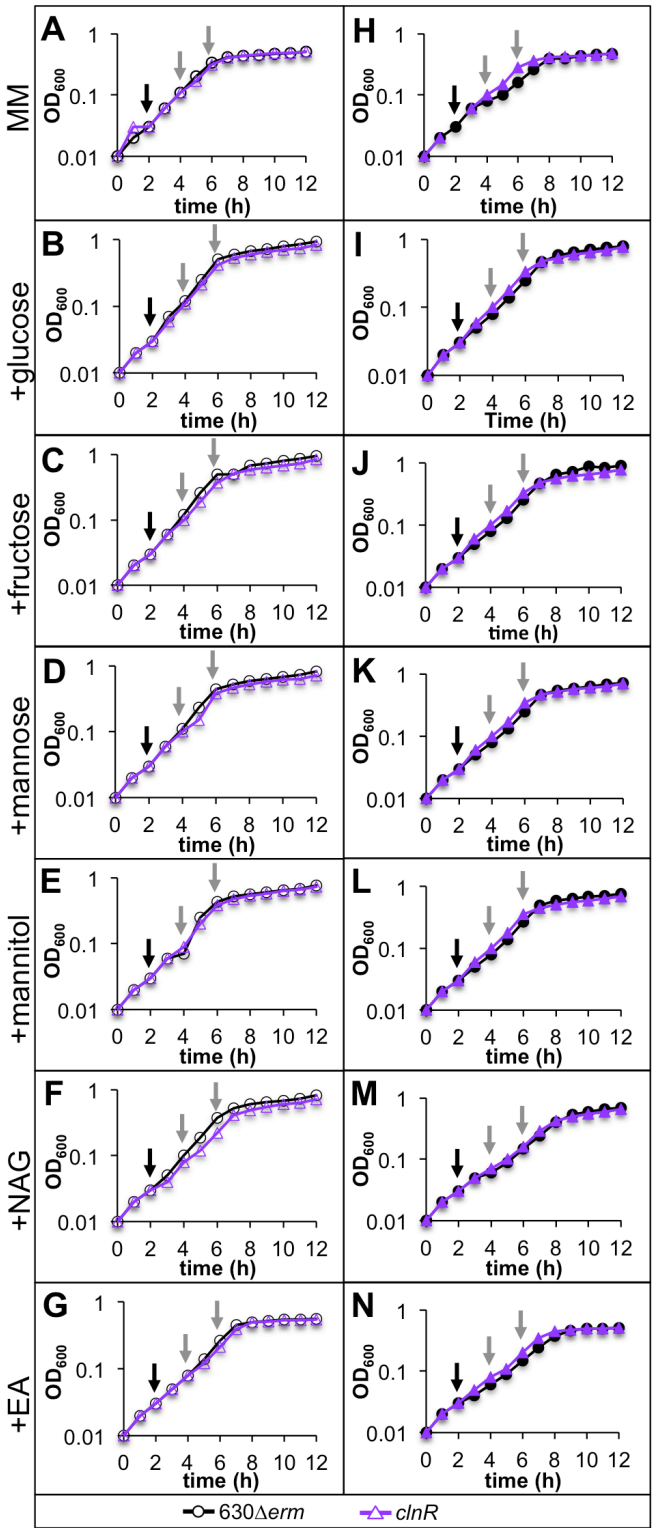

Figure S5. ClnR and LL-37 regulate the metabolism of nutrients. Active cultures of strain 630Δ*erm* (black) and the *clnR* mutant (MC885, purple) were diluted to an OD_{600} in

0.01 in MM either without **(A-G)** or with **(H-N)** 0.5 µg/ml LL-37. (**A, H)** or supplemented with **B, I)** 10 mM glucose, **C, J)** 10 mM fructose, **D, K)** 10 mM mannose, **E, L)** 20 mM mannitol, **F, M)** 20 mM N-acetylglucoseamine (NAG), or **G, N)** 20 mM ethanolamine (EA). Black arrows denote the end of initial peptide-fueled growth; gray arrows delineate the period of maximal carbohydrate-influenced growth. Graphs are representative of three independent replicates.

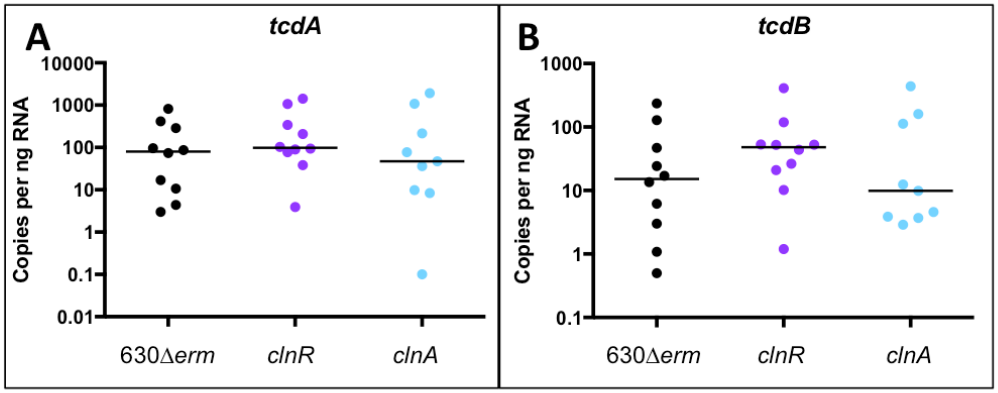

Figure S6. **Toxin expression in *clnR* and clnA-infected animals at the time of morbidity.** RNA was extracted from cecal contents of hamsters infected with strain 630Δ*erm,* the *clnR* mutant (MC885), or the *clnA* mutant (MC935) at the time of morbidity. RNA was used to generate cDNA and analyzed by droplet digital PCR, as described in Methods. Values shown are absolute copies of *tcdA* (**A**) and *tcdB* (**B**) detected per ng of RNA. Solid lines indicate the median. No statistically significant differences were found by one-way ANOVA.

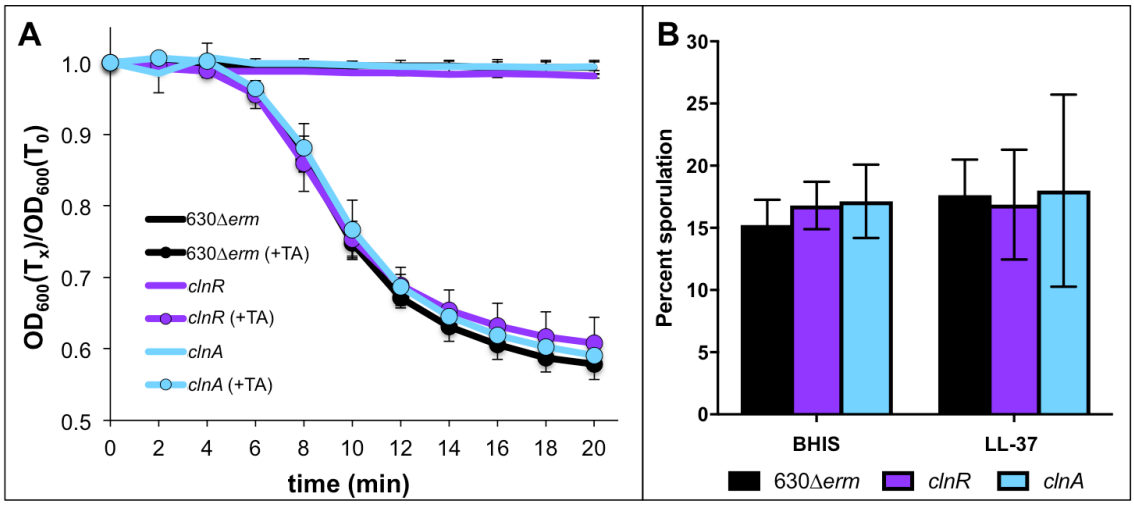

Figure S7. *clnR* and *clnA* mutant germination and sporulation. A) Germination assessment for strains 630Δ*erm, clnR* (MC885), and *clnA* (MC935). Spores were purified as described in methods. Heat-activated spores were added to BHIS for a starting OD_{600} of approximately 0.3. Taurocholic acid (5 mM) was added at T_0 to the indicated samples, and the OD_{600} of the samples was assessed every two minutes for the duration of the experiment. Ratios of the OD_{600} at each timepoint (T_x) were plotted against the density observed at T_0. Three independent biological replicates are shown with error bars indicating the SD. * indicates an adjusted P-value ≤ 0.05 by one-way ANOVA and Dunnett's test for multiple comparisons, comparing the mutant strains to 630Δ*erm*. **B)** Sporulation frequency. Ethanol-resistant spore formation frequency per total viable CFU of the 630Δ*erm, clnR,* and *clnA* strains grown on 70:30 sporulation agar with or without 1 µg/ml LL-37 for 24 h. Sporulation frequencies were calculated as described in the Methods. The mean and and standard error of the mean are shown for a minimum of three independent experiments. No statistically significant differences were observed by ANOVA assessment.

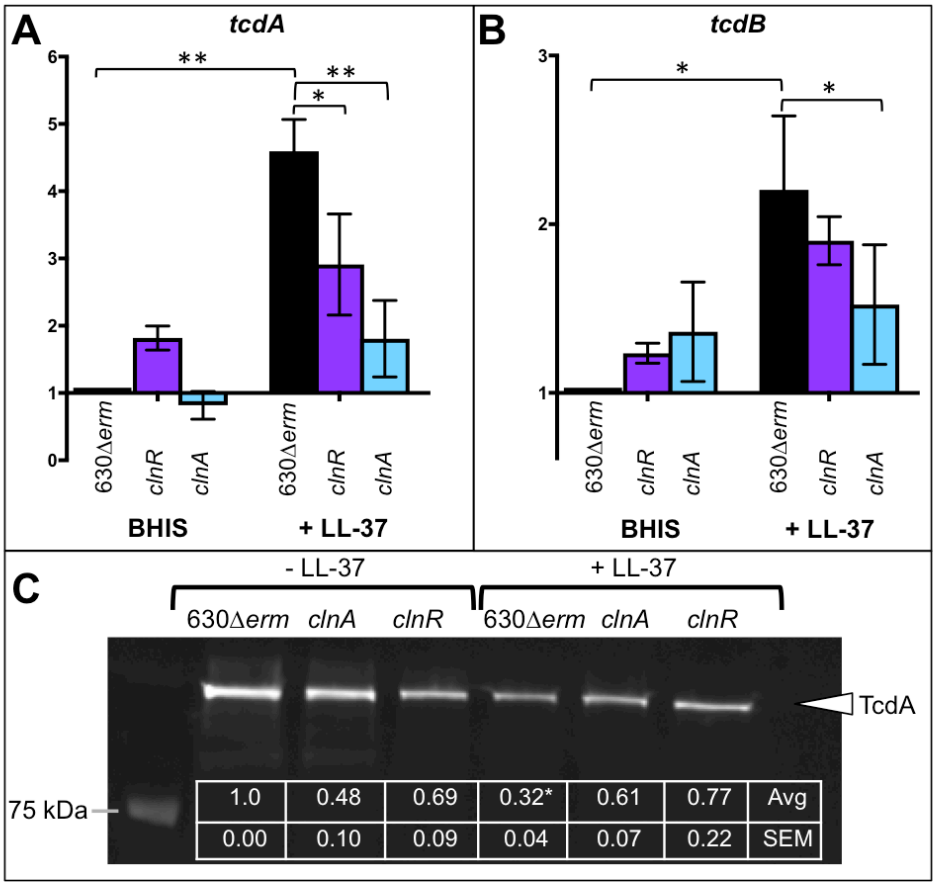

Figure S8. LL-37 promotes toxin expression in a ClnRAB-dependent manner. qRT-PCR analysis of *tcdA* and *tcdB* from strains 630Δ*erm, clnR* (MC885), and *clnA* (MC935) grown in BHIS or BHIS with 2 µg/ml LL-37. Graphs show the mean mRNA expression of **A)** *tcdA* and **B)** *tcdB* relative to expression for 630Δ*erm* in BHIS. Error bars represent the standard error of the mean. Data were analyzed by two-way ANOVA and Dunnett's test for multiple comparisons, comparing to 630Δ*erm* in the same condition. * indicates adjusted P value of < 0.05, ** indicates adjusted P value of ≤ 0.0001. (**C**) TcdA western blot for culture lysates from strains grown 24 h in TY medium with or without 2 µg/ml LL-37. Results shown are representative of three independent replicates. * indicates adjusted P-value < 0.05, compared to 630Δ*erm* without LL-37 by 2-way ANOVA with Sidak's multiple comparisons test.

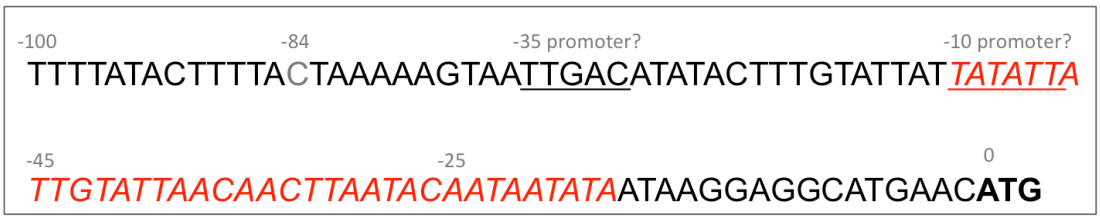

Figure S9. Features of the sequence upstream of *clnR*. 100 nucleotides upstream of the *clnR* translational start site (bold) are shown. The underlines indicate putitive -35 and -10 promoter sites. The italicized red region is a tandem repeat sequence that we hypothesize is a ClnR binding site. The construct used in EMSA experiments contained the 84 base pairs upstream of the transcriptional start site, with the final nucleotide indicated in gray.

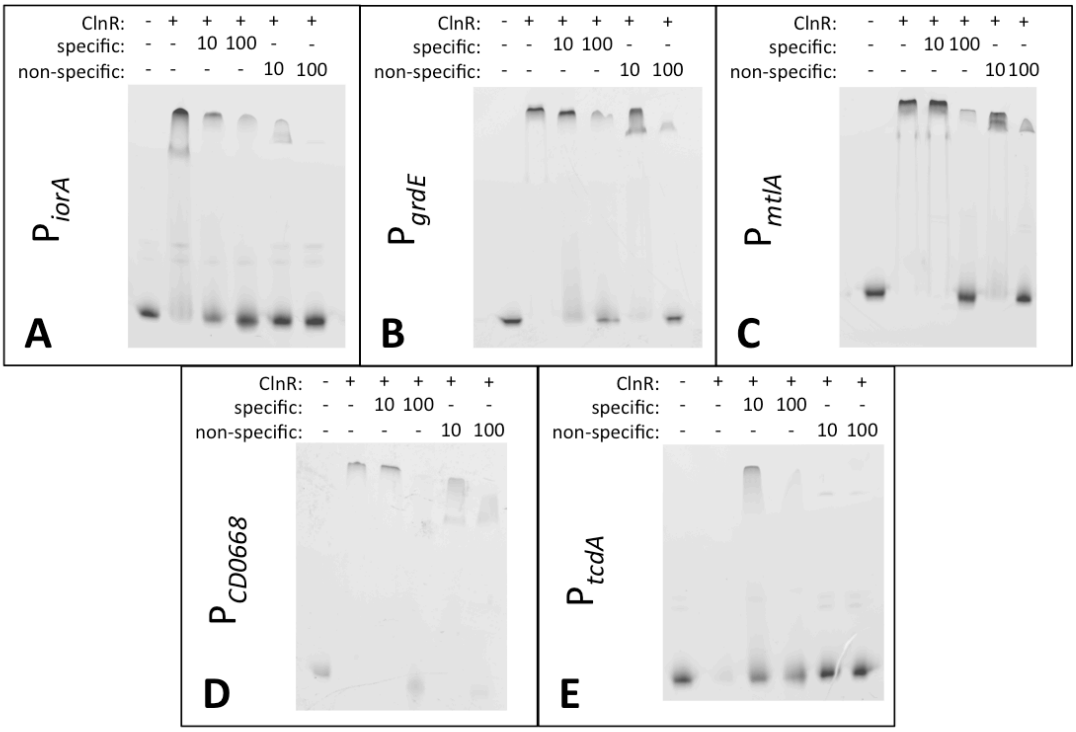

Figure S10. Competitive Electrophoretic Mobility Shift Assays (EMSA) of ClnR-dependent genes. Competitive elecrophoretic mobility shift assays were performed as described in Methods using His-tagged ClnR and fluorescein-labeled DNA encompassing regions upstream of **A**) *iorA,* **B**) *grdE,* **C**) *mtlA,* **D**) *CD0668*, or **E**) *tcdA*. ClnR was added at 8 μM and specificity was assessed with the addition of unlabeled target DNA or unlabeled P*spo0A* DNA at either 10x or 100x the concentration of labeled target DNA.

REFERENCES

1. **Lessa FC, Mu Y, Bamberg WM, Beldavs ZG, Dumyati GK, Dunn JR, Farley MM, Holzbauer SM, Meek JI, Phipps EC, Wilson LE, Winston LG, Cohen JA, Limbago BM, Fridkin SK, Gerding DN, McDonald LC.** 2015. Burden of *Clostridium difficile* infection in the United States. N Engl J Med **372:**825-834.
2. **Postma N, Kiers D, Pickkers P.** 2015. The challenge of Clostridium difficile infection: Overview of clinical manifestations, diagnostic tools and therapeutic options. Int J Antimicrob Agents doi:10.1016/j.ijantimicag.2015.11.001.
3. **Borriello SP.** 1990. The influence of the normal flora on *Clostridium difficile* colonisation of the gut. Ann Med **22:**61-67.
4. **Rolfe RD, Helebian S, Finegold SM.** 1981. Bacterial interference between Clostridium difficile and normal fecal flora. J Infect Dis **143:**470-475.
5. **Wah J, Wellek A, Frankenberger M, Unterberger P, Welsch U, Bals R.** 2006. Antimicrobial peptides are present in immune and host defense cells of the human respiratory and gastrointestinal tracts. Cell Tissue Res **324:**449-456.
6. **Tollin M, Bergman P, Svenberg T, Jornvall H, Gudmundsson GH, Agerberth B.** 2003. Antimicrobial peptides in the first line defence of human colon mucosa. Peptides **24:**523-530.
7. **Muller CA, Autenrieth IB, Peschel A.** 2005. Innate defenses of the intestinal epithelial barrier. Cell Mol Life Sci **62:**1297-1307.
8. **Dommett R, Zilbauer M, George JT, Bajaj-Elliott M.** 2005. Innate immune defence in the human gastrointestinal tract. Mol Immunol **42:**903-912.

9. **Peschel A, Sahl HG.** 2006. The co-evolution of host cationic antimicrobial peptides and microbial resistance. Nat Rev Microbiol **4:**529-536.

10. **Dürr UHN, Sudheendra US, Ramamoorthy A.** 2006. LL-37, the only human member of the cathelicidin family of antimicrobial peptides. BBA - Biomembranes **1758:**1408-1425.

11. **Cowardin CA, Petri WA, Jr.** 2014. Host recognition of *Clostridium difficile* and the innate immune response. Anaerobe **30:**205-209.

12. **Kelly CP, Kyne L.** 2011. The host immune response to *Clostridium difficile*. J Med Microbiol **60:**1070-1079.

13. **McQuade R, Roxas B, Viswanathan VK, Vedantam G.** 2012. *Clostridium difficile* clinical isolates exhibit variable susceptibility and proteome alterations upon exposure to mammalian cationic antimicrobial peptides. Anaerobe **18:**614-620.

14. **Kazamias MT, Sperry JF.** 1995. Enhanced fermentation of mannitol and release of cytotoxin by *Clostridium difficile* in alkaline culture media. Appl Environ Microbiol **61:**2425-2427.

15. **Janoir C, Deneve C, Bouttier S, Barbut F, Hoys S, Caleechum L, Chapeton-Montes D, Pereira FC, Henriques AO, Collignon A, Monot M, Dupuy B.** 2013. Adaptive strategies and pathogenesis of *Clostridium difficile* from *in vivo* transcriptomics. Infect Immun **81:**3757-3769.

16. **Ferreyra JA, Wu KJ, Hryckowian AJ, Bouley DM, Weimer BC, Sonnenburg JL.** 2014. Gut microbiota-produced succinate promotes *C. difficile* infection after antibiotic treatment or motility disturbance. Cell host & microbe **16:**770-777.

17. **Ho TD, Ellermeier CD.** 2011. PrsW is required for colonization, resistance to antimicrobial peptides, and expression of extracytoplasmic function sigma factors in *Clostridium difficile*. Infect Immun **79:**3229-3238.

18. **Theriot CM, Koenigsknecht MJ, Carlson PE, Jr., Hatton GE, Nelson AM, Li B, Huffnagle GB, J ZL, Young VB.** 2014. Antibiotic-induced shifts in the mouse gut microbiome and metabolome increase susceptibility to *Clostridium difficile* infection. Nat Commun **5:**3114.

19. **Dineen SS, McBride SM, Sonenshein AL.** 2010. Integration of metabolism and virulence by *Clostridium difficile* CodY. J Bacteriol **192:**5350-5362.

20. **Nawrocki KL, Edwards AN, Daou N, Bouillaut L, McBride SM.** 2016. CodY-dependent regulation of sporulation in *Clostridium difficile*. J Bacteriol **198:**2113-2130.

21. **Edwards AN, Nawrocki KL, McBride SM.** 2014. Conserved oligopeptide permeases modulate sporulation initiation in *Clostridium difficile*. Infect Immun **82:**4276-4291.

22. **Woods EC, McBride SM.** 2017. Regulation of antimicrobial resistance by extracytoplasmic function (ECF) sigma factors. Microbes Infect **19:**238-248.

23. **Woods EC, Nawrocki KL, Suarez JM, McBride SM.** 2016. The *Clostridium difficile* Dlt pathway is controlled by the ECF sigma factor, SigmaV, in response to lysozyme. Infect Immun doi:10.1128/IAI.00207-16.

24. **Utaida S, Dunman PM, Macapagal D, Murphy E, Projan SJ, Singh VK, Jayaswal RK, Wilkinson BJ.** 2003. Genome-wide transcriptional profiling of the

response of *Staphylococcus aureus* to cell-wall-active antibiotics reveals a cell-wall-stress stimulon. Microbiology **149:**2719-2732.

25. **Poole K.** 2012. Bacterial stress responses as determinants of antimicrobial resistance. J Antimicrob Chemother **67:**2069-2089.

26. **Durr UH, Sudheendra US, Ramamoorthy A.** 2006. LL-37, the only human member of the cathelicidin family of antimicrobial peptides. Biochim Biophys Acta **1758:**1408-1425.

27. **Skerlavaj B, Benincasa M, Risso A, Zanetti M, Gennaro R.** 1999. SMAP-29: a potent antibacterial and antifungal peptide from sheep leukocytes. FEBS Lett **463:**58-62.

28. **Wang G.** 2008. Structures of human host defense cathelicidin LL-37 and its smallest antimicrobial peptide KR-12 in lipid micelles. J Biol Chem **283:**32637-32643.

29. **Hoskisson PA, Rigali S.** 2009. Chapter 1: Variation in form and function the helix-turn-helix regulators of the GntR superfamily. Adv Appl Microbiol **69:**1-22.

30. **Rigali S, Derouaux A, Giannotta F, Dusart J.** 2002. Subdivision of the helix-turn-helix GntR family of bacterial regulators in the FadR, HutC, MocR, and YtrA subfamilies. J Biol Chem **277:**12507-12515.

31. **Bouillaut L, Self WT, Sonenshein AL.** 2013. Proline-dependent regulation of *Clostridium difficile* Stickland metabolism. J Bacteriol **195:**844-854.

32. **Dubois T, Dancer-Thibonnier M, Monot M, Hamiot A, Bouillaut L, Soutourina O, Martin-Verstraete I, Dupuy B.** 2016. Control of *Clostridium*

difficile physiopathology in response to cysteine availability. Infect Immun **84:**2389-2405.

33. **Karlsson S, Burman LG, Akerlund T.** 1999. Suppression of toxin production in *Clostridium difficile* VPI 10463 by amino acids. Microbiology **145 (Pt 7):**1683-1693.

34. **Martin-Verstraete I, Peltier J, Dupuy B.** 2016. The regulatory networks that control *Clostridium difficile* toxin synthesis. Toxins (Basel) **8**.

35. **Gellatly SL, Needham B, Madera L, Trent MS, Hancock RE.** 2012. The *Pseudomonas aeruginosa* PhoP-PhoQ two-component regulatory system is induced upon interaction with epithelial cells and controls cytotoxicity and inflammation. Infect Immun **80:**3122-3131.

36. **Froehlich BJ, Bates C, Scott JR.** 2009. *Streptococcus pyogenes* CovRS mediates growth in iron starvation and in the presence of the human cationic antimicrobial peptide LL-37. J Bacteriol **191:**673-677.

37. **Nizet V, Ohtake T, Lauth X, Trowbridge J, Rudisill J, Dorschner RA, Pestonjamasp V, Piraino J, Huttner K, Gallo RL.** 2001. Innate antimicrobial peptide protects the skin from invasive bacterial infection. Nature **414:**454-457.

38. **Velarde JJ, Ashbaugh M, Wessels MR.** 2014. The human antimicrobial peptide LL-37 binds directly to CsrS, a sensor histidine kinase of group A Streptococcus, to activate expression of virulence factors. J Biol Chem **289:**36315-36324.

39. **Tran-Winkler HJ, Love JF, Gryllos I, Wessels MR.** 2011. Signal transduction through CsrRS confers an invasive phenotype in group A Streptococcus. PLoS Pathog **7:**e1002361.

40. **Majchrzykiewicz JA, Kuipers OP, Bijlsma JJ.** 2010. Generic and specific adaptive responses of *Streptococcus pneumoniae* to challenge with three distinct antimicrobial peptides, bacitracin, LL-37, and nisin. Antimicrob Agents Chemother **54:**440-451.

41. **Strempel N, Neidig A, Nusser M, Geffers R, Vieillard J, Lesouhaitier O, Brenner-Weiss G, Overhage J.** 2013. Human host defense peptide LL-37 stimulates virulence factor production and adaptive resistance in *Pseudomonas aeruginosa*. PLoS One **8:**e82240.

42. **Liu W, Dong SL, Xu F, Wang XQ, Withers TR, Yu HD, Wang X.** 2013. Effect of intracellular expression of antimicrobial peptide LL-37 on growth of *Escherichia coli* strain TOP10 under aerobic and anaerobic conditions. Antimicrob Agents Chemother **57:**4707-4716.

43. **Sonenshein AL.** 2005. CodY, a global regulator of stationary phase and virulence in Gram-positive bacteria. Curr Opin Microbiol **8:**203-207.

44. **Dineen SS, Villapakkam AC, Nordman JT, Sonenshein AL.** 2007. Repression of *Clostridium difficile* toxin gene expression by CodY. Mol Microbiol **66:**206-219.

45. **Dupuy B, Sonenshein AL.** 1998. Regulated transcription of *Clostridium difficile* toxin genes. Mol Microbiol **27:**107-120.

46. **Antunes A, Martin-Verstraete I, Dupuy B.** 2011. CcpA-mediated repression of *Clostridium difficile* toxin gene expression. Mol Microbiol **79:**882-899.

47. **Antunes A, Camiade E, Monot M, Courtois E, Barbut F, Sernova NV, Rodionov DA, Martin-Verstraete I, Dupuy B.** 2012. Global transcriptional

control by glucose and carbon regulator CcpA in *Clostridium difficile*. Nucleic Acids Res **40:**10701-10718.

48. **Bouillaut L, Dubois T, Sonenshein AL, Dupuy B.** 2015. Integration of metabolism and virulence in *Clostridium difficile*. Res Microbiol **166:**375-383.

49. **Karlsson S, Burman LG, Akerlund T.** 2008. Induction of toxins in *Clostridium difficile* is associated with dramatic changes of its metabolism. Microbiology **154:**3430-3436.

50. **Pitts AC, Tuck LR, Faulds-Pain A, Lewis RJ, Marles-Wright J.** 2012. Structural insight into the *Clostridium difficile* ethanolamine utilisation microcompartment. PLoS One **7:**e48360.

51. **Kopke M, Straub M, Durre P.** 2013. *Clostridium difficile* is an autotrophic bacterial pathogen. PLoS One **8:**e62157.

52. **Luria SE, Burrous JW.** 1957. Hybridization between *Escherichia coli* and *Shigella*. J Bacteriol **74:**461-476.

53. **Putnam EE, Nock AM, Lawley TD, Shen A.** 2013. SpoIVA and SipL are *Clostridium difficile* spore morphogenetic proteins. J Bacteriol **195:**1214-1225.

54. **Edwards AN, Suarez JM, McBride SM.** 2013. Culturing and maintaining *Clostridium difficile* in an anaerobic environment. J Vis Exp doi:10.3791/50787**:**e50787.

55. **Bouillaut L, McBride SM, Sorg JA.** 2011. Genetic manipulation of *Clostridium difficile*. Curr Protoc Microbiol **Chapter 9:**Unit 9A 2.

56. **Sorg JA, Dineen SS.** 2009. Laboratory maintenance of *Clostridium difficile*. Curr Protoc Microbiol **Chapter 9:**Unit9A 1.

57. **Suarez JM, Edwards AN, McBride SM.** 2013. The *Clostridium difficile cpr* locus is regulated by a noncontiguous two-component system in response to type A and B lantibiotics. J Bacteriol **195:**2621-2631.

58. **Dobin A, Davis CA, Schlesinger F, Drenkow J, Zaleski C, Jha S, Batut P, Chaisson M, Gingeras TR.** 2013. STAR: ultrafast universal RNA-seq aligner. Bioinformatics **29:**15-21.

59. **Anders S, Pyl PT, Huber W.** 2015. HTSeq--a Python framework to work with high-throughput sequencing data. Bioinformatics **31:**166-169.

60. **Love MI, Huber W, Anders S.** 2014. Moderated estimation of fold change and dispersion for RNA-seq data with DESeq2. Genome Biol **15:**550.

61. **Tatusov RL, Koonin Ev Fau - Lipman DJ, Lipman DJ.** 1997. A genomic perspective on protein families. Science.

62. **Schmittgen TD, Livak KJ.** 2008. Analyzing real-time PCR data by the comparative C(T) method. Nat Protoc **3:**1101-1108.

63. **Liu R, Suarez JM, Weisblum B, Gellman SH, McBride SM.** 2014. Synthetic polymers active against *Clostridium difficile* vegetative cell growth and spore outgrowth. J Am Chem Soc **136:**14498-14504.

64. **Edwards AN, Tamayo R, McBride SM.** 2016. A Novel Regulator Controls Clostridium difficile Sporulation, Motility and Toxin Production. Mol Microbiol doi:10.1111/mmi.13361.

65. **Mercante J, Suzuki K, Cheng X, Babitzke P, Romeo T.** 2006. Comprehensive alanine-scanning mutagenesis of Escherichia coli CsrA defines two subdomains of critical functional importance. J Biol Chem **281:**31832-31842.

66. **Cartman ST, Kelly ML, Heeg D, Heap JT, Minton NP.** 2012. Precise manipulation of the *Clostridium difficile* chromosome reveals a lack of association between the *tcdC* genotype and toxin production. Appl Environ Microbiol **78:**4683-4690.

67. **Bartlett JG, Onderdonk AB, Cisneros RL, Kasper DL.** 1977. Clindamycin-associated colitis due to a toxin-producing species of *Clostridium* in hamsters. J Infect Dis **136:**701-705.

68. **Chang TW, Bartlett JG, Gorbach SL, Onderdonk AB.** 1978. Clindamycin-induced enterocolitis in hamsters as a model of pseudomembranous colitis in patients. Infect Immun **20:**526-529.

69. **Sorg JA, Sonenshein AL.** 2010. Inhibiting the initiation of *Clostridium difficile* spore germination using analogs of chenodeoxycholic acid, a bile acid. J Bacteriol **192:**4983-4990.

70. **Edwards AN, McBride SM.** 2016. Isolating and Purifying Clostridium difficile Spores. Methods Mol Biol **1476:**117-128.

71. **Dalgaard P, Koutsoumanis K.** 2001. Comparison of maximum specific growth rates and lag times estimated from absorbance and viable count data by different mathematical models. J Microbiol Methods **43:**183-196.

72. **Pope CF, McHugh TD, Gillespie SH.** 2010. Methods to determine fitness in bacteria. Methods Mol Biol **642:**113-121.

73. **McBride SM, Sonenshein AL.** 2011. Identification of a genetic locus responsible for antimicrobial peptide resistance in Clostridium difficile. Infect Immun **79:**167-176.

74. **Edwards AN, Tamayo R, McBride SM.** 2016. A novel regulator controls *Clostridium difficile* sporulation, motility and toxin production. Mol Microbiol **100:**954-971.

Chapter 4: Discussion

C. difficile infections are a serious public health issue (1). The predominantly nosocomial nature of these infections presents an opportunity for preventative, or at the least, early interventions to lessen the incidence or severity of disease (2). An understanding of the early colonization events that lead to establishment of infection is critical for developing such preventative and early-acting therapeutics. The innate immune system delivers the initial host response to combat infections, so how *C. difficile* responds to components of the host's innate immune system is likely to be important for *C. difficile* colonizion of the colon. Cationic antimicrobial peptides comprise a significant part of the innate immune system in the gut and neutrophilic response to CDI, yet how *C. difficile* interacts with these compounds is currently poorly understood (3). In this work, we sought to define the response of *C. difficile* to the host CAMPs lysozyme and LL-37.

I. Lysozyme

It was known previously that the Dlt pathway, which adds D-alanine to teichoic acids and increases the cell surface charge, was involved in *C. difficile* resistance to a variety of CAMPs (4). It was not known, however, how this resistance mechanism is regulated or whether this resistance mechanism applied to the host CAMP, lysozyme. In this work we elucidated the regulatory pathway controlling the Dlt pathway in response to lysozyme and demonstrated the importance of this pathway to virulence *in vivo*.

Our results indicated that *dlt* expression is induced in response to lysozyme and confers resistance to lysozyme (**Chap. 2 Fig. 1, 2**). This induction is dependent on the extracytoplasmic sigma factor, σ^V (**Chap. 2 Fig. 2**). We determined regions of the *dlt* promoter that are necessary for both σ^V- and lysozyme-dependent regulation (**Chap. 2**

Table 3, 4). Moreover, we demonstrated that a *sigV* and a *dlt* mutant are both more virulent *in vivo*, even though a *dlt* mutant does not have a competitive advantage (**Chap. 2 Fig. 6**). These findings are significant because they underscore the importance of the interaction between the bacterium and host-produced CAMPs to bacterial pathogenesis.

There remains much to be learned about this system. For example, why is a *dlt* mutant more virulent *in vivo?* We had originally hypothesized that with a severely reduced capacity to resist killing by lysozyme, a *dlt* mutant would fare much worse than the parent strain in the lysozyme-rich environment of an infection. It is possible that the addition of D-alanines to teichoic acids on the cell surface is also important for interactions with the host immune receptors, and the lack of this moiety on the surface of the *dlt* mutant impacts the host immune response (5, 6). However, given that we observed no competitive advantage or disadvantage of a *dlt* mutant in co-infections with the parent strain, it is unlikely that the host mounts a different immune response against *C. difficile* with or without D-alanylated teichoic acids. Given the dearth of reagents to study hamster immune responses, an alternate model for infection or additional reagents would be necessary for further exploration of this question.

Another open question is how the Dlt pathway is regulated in response to other antimicrobial triggers. A variety of other CAMPs, including polymyxin B, can induce *dlt* expression (4). This induction, however, is not σ^V-dependent (**Chap. 2 Fig. 2**). It appears that the other main *C. difficile* ECF sigma factor, σ^T, may contribute to *dlt* regulation in response to polymyxin B, and indeed a *sigT* mutant has a slight growth defect in polymyxin B (**Chap. 2 Fig. 1**). A *sigT* mutant is incapable of inducing *dlt* expression to the same level as the parent strain in response to polymyxin B, but a small level of

induction is still possible in a *sigT* mutant (**Chap. 2 Supl. Fig. S3**). Therefore, σ^T is not the only factor responsible for inducing *dlt* expression in response to polymyxin B.

Adding to the complexity of how the Dlt pathway is regulated, we noted striking differences between strains. Our studies focused on *C. difficile* strains 630Δ*erm* (ribotype 012) and R20291 (ribotype 027). We noted that strain R20291 is more sensitive to lysozyme than 630Δ*erm* (**Chap. 2 Fig. 1**), induces both *sigV* and *dltD* to relatively higher levels in response to lysozyme (**Chap. 2 Fig. 2**), and has less D-alanine on the cell surface (**Chap. 2 Fig. 4**). These differences between strains raise several questions. Does R20291 contain additional regulatory factors that account for the greater induction of gene expression in response to lysozyme? Do the enzymes of the Dlt pathway not function as efficiently in R20291 as those in 630Δ*erm*, thereby leading to less D-alanylation of teichoic acids despite higher *dlt* gene expression? Or are there other differences in post-transcriptional regulation between these strains? How widespread are differences in *dlt* regulation between strains of other ribotypes?

Many of these remaining questions revolve around identifying which factors bind and regulate the *dlt* promoter. DNA-affinity pulldowns would be one way to discover which regulators bind the *dlt* promoter. In these experiments, a biotin-labeled segment of the *dlt* promoter region would be anchored to streptavidin beads and exposed to lysates of cells grown in a variety of conditions (such as +/- lysozyme or +/- polymyxin B). Regulators that bind to this region of DNA would remain bound after several washes to remove non-specific binding, and can subsequently be identified with mass spectrometry. This technique could help resolve whether σ^V regulates *dlt* expression directly, which factors regulate *dlt* expression in response to other CAMPs like polymyxin B, and

whether different factors regulate transcription of this operon in R20291.

Clearly, the regulation of the Dlt pathway is complex. Given the importance of this pathway to virulence, as demonstrated in this work, it is perhaps not surprising that *C. difficile* has evolved multiple pathways to control and fine-tune the expression of this pathway.

II. LL-37

Although an earlier study had suggested that *C. difficile* harbors inducible mechanisms of LL-37 resistance, specific resistance mechanisms had not been identified (7). We therefore sought to identify inducible mechanisms of resistance to this important host CAMP. In this work, we did not identify a specific LL-37 resistance mechanism, but instead we discovered a novel global regulator that uses LL-37 as a signal for the host environment, which orchestrates a broad range of adaptations to enable adaptation to the host.

We hypothesized that LL-37 resistance mechanisms would be induced in LL-37, so we began by determining which genes are induced in LL-37. Using RNA-seq we identified that the *clnRAB* operon is highly induced in LL-37 (**Chap. 3 Table S1)**. This operon contains a GntR-family transcriptional regulator (*clnR*) and a predicted ABC-transporter (*clnAB*). Similar to other GntR-family transcriptional regulators, ClnR autoregulates its expression; ClnR represses *clnRAB* expression in the absence of LL-37, and is necessary for induction of *clnRAB* expression in the presence of LL-37 (**Chap. 3 Fig. 4**). Unexpectedly, we also found that the ABC-transporter contributes to the regulation of *clnRAB*, as a *clnA* mutant, like a *clnR* mutant, is unable to induce *clnRAB* expression in response to LL-37 (**Chap. 3 Fig. 4**). Despite the high level of induction of

clnRAB in LL-37, neither a *clnR* nor a *clnA* mutant has significantly altered resistance to LL-37 compared to the parent strain (**Chap. 3 Table S2**). Using RNA-seq to define the transcriptome of the *clnR* mutant, we found that dozens of genes are dysregulated in this mutant both with and without LL-37, indicating that ClnR acts as a global regulator (**Chap. 3 Table S4**). The genes with ClnR-dependent expression serve a wide variety of functions, including toxin production, alternative metabolic pathways, transcriptional regulation, and transmembrane transport (**Chap. 3 Fig. 3**). Both a *clnR* and a *clnA* mutant are more virulent *in vivo,* which demonstrates the importance of these ClnR-dependent genes to the disease process (**Chap. 3 Fig. 5**).

At first it may seem contradictory that *clnR* and *clnA* mutants are more virulent *in vivo*, because mutants lacking the *clnRAB* system are unable to properly adapt to the host environment. There are, however, several possible explanations for this finding. For one, we found that *in vitro* in TY medium, LL-37 reduces toxin expression in 630Δ*erm*, but *clnR* and *clnA* mutants are unable to respond to LL-37 (**Chap. 3 Fig. S8**). Therefore, in the presence of LL-37, *clnR* and *clnA* mutants produce more toxin than 630Δ*erm*. During infection, presumably high concentrations of LL-37 are present, so the *clnR* and *clnA* mutants may be producing more toxin than the parent strain, leading to more rapid host morbidity. In addition, the many metabolic pathways controlled by ClnR could provide the bacterium with additional sources of nutrition in the host environment. Access to additional nutritional sources would delay toxin production, because toxin production is triggered only when nutrition is scare (8). Without the ability to induce expression of alternate metabolic pathways during infection, the *clnR* and *clnA* mutants would likely run out of nutrients faster than the parent strain, and therefore would begin toxin

production earlier. It appears that the ClnRAB system may have evolved as a mechanism to help prolong survival and replication in the host and delay the induction of the virulence mechanisms that ultimately lead to the expulsion of the bacterium from the intestine. Dissecting which of the ClnR-dependent metabolic pathways contribute significantly to survival in the host would help to define how individual metabolites impact *C. difficile* colonization and virulence.

Another aspect that merits additional investigation is whether any of the factors in the ClnR regulon are LL-37 resistance mechanisms. Although a *clnR* mutant is not more sensitive to LL-37, ClnR may still regulate LL-37 resistance mechanisms. There are several explanations for why a *clnR* mutant is not more sensitive to LL-37, even if resistance genes within the ClnR regulon exist. For one, resistance genes could have a high enough baseline expression in the *clnR* mutant to maintain resistance to LL-37. In addition, the effects of ClnR are pleiotropic and cause expression of some genes to increase whereas others are decreased. Mutants of individual genes are therefore needed in order to evaluate whether these genes impact resistance. We identified many candidate resistance genes that are induced by LL-37. These genes include the *cdd* putative lantibiotic transporter, several *van* genes, additional ABC transporters, and several transcriptional regulators (**Chap. 3 Table S4**). Generating mutants in each of these putative resistance genes would enable an assessment of their role in the LL-37 response.

In addition, determining which genes are directly regulated by ClnR would increase our understanding of the nature of the response to LL-37. We were able to demonstrate that ClnR does directly bind upstream of *clnR,* as well as the antimicrobial resistance gene, *vanZ1*, and the regulators, *sigU* and *CD1606* (**Chap. 3 Fig. 6**). We found

that ClnR binding to several other ClnR-dependent genes is non-specific (**Chap. 3, Fig. S10**), indicating that many effects of ClnR may be through indirect mechanisms. Given that ClnR regulates the expression of a number of other transcriptional regulators, it would not be surprising if these regulators are responsible for direct regulation of many of the ClnR-dependent genes. Effects of ClnR could also be indirect if genes under direct control of ClnR alter the state of the cell (i.e. altering the redox state, producing metabolic byproducts) in ways that trigger other transcriptional changes. In future studies, chromatin immunoprecipitation could be a useful method to determine the direct regulon of ClnR and define the network of ClnR-dependent gene regulation.

Because by nature global regulators induce complex changes, it often takes a great number of studies to gain a full picture of the roles of pleiotropic regulators, such as ClnR. This work has provided a preliminary exploration of the ClnR regulon and defines ClnR as a novel regulator that coordinates a response to a specific host environment cue.

III. Final Summary

In this work, we have explored several aspects of how *C. difficile* responds to the host environment. Specifically, we elucidated the mechanism by which *C. difficile* is able to induce lysozyme resistance upon exposure to lysozyme. In this pathway, lysozyme exposure leads to activation of σ^V, which in turn activates *dlt* transcription to augment the cell wall of *C. difficile* and provide lysozyme resistance. In addition, we showed that LL-37 activates the global regulator, ClnR, and the ABC-transporter ClnAB, which coordinate an adaptive response to the intestinal environment.

Overall this work furthers our understanding of the early stages of *C. difficile* infection, which is a critical stage for preventative and therapeutic interventions.

Surviving the innate immune response is an important step in the process of disease progression and therefore represents a key window of opportunity for therapeutic intervention and prevention of pathogenesis. Identifying ways to increase *C. difficile* susceptibility to innate immune responses may help extend the utility and efficacy of our current antibiotic therapies so that we can better prevent and treat this threatening disease.

References

1. **Lessa FC, Mu Y, Bamberg WM, Beldavs ZG, Dumyati GK, Dunn JR, Farley MM, Holzbauer SM, Meek JI, Phipps EC, Wilson LE, Winston LG, Cohen JA, Limbago BM, Fridkin SK, Gerding DN, McDonald LC.** 2015. Burden of *Clostridium difficile* infection in the United States. N Engl J Med **372:**825-834.
2. **Louh IK, Greendyke WG, Hermann EA, Davidson KW, Falzon L, Vawdrey DK, Shaffer JA, Calfee DP, Furuya EY, Ting HH.** 2017. *Clostridium difficile* infection in acute care hospitals: systematic review and best practices for prevention. Infect Control Hosp Epidemiol **38:**476-482.
3. **Muller CA, Autenrieth IB, Peschel A.** 2005. Innate defenses of the intestinal epithelial barrier. Cell Mol Life Sci **62:**1297-1307.
4. **McBride SM, Sonenshein AL.** 2011. The *dlt* operon confers resistance to cationic antimicrobial peptides in *Clostridium difficile*. Microbiology **157:**1457-1465.
5. **Tabuchi Y, Shiratsuchi A, Kurokawa K, Gong JH, Sekimizu K, Lee BL, Nakanishi Y.** 2010. Inhibitory role for D-alanylation of wall teichoic acid in activation of insect Toll pathway by peptidoglycan of *Staphylococcus aureus*. J Immunol **185:**2424-2431.
6. **Grangette C, Nutten S, Palumbo E, Morath S, Hermann C, Dewulf J, Pot B, Hartung T, Hols P, Mercenier A.** 2005. Enhanced antiinflammatory capacity of a *Lactobacillus plantarum* mutant synthesizing modified teichoic acids. Proc Natl Acad Sci U S A **102:**10321-10326.

7. **McQuade R, Roxas B, Viswanathan VK, Vedantam G.** 2012. *Clostridium difficile* clinical isolates exhibit variable susceptibility and proteome alterations upon exposure to mammalian cationic antimicrobial peptides. Anaerobe **18:**614-620.

8. **Bouillaut L, Dubois T, Sonenshein AL, Dupuy B.** 2014. Integration of metabolism and virulence in *Clostridium difficile*. Res Microbiol doi:10.1016/j.resmic.2014.10.002.